EPRI

BEST ESTIMATE ANALYSIS OF THE LARGE BREAK LOSS OF COOLANT ACCIDENT FOR INDIAN POINT UNIT 2 NUCLEAR PLANT

TR-103391
Research Project 2956-1&3
(WCAP-13837)
October 1993

Prepared by

WESTINGHOUSE ELECTRIC CORPORATION
Energy Systems Business Unit
P.O. Box 355
Pittsburgh, PA 15230-0355

S.K. Chow
M.Y. Young

Prepared for
Consolidated Edison Co.
4 Irving Place
New York, NY 10003

Consolidated Edison Project Manager
Arthur P. Ginsberg

and

Electric Power Research Institute
3412 Hillview Avenue
Palo Alto, CA 94303

EPRI Project Manager
S. Pal Kalra
Risk & Reliability Program
Nuclear Power Division

285T/SPK/DGO

TABLE OF CONTENTS

LIST OF TABLES

LIST OF FIGURES

LIST OF FIGURES (Cont'd)

SECTION 1
INTRODUCTION

When the Final Acceptance Criteria (FAC) governing the loss of coolant accident (LOCA) for light water reactors was issued in Appendix K of 10CRF50.46 (1988) in 1973, both the NRC and the industry recognized that the rule was highly conservative. That is, using the then accepted analysis methods, the performance of the Emergency Core Cooling System (ECCS) would be conservatively underestimated, resulting in predicted peak cladding temperatures much higher than expected. At that time, however, the degree of conservatism in the analysis could not be quantified. As a result, the NRC began a large scale confirmatory research program with the following objectives:

(1) Identify through separate effects and integral effects experiments, the degree of conservatism in those models permitted in the Appendix K rule. In this fashion, those areas in which a purposely prescriptive approach was used in the Appendix K rule could be quantified with additional data so that a less prescriptive future approach might be allowed.

(2) Develop improved thermal-hydraulic computer codes and models so that more accurate and realistic accident analysis calculations could be performed. The purpose of this research was to develop an accurate predictive capability so that the uncertainties in the ECCS performance and the degree of conservatism with respect to the Appendix K limits could be quantified.

Over the past decade, the NRC, and the nuclear industry have sponsored reactor safety research programs directed at meeting the above two objectives. The overall results have quantified the conservatism in the Appendix K rule for LOCA analysis and confirmed that some relaxation of the rule can be made without a loss in safety to the public. It was also found that some plants were being restricted in operating flexibility by overly conservative Appendix K requirements. In recognition of the Appendix K conservatism that was being quantified by the research programs, the NRC adopted an interim approach for evaluation methods. This interim approach is described in SECY-83-472 (1983). The SECY-83-472

approach retained those features of Appendix K that were legal requirements, but permitted applicants to use best-estimate thermal-hydraulic models in their ECCS evaluation model. Thus, SECY-83-472 represented an important step in basing licensing decisions on realistic calculations, as opposed to those calculations prescribed by Appendix K.

In 1988, as a result of the improved understanding of LOCA thermal-hydraulic phenomena gained by these extensive research programs, the NRC staff amended the requirements of 10CFR50.46 and Appendix K, "ECCS Evaluation Models," so that a realistic evaluation model may be used to analyze the performance of the ECCS during a hypothetical LOCA (Federal Register V53, 1988). Under the amended rules, best estimate thermal-hydraulic models may be used in place of models with Appendix K features. The rule change also requires, as part of the analysis, an assessment of the uncertainty of the best estimate calculations. It further requires that this analysis uncertainty be included when comparing the results of the calculations to the prescribed acceptance limits.

To demonstrate use of the revised ECCS rule, the NRC and its consultants developed a method called the Code Scaling, Applicability, and Uncertainty (CSAU) evaluation methodology (Wilson, 1989). This method outlined an approach for defining and qualifying a best estimate thermal-hydraulic code and quantifying the uncertainties in a LOCA analysis.

This report describes in summary form a new evaluation model developed by Westinghouse and the Electric Power Research Institute (EPRI) to apply realistic methods to the analysis of the large break LOCA for PWR's. The evaluation model is used to calculate the peak cladding temperature (PCT) at 95 percent probability for the Indian Point Unit 2 (IP2) nuclear power station. The calculated results and associated Technical Specification and Final Safety Analysis Report changes required for implementation of this methodology for IP2 are presented in this report.

SECTION 2
EVALUATION MODEL DESCRIPTION

2-1 WCOBRA/TRAC Computer Code

The COBRA/TRAC code was originally developed by Thurgood et al. (1983) at Pacific Northwest Laboratory by combining the COBRA-TF code as developed by Thurgood et al. (1980) and the TRAC-PD2 codes as developed by Liles et al. (1981). The COBRA-TF code, which has the capability to model three dimensional flow behavior in a reactor vessel, was incorporated into TRAC-PD2 to replace its vessel model. TRAC-PD2 is a systems transient code designed to model all major components in the primary system. Westinghouse continued the development and validation of COBRA/TRAC through the FLECHT-SEASET program (Paik and Hochreiter, 1986). To allow the code to model phenomena specific to plants with upper plenum injection, Westinghouse made modifications and improvements to COBRA/TRAC and renamed the new version WCOBRA/TRAC. This computer code is described in detail in a report referred to as the Code Qualification Document (CQD) (Westinghouse, 1992 and 1993).

WCOBRA/TRAC uses a two-fluid, three-field representation of flow in the vessel component. The three fields are a vapor field, a continuous liquid field and an entrained liquid drop field. Each field in the vessel uses a set of three dimensional continuity, momentum, and energy equations with one exception. A common energy equation is used by both the continuous liquid and the entrained liquid drop fields.

The one-dimensional components consist of all the major components in the primary system, such as pipes, pumps, valves, steam generators, and the pressurizer. The one-dimensional components are represented by a two-phase, five equation drift flux model. This formulation consists of two equations for the conservation of mass, two equations for the conservation of energy, and a single equation for the conservation of momentum. Closure for the field equations requires specification of the interphase relative velocities, interfacial heat and mass transfer, and other thermodynamic and constitutive relationships.

2-2 Methodology

Volumes I, II, and III of the CQD (Westinghouse, 1992 and 1993) presented a detailed assessment of the computer code WCOBRA/TRAC through comparisons to experimental data. From this assessment, a quantitative estimate was obtained of the code's ability to predict peak cladding temperatures in a PWR large break LOCA. Modeling of a PWR introduced additional uncertainties which were identified and discussed in Section 21 of CQD Volume IV (Westinghouse, 1992 and 1993). A list of key LOCA parameters was compiled as a result of these studies. Models of several PWR's were used to perform sensitivity studies and establish the relative importance of these parameters. The final step of the best estimate methodology, in which all the uncertainties of the LOCA parameters are accounted for to estimate a PCT at 95 percent probability, is described in the following sections. The methodology is summarized below:

1. Plant Model Development

   In this step, a WCOBRA/TRAC model of the plant is developed. A high level of noding detail is used, to provide an accurate simulation of the transient. However, specific guidelines are followed to assure that the model is consistent with models used in the code validation. This results in a high level of consistency among plant models, except for specific areas dictated by hardware differences such as in the upper plenum of the reactor vessel or the ECCS injection configuration.

2. Determination of Plant Operating Conditions

   In this step, the expected or desired operating range of the plant to which the analysis is to be applied is established. The parameters considered are based on a "key LOCA parameters" list which was developed as part of the methodology. A conservative (based on prior experience) set of these parameters is chosen for input as initial conditions to the plant model. This set of conditions will generate a result with a relatively high PCT, and is called the "scoping study base case".

3. Scoping Study Calculations

Calculations are performed using the plant model in which most of the key LOCA parameters are varied one at a time over the range defined in step 2. Information is generated on the sensitivity of PCT to parameter variations which will be used to quantify certain uncertainty elements, and to identify where margin is available for plant improvements in operation.

4. Response Surface Calculations

Using the results from the scoping study, several parameters are set at more realistic values. This set of conditions is called the "response surface base case" and is used as a starting point for sensitivity studies to generate additional PCT data. In this step, the focus is on the effect of core power distribution parameters, and on break flow parameters. In addition to one at a time studies, parameters are varied in combination. Regression analyses are performed to derive PCT response surfaces from these results.

5. Uncertainty Evaluation

The PCT uncertainty in four categories (described below) is derived from the scoping studies and the response surfaces using the methodology described in Volume V of the CQD. The uncertainty calculations assume certain plant operating ranges which may be varied depending on the results obtained. These uncertainties are then combined to determine the overall PCT uncertainty at the 95 percent probability level.

6. Plant Operating Range

The plant operating range over which the uncertainty evaluation applies is defined. Depending on the results obtained in the scoping and response surface calculations, this range may be the desired range established in step 2, or may be narrower in some parameters to regain needed margin.

2-3 Uncertainty Elements and PCT Equation

There are four uncertainty categories or elements:

1. Code bias and uncertainty
2. Power distribution bias and uncertainty
3. Break flow bias and uncertainty
4. Initial condition uncertainty

These elements are considered to affect the base case PCT as shown below

$$PCT_j = PCT_j^B + \Delta PCT_{1_j} + \Delta PCT_{2_j} + \Delta PCT_{3_j} + \Delta PCT_{4_j} \qquad (2\text{-}1)$$

where

PCT_j^B = **Base case PCT:** The base case PCT is calculated using WCOBRA/TRAC at the nominal conditions identified in Section 4, for blowdown (j=1) and reflood (j=2, 3)

Each element includes a correction or bias, which is added to the base case PCT to move it closer to the expected, or average PCT. The bias from each element has an uncertainty associated with the data and calculational methods used to derive the bias. Each element of uncertainty is assumed independent.

ΔPCT_{1_j} = **Code bias and uncertainty:** The code bias accounts for differences between the code prediction of tests which simulate the PWR LOCA transient, and the measured data. It is independent of the plant type. Different values are used for the blowdown and reflood PCTs.

ΔPCT_{2_j} = **Power distribution bias and uncertainty:** This bias is the difference between the base case PCT, which assumes a nominal power distribution, and the average PCT taking into account all

possible power distributions during normal plant operation. Elements which contribute to the uncertainty of this bias are calculational uncertainties, and variations due to transient operation of the reactor.

ΔPCT_{3_j} = **Break flow bias and uncertainty:** This bias is the difference between the base case PCT, which assumes best estimate break flow parameters, and the average PCT taking into account all possible values of the break flow parameters. The uncertainty of this bias takes into account the effects of break discharge coefficient and broken loop resistance, which were found to have a strong effect on PCT.

ΔPCT_{4_j} = **Initial condition bias and uncertainty:** This bias is the difference between the base case PCT, which assumes several nominal or average initial conditions, and the average PCT taking into account all possible values of the initial conditions. This bias takes into account plant variations which have a relatively small effect on PCT. The elements which make up this bias and its uncertainty are plant specific.

The separability of the uncertainty components in the manner described is an approximation, since the parameters in each element may be affected by parameters in other elements. However, the way in which each element is derived should result in a reasonable estimate of the uncertainty, for the following reasons:

a) The physical phenomena have been grouped in such a way that their expected dependencies have been maintained to the greatest extent possible. Physical parameters affecting break flow have been grouped together, as have core power distribution parameters. Where the parameters have been separated, the dependencies are expected to be weak. Break flow, for example, would not be expected to depend significantly on the core power distribution. By the same token, variations in break

flow parameters did not significantly alter the nature of the transient, so that the calculated power distribution sensitivities would still apply.

b) The several combined sensitivity studies performed during the scoping studies do not show any effects which would indicate that a linear combination of the remaining parameters is not a conservative approach.

c) The base cases from which the variations and the response surfaces were derived represent points between the expected mean and expected 95 percent probability PCT. This will result in accurate estimates of the effects of uncertainties near the upper tail of the PCT distribution. While this approach leads to increasing inaccuracy in the lower half of the distribution, even wide variations in the results at these points will have little effect on the 95 percent estimate.

SECTION 3
PLANT SIMULATION MODEL

3-1 WCOBRA/TRAC Model for Indian Point Unit 2

Indian Point Unit 2 (IP2) is a four-loop Westinghouse PWR located just north of New York City, and is owned and operated by Consolidated Edison. It is one of the first large PWR's completed, and has been operational for about twenty years. Figure 3-1 is a drawing of the reactor vessel, showing the internals design.

A major portion of a WCOBRA/TRAC analysis involves generating the plant specific vessel and loop model, and the appropriate inputs to that model, to properly describe the plant. The vessel model, in particular, requires detailed information regarding the vessel internals. As-built drawings for the plant are used to define the inputs to the plant specific model.

Vessel Model

Figure 3-2 shows the vessel elevation layout for IP2. The elevations shown at right are relative to the inside bottom of the vessel. This elevation layout contained most of the information needed to divide the vessel into nine vertical sections. Except for the elevation of the boundary between section 1 and section 2, all the other section boundaries were determined from Figure 3-2. Proceeding up the vessel, the bottom of section 1 is the inside vessel bottom. The bottom of section 3 is defined as the beginning of the active fuel. The bottom of section 4 is the top of the active fuel. The bottom of section 5 is the elevation at the top of the upper core plate. The bottom of 7 is equal to the elevation of the bottom of the hot leg inner wall. The bottom of section 8 is the elevation at the bottom of the upper support plate. The bottom of section 9 is the elevation at the top of the upper guide tube in the upper head. The top of section 9 is the inside top of the vessel upper head. The bottom of section 2 is the only section boundary that cannot be determined by viewing Figure 3-3. The bottom of section 2 is defined by an elevation such that the flow area of the curved

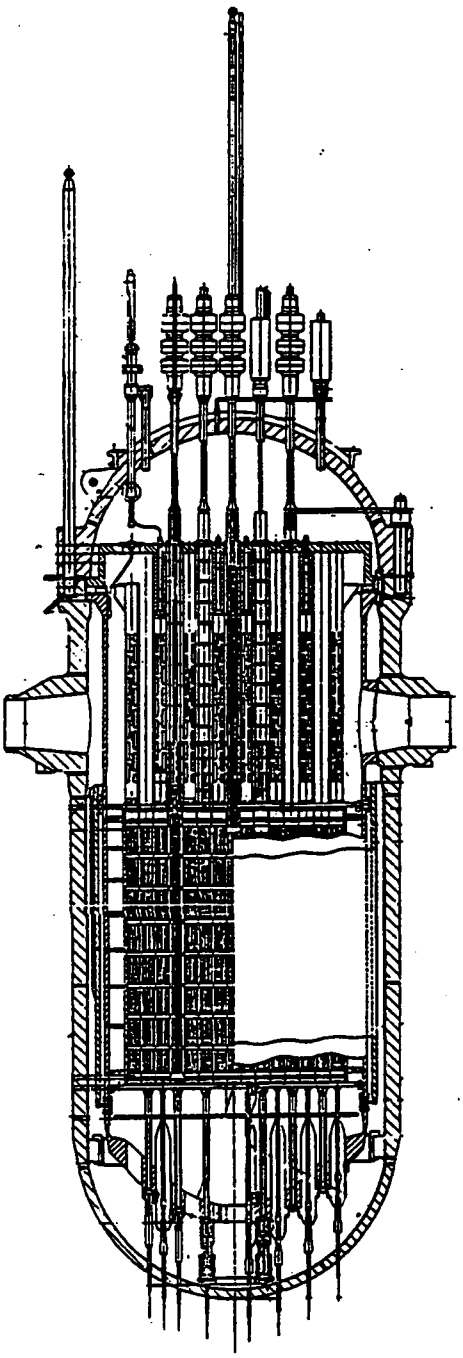

Figure 3-1. IP2 Vessel Profile

lower support plate (or the lower support dome) below this elevation is approximately equal to that above this elevation. Figures 3-3 and 3-4 show the location of the section boundary between sections 1 and 2.

After defining the elevations for each section, a noding scheme was defined following the same basic rules applied to the LOFT model described in the CQD report. These rules include: 1) Cell boundaries at all significant area changes, pressure loss locations, and changes in flow direction. 2) Changes in axial dimension between adjacent cells less than 50 percent. 3) A minimum of two lateral subregions(channels) in each section where multi-dimensional flow is expected. 4) A hot assembly in the core section of the PWR model, as in all large scale integral test simulations.

Figures 3-5, 3-6 and 3-7 illustrate the IP2 vessel noding. Figure 3-5 is a vertical section noding diagram, and Figures 3-6 and 3-7 are horizontal views of each section. In these figures, the values within the squares are the channel numbers, and the values within the circles with arrows attached to them are the horizontal flow gap numbers. A gap is used to define lateral flow path within a section between channels. Positive flow is in the direction indicated by the arrow. WCOBRA/TRAC assumes a vertical flow path for vertically stacked channels, unless specified otherwise in the input. Upward axial flow is considered as positive flow. As can be seen in Figures 3-5, 3-6 and 3-7, 61 channels and 66 gaps are used in the IP2 model to define the vessel. Figure 3-5 also illustrates that several of the nine sections were sub-divided into two or more levels. For example, the active fuel region, section 3, is divided into 16 vertical levels. By accounting for the vertical sub-division within sections 2, 3, 5 and 7, the vessel model for IP2 has a total of 221 fluid cells.

Vessel section 1 models the vertical section of the vessel from the inside bottom of the vessel to an elevation which splits equally (approximately) the through-flow area of the curved lower support dome above and below this elevation. This section contains five channels (designed 1 through 5) and eight horizontal flow gaps (numbered 1 through 8) to model this portion of the vessel. Channels 1 to 4 represent the annulus volume continued downward from the downcomer, and channel 5 models the center portion of this section underneath the curved dome. Gaps 1 to 4 are the lateral connections between the four peripheral channels, and gaps 5 to 8 are the radial connections between the peripheral channels and channel 5.

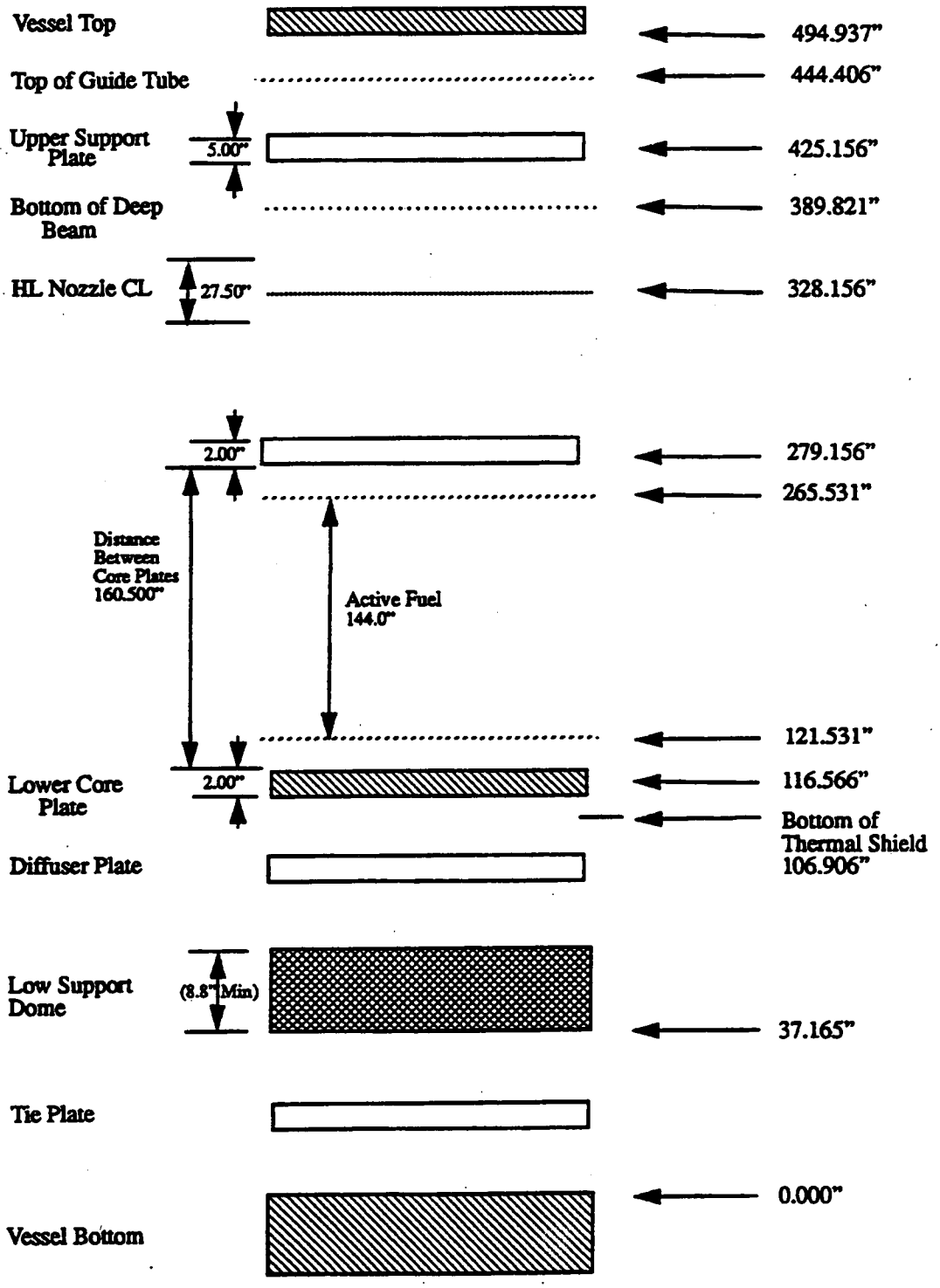

Figure 3-2. Vessel Component Elevations

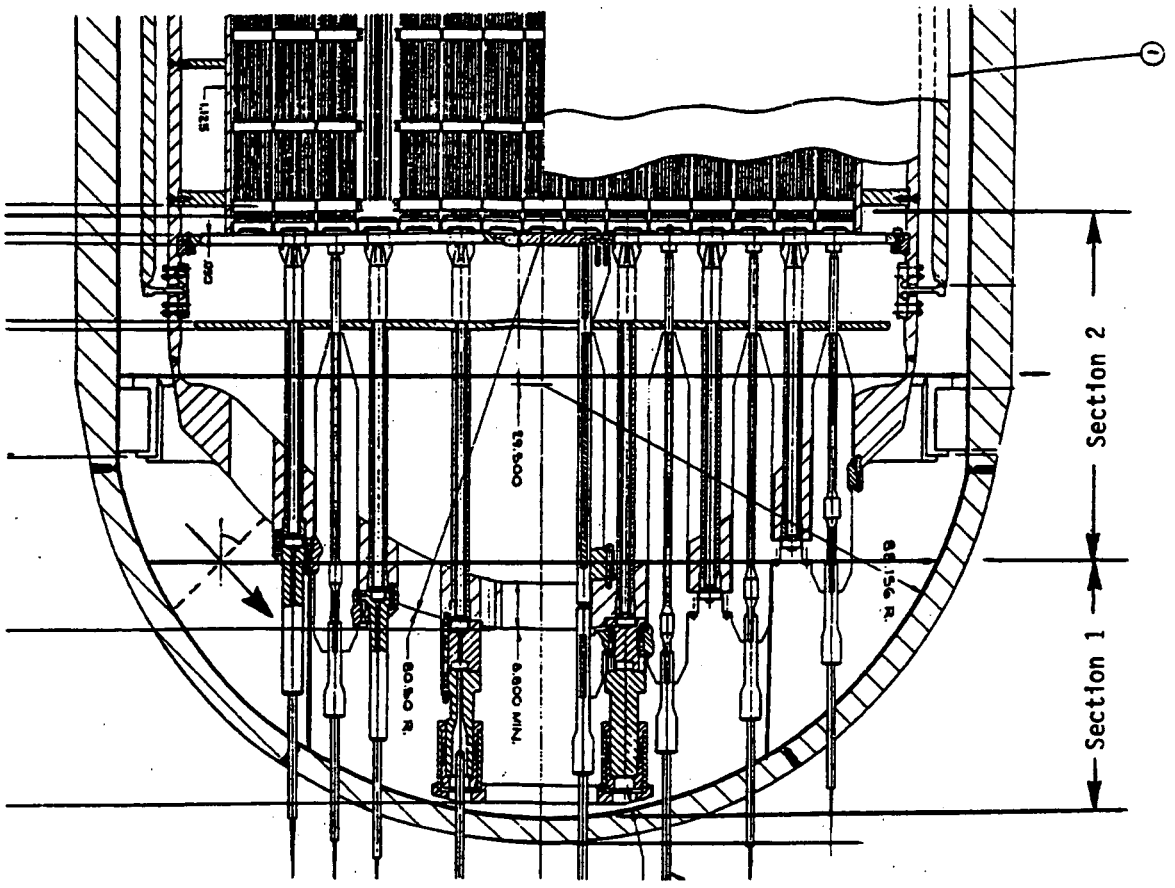

Figure 3-3. Front View of Sections 1 and 2

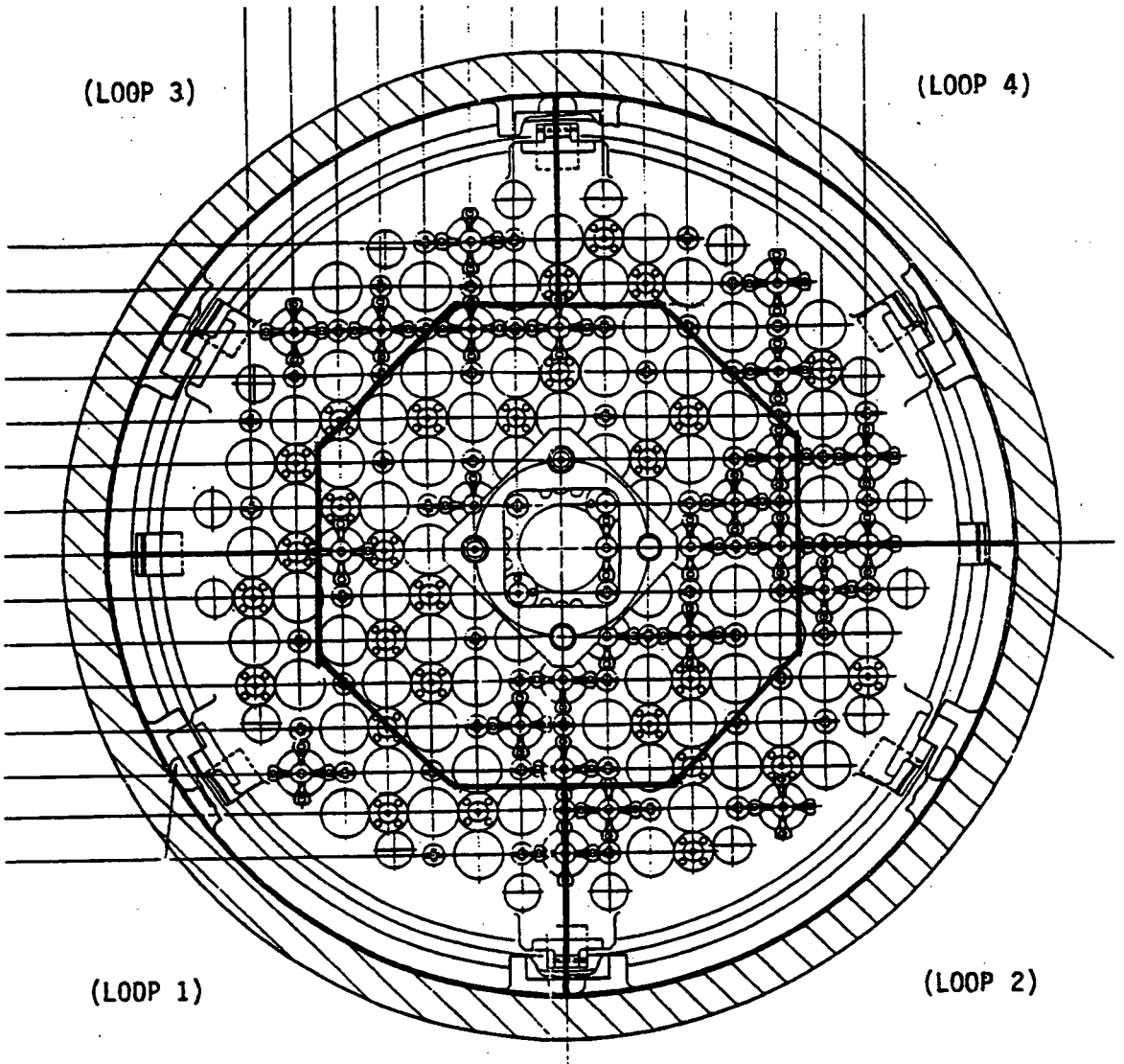

Figure 3-4. Top View of Lower Support Dome and Channel Divisions in Section 1

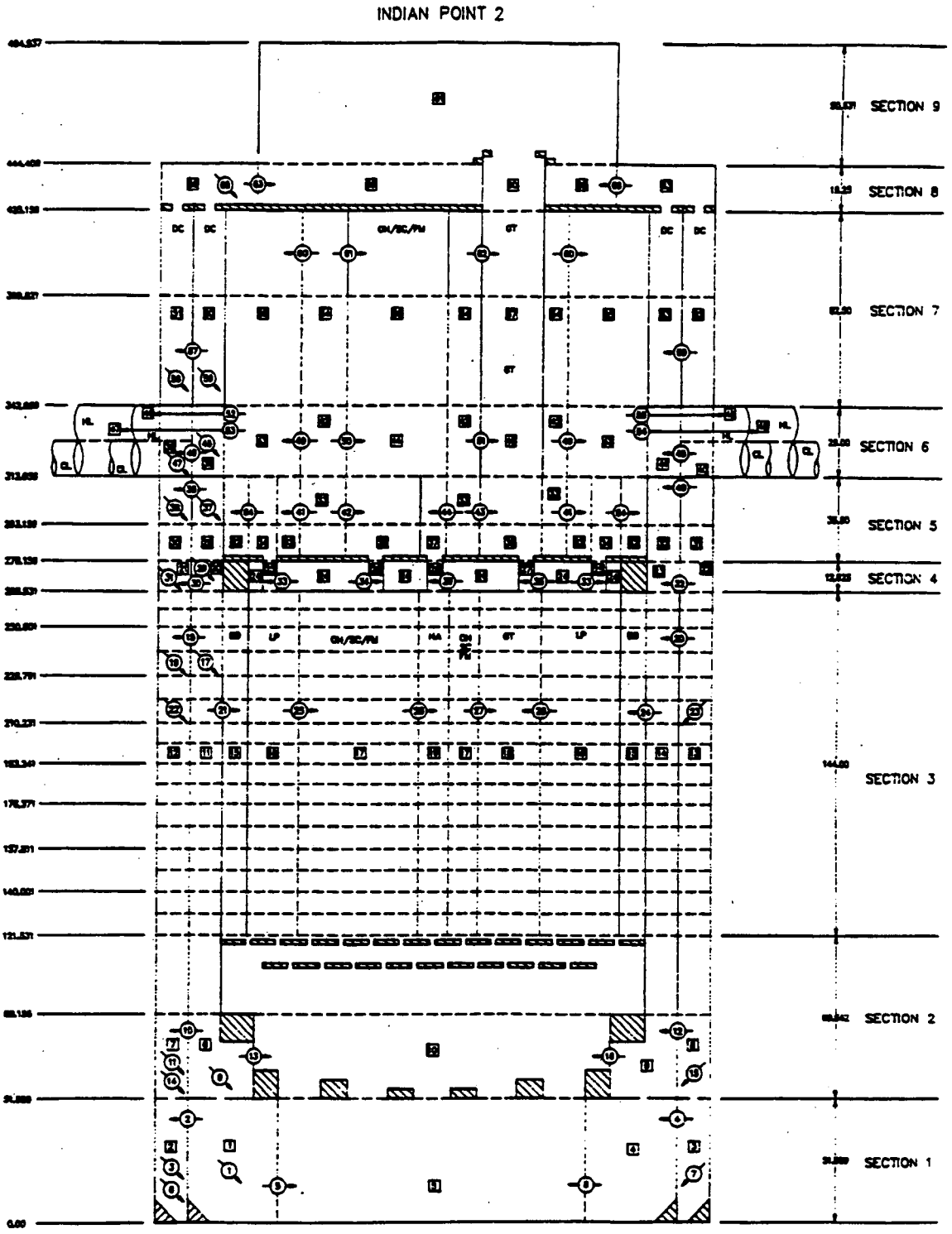

Figure 3-5. IP2 Vessel Noding (Vertical View)

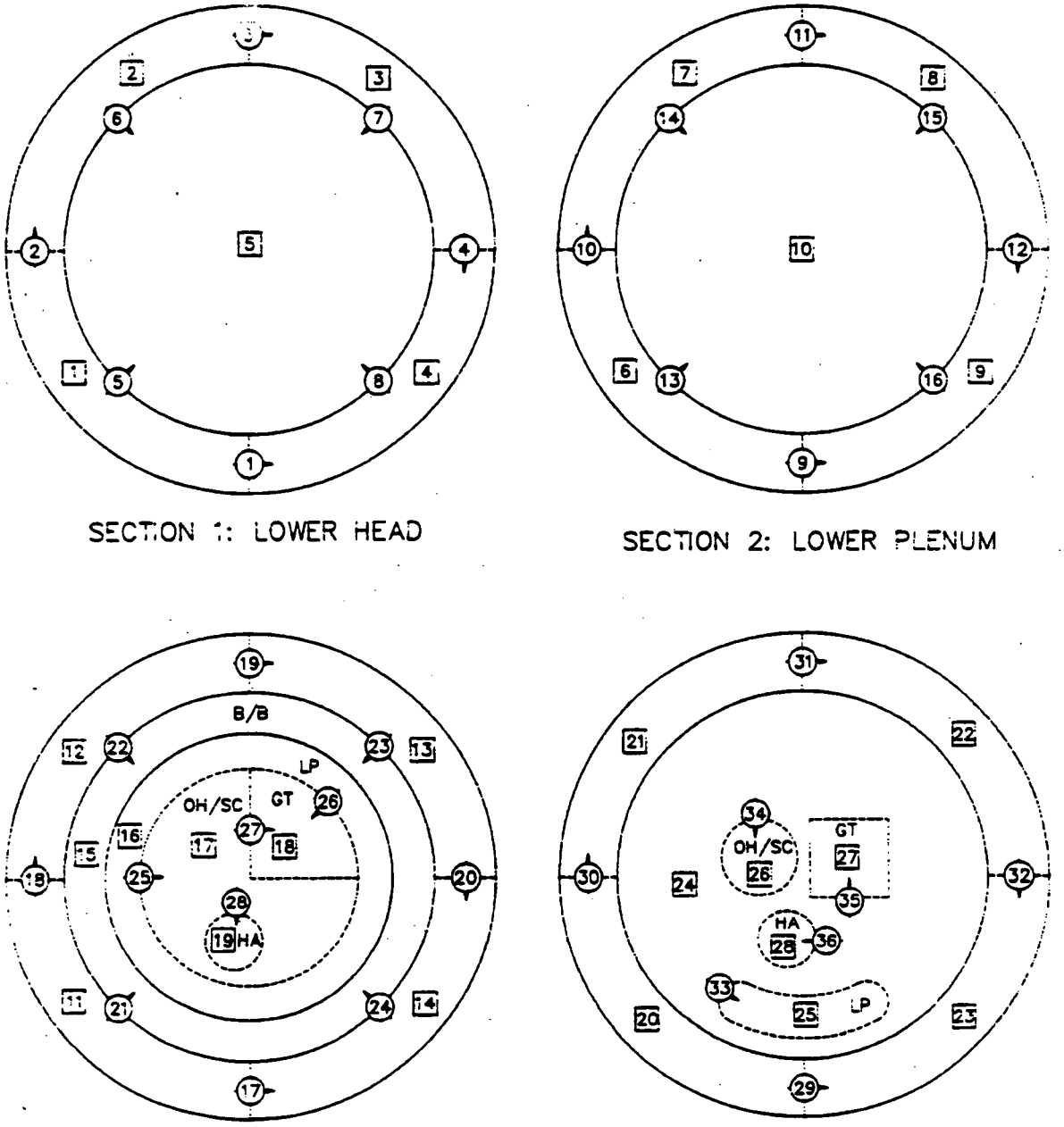

Figure 3-6. IP2 Noding (Horizontal View)

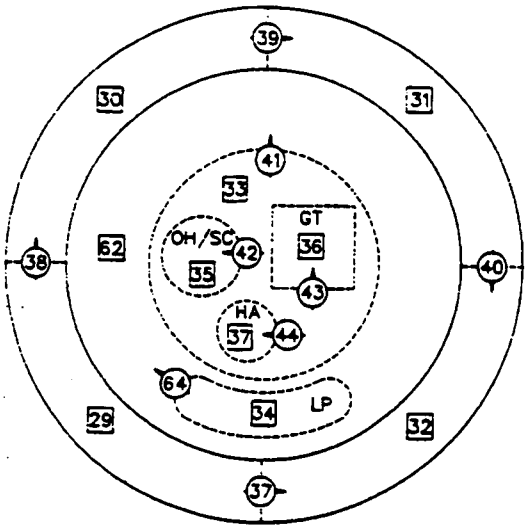

SECTION 5: UPPER PLENUM BELOW NOZZLES

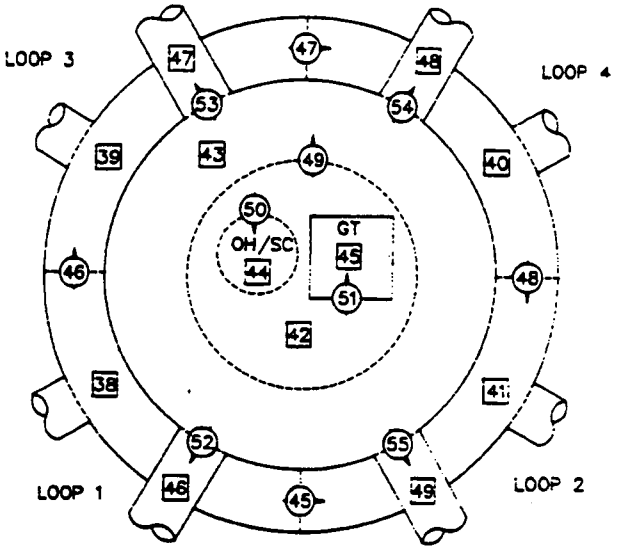

SECTION 6: NOZZLE REGION

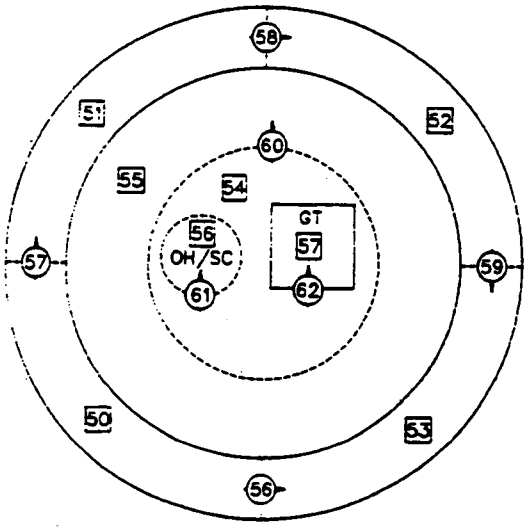

SECTION 7: UPPER PLENUM ABOVE NOZZLES

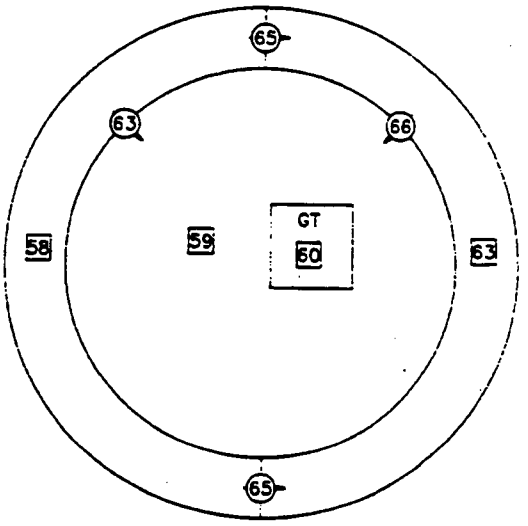

SECTION 8: UPPER HEAD UP TO THE TOP OF GUIDE TUBES

Figure 3-7. Section Views

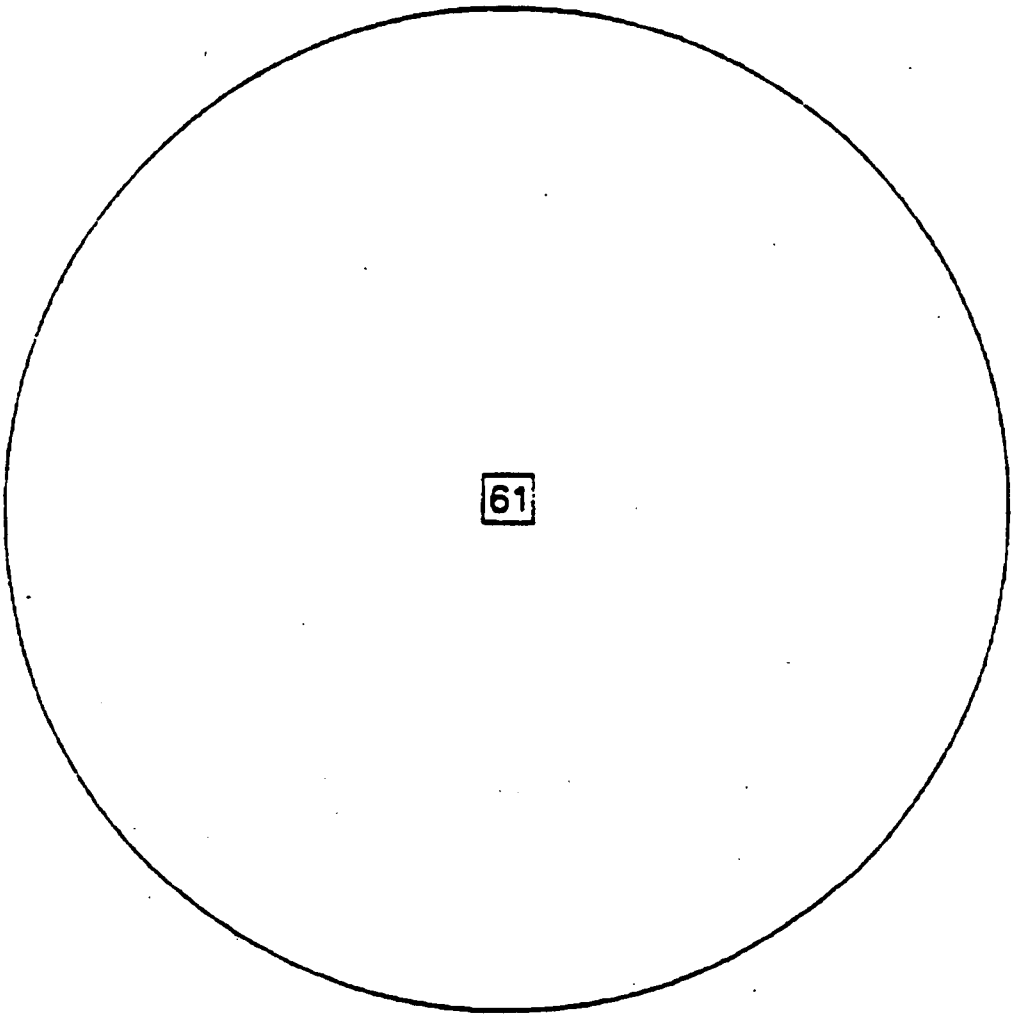

SECTION 9: UPPER HEAD ABOVE THE GUIDE TUBES

Figure 3-7. (Cont'd) Section Views

Positive flow is in the arrow direction indicated in the figure. While channel 1 is in the vessel quadrant that connects to Loop 1 (the assumed broken loop), channels 2, 3, and 4 are in the quadrants that connect Loops 3, 4 and 2, respectively.

Vessel section 2 models the vertical section of the vessel from the top of section 1 to the bottom of the active fuel region. This section contains two vertical sub-levels. The intermediate level interface is set at the top edge of the lower support dome which is at about the same elevation of the top surface of the radial keys. This section contains five channels (designated 6 through 9) and eight lateral horizontal flow gaps (numbered 9 to 16). Channels 6 to 9 model the annulus volume outside the curved dome, channel 10 models the volume inside the dome; the top cell of channel 10 contains the flow distribution plate, lower core plate, bottom fuel nozzle, non-active portion of the fuel rods, etc. The through-flow area in the lower core plate was used as the momentum area at the top of channel 10. Gaps 9 to 12 model the lateral connections between the peripheral channels (channels 6 through 9) in the extended downcomer region, and gaps 13 to 16 models the horizontal radial connections between the peripheral channels and channel 10. Because this section has two sub-levels, each channel has 2 cells and each gap has 2 levels. The upper level of the radial gaps, however, are blocked since there is no flow across the core barrel extension (sometimes referred to as the flow skirt). The lower level of the radial gaps models the flow across the lower support dome in this section. Area variation inputs are used to vary the axial and gap flow areas in this section to account for the area changes due to the curved walls and other structure blockages.

Vessel section 3 models the vertical section of the vessel from the bottom to the top of the active fuel region. The modeling is accomplished using 16 vertical cells in nine channels (designated 11 through 19), and twelve horizontal flow gaps (17 through 28). Channels 11 to 14 represent the downcomer annulus volume between the vessel inner wall and the core barrel outer wall. Channel 15 is the annulus volume between the barrel inner wall and the baffle plates (barrel/baffle region), and is designated as the B/B channel. Channels 16 through 19, combined, represent the total volume within the baffle plates (minus the thimble bypass volume), i.e., the entire core active fuel region. Channel 16 includes assemblies on the periphery of the core which have relative low power. For IP2, 44 assemblies are in channel 16, which is designated as the LP (low power) channel. In order to determine the

breakdown of the remaining 149 assemblies, in particular, the designation for the hot assembly, the upper plenum (vessel section 5) structure layout was examined. Figure 20-2-8 shows that four types of internals existed in the upper plenum: guide tubes, orifice holes, support columns, and free standing mixers. Among the four types of structures, the free-standing mixer is expected to be the most flow limiting during the blowdown transient. The free standing mixer is a vertical solid-wall tube with the top standing at an elevation 13 inches above the top surface of the upper core plate. Only axial flow can enter or exit the tube at its top end, there is no lateral flow passage through the tube wall within this 13-inch distance. During blowdown, when the liquid level in the upper plenum drops below 13 inches, less cooling flow from the upper plenum may enter the fuel assemblies beneath the free-standing mixers. On the other hand, there is no such flow restriction for the orifice hole or the guide tube in this elevation range to limit the downward cooling flow because the lateral flow paths are wide open. During reflood de-entrained liquid collected on the core plate will flow preferentially through the open holes. Although the support column has also a solid tube wall up to nearly 13 inches above the upper core plate, its axial flow area and the equivalent hydraulic diameter of the support column, are larger than those of the free-standing mixer. Consequently the free-standing mixer is considered to be the most flow limiting internal, and one of the fuel assemblies underneath one of the free-standing mixers is to be designated as the hot assembly channel (HA channel), channel 19. All assemblies under the guide tube internals are modeled in channel 18. The remaining assemblies under the support columns, open holes, and the rest of the free-standing mixers are modeled in channel 17. Channels 17 and 18 are designated as the SC/OH/FM channel (under support column/open hole/free-standing mixer of section 5) and the GT channel (under the guide tubes of section 5), respectively. As indicated by Figure 3-9, the lateral flow path of the guide tubes just above the free-standing mixer's axial flow entrance (top cell of section 5) are wide open, while that of the support columns are limited by the slot opening. For this reason, flow mixers that are adjacent to support columns, such as those located in E5, E11, G9, J17, L5 or L11 (Figure 3-8) are judged to be more flow limiting than those adjacent to guide tubes. Consequently one of the assemblies under these locations is considered to be the hot assembly. The grids are modeled within this length range at their specified elevations. The axial form loss coefficients, however, are modeled at the momentum cell centers that are closest to the grids. The axial loss coefficient in the hot assembly includes additional flow resistance from intermediate flow mixers to conservatively account for transitions to this type

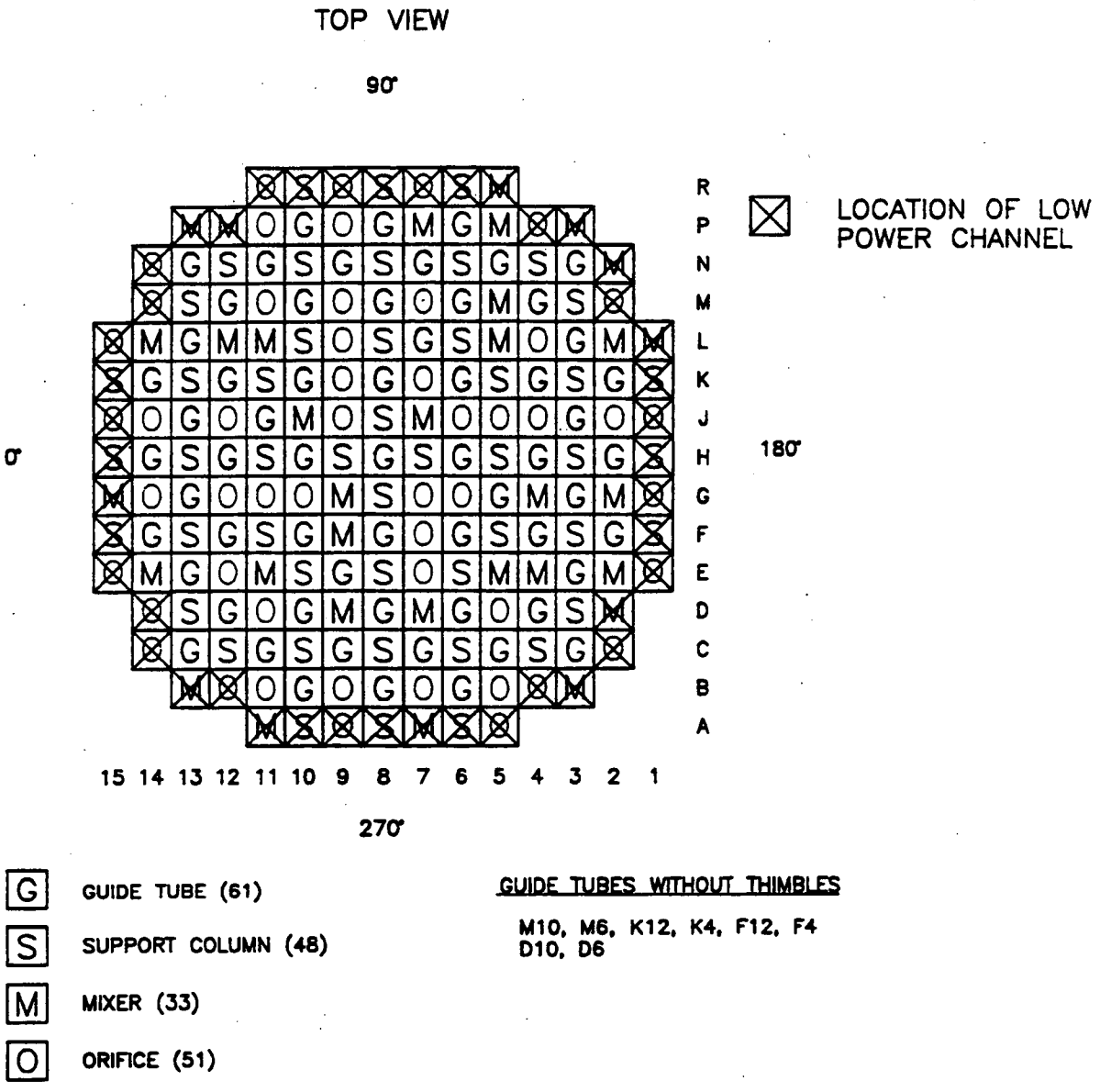

Figure 3-8. Upper Plenum Internal Distribution

of fuel in the future. The momentum area at the bottom of channels 15 through 19 uses the through-flow area of the lower core plate, the sum of them is equal to the momentum area at the top of channel 10 of section 2.

Section 4 models the vertical section of the vessel from the top of the active fuel to the bottom of the upper core plate. This section has one vertical cell and uses nine channels (designated 20 through 28) and eight horizontal gaps (29 to 36) to model this portion of the vessel. Channels 20 to 23 each represents one-quarter of the downcomer annulus volume between the vessel inner wall and the core barrel. Channels 24 to 28 model the vessel volume inside the baffle which is referred to as the countercurrent flow limit (CCFL) region. Channels 25 to 28 represent the jet flow coming out of the core channels 16 to 19, respectively, and channel 24 (the global channel) models the fluid volume of this region which does not have any axial flow connection. This region is so named because during a LOCA the liquid from the upper plenum attempts to penetrate through upward flowing vapor and is limited by the interfacial shear which exists at the minimum flow area in this region.

Section 5 extends vertically from the elevation of the bottom of the upper core plate to the elevation of the bottom of the hot leg. This section contains two vertical cells for ten channels (designated 29 through 37, and 62) and nine horizontal flow gaps (37 through 44, and 64). Channels 29 to 32 are the downcomer channels each representing one-fourth the downcomer annulus volume between the vessel wall and the barrel outer wall. Channels 34, 36, and 37 model the regions above the LP, SC/OH/FM, GT, and HA fuel channels, respectively. Channel 33 is the inner global channel representing the fluid volume outside of the cylindrical volumes above the fuel assemblies in the SC/OH/FM, GT, and HA channels. Channel 62 is the outer global channel representing the rest of the volume in the upper plenum which is not included in the inner global channel.

Section 6 models the vertical section of the vessel from the bottom to the top of the hot leg (inner diameter). This section uses one vertical cell in twelve channels (designated 38 through 49) and eleven horizontal flow gaps (45 to 55) to model this section. Figures 3-5 and 3-6 provide an illustration for the vertical and radial representation of this section of the vessel model. Channels 38 to 41 each represents one-fourth of the downcomer annulus

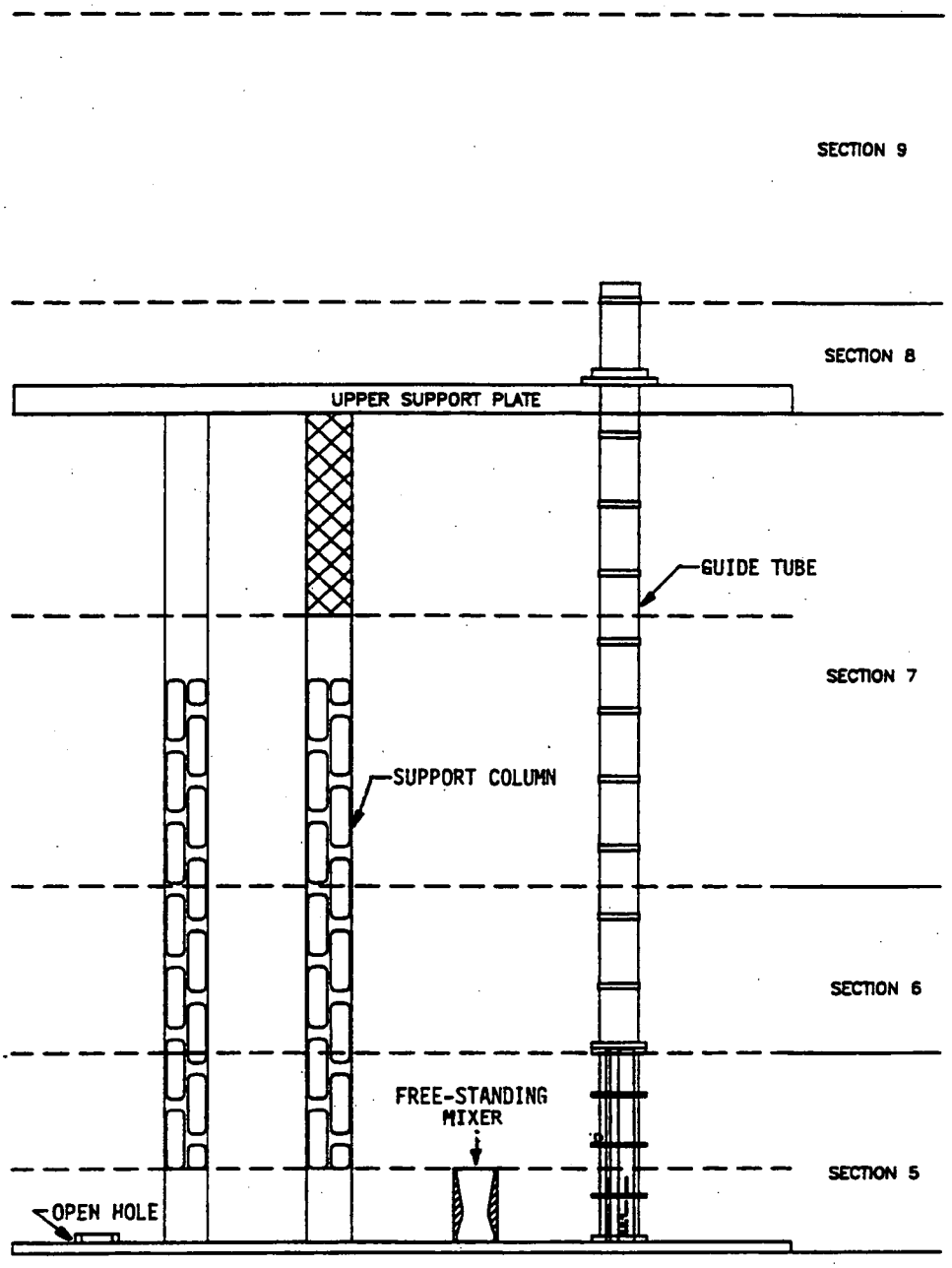

Figure 3-9. Vertical View of Open Hole, Support Column, Free-Standing Mixer, and Guide Tube in Upper Plenum

volume between the vessel inner wall and the core barrel outer wall, excluding the hot leg which passes through this region. Channel 42, the inner global channel in this section, includes the volume above the single hot assembly combined with the volume above the inner global channel in the section below. Channels 44 and 45 model the fluid volumes inside the support columns and the guide tubes in this section, respectively. Channel 43, the outer global channel, models the rest of the fluid volume in the section. Channels 46 to 49 each represents the volume of the hot leg within the vessel. Gaps 52 to 55 model the lateral flow connections between the upper plenum and the hot legs.

Section 7 extends vertically from the top of the hot leg to the bottom of the upper support plate, yielding an overall height of 82.50 inches for this section. This section is divided into two levels with the lower level cell from the bottom of the hot legs to the bottom of the deep beam. This section contains two cells for eight channels (designated 50 through 57) and seven horizontal flow gaps (56 to 62). Channels 50 through 53 each represents one-quarter the downcomer volume annulus volume between the vessel inner wall and the core barrel outer wall, and are connected to the upper plenum through the spray nozzle holes. Channel 54 is the inner global region and is a vertical extension of channel 42. Channel 55 is the outer global region and is a vertical extension of channel 43. Similarly, channels 57 and 58 are the vertical extensions of channels 44 and 45, respectively, in the section below. There is no vertical flow connection at the top of channels 54, 55, and 56 between the upper plenum and the upper head. Channel 57 connects vertically to the upper head through the guide extension.

Section 8 extends vertically from the bottom of the upper support plate to the upper guide tube's top plate (elevation 444.406 inches), yielding an overall height of 19.25 inches. This section has one vertical cell for four channels (designated 58 through 60, and 63) and three horizontal flow gaps (63, 65, and 66). Channels 58 and 60 model the peripheral region. Channel 58 is connected to the downcomer channels 50 and 51, and channel 60 is connected to the downcomer channels 52 and 53 in section 7. Channel 60 models the volume inside the guide tube, and channel 59 models the rest of the volume in the upper head in this section. The boundary between this channel and the peripheral channels is defined by an imaginary cylindrical surface which intersects the upper head's vessel wall at an elevation of 444.406 inches.

Vessel section 9 models the vertical section of vessel extending from the top plate of the upper guide tube to the inside top of the vessel head, yielding an overall height of 50.531 inches for section 9. This section is modeled by one channel (designated 61). There is no horizontal flow gap in this section. The flow area at the bottom of channel 61 is equal to the sum of the flow area at the top of channels 59 and 60 from section 8.

Tables 3-1 and 3-2 give the channel noding and gap connection summary for the IP2 vessel model.

Core Model

The WCOBRA/TRAC code allows for modeling of heated and unheated conductor geometries. Unheated conductors are used to model metal mass in the reactor vessel such as the lower core plate. These conductors are connected to appropriate vessel channels. For heated conductors, the code allows for detailed radial and axial noding, and for the nuclear rod, other fuel related inputs (rod internal pressure, fuel rod molar fractions, clad thickness, fuel theoretical density, etc.) can be specified. For the 15X15 fuel, each fuel bundle contains 204 fuel rods and 21 thimble tubes. Five fuel assembly groups are modeled in the IP2 vessel model: 1) the hot rod, 2) the hot assembly (channel 19 under a free-standing mixer), 3) the interior assemblies under support columns/open holes and the balance of the free-standing mixers (channel 17), 4) the interior assemblies under all the guide tubes (channel 18), and 5) the periphery low power assemblies (channel 16). Rod 1 represents a single fuel rod, known as the hot rod and is located in the hot assembly. Rod 2 represents the remaining fuel rods in the hot assembly and has a power equivalent to the hot assembly average fuel rods. Rod 3 represents the fuel assemblies contained in the guide tube channel. Rod 4 represents the fuel assemblies contained in the support column/open hole/free-standing mixer channel. Rod 5 represents the assemblies contained in the periphery low power channel.

The nuclear fuel rods were initialized with internal gas properties, radial power profiles and fuel average temperatures from the PAD code (Weiner, 1988).

Each fuel rod is also assigned an axial power profile. The profile used for the scoping studies is illustrated in Figure 3-10.

Table 3-1
Channel Descriptions for WCOBRA/TRAC IP2 Vessel Model

Section	Channel	Description	Connections to Channels	
			Above	Below
1	1	Lower Plenum - Broken Quarter	6	--
	2	Lower Plenum - Intact Quarter	7	--
	3	Lower Plenum - Intact Quarter	8	--
	4	Lower Plenum - Intact Quarter	9	--
	5	Lower Plenum - Center Portion	10	--
2	6	Lower Plenum - Broken Quarter	11	6
	7	Lower Plenum - Intact Quarter	12	7
	8	Lower Plenum - Intact Quarter	13	8
	9	Lower Plenum - Intact Quarter	14	9
	10	Lower Plenum - Core Inlet	15,16,17,18,19	5
3	11	Downcomer - Broken Quarter	20	6
	12	Downcomer - Intact Quarter	21	7
	13	Downcomer - Intact Quarter	22	8
	14	Downcomer - Intact Quarter	23	9
	15	Barrel-Baffle region	--	10
	16	Low Power/Periphery Assemblies	25	10
	17	Assemblies Below Support Columns/Open Holes/Free-Standing Mixers	26	10
	18	Assemblies Below Guide Tubes	27	10
	19	Hot Assembly Under Free-Standing Mixer	28	10

Table 3-1 (Cont'd)
Channel Descriptions for WCOBRA/TRAC IP2 Vessel Model

Section	Channel	Description	Connections to Channels	
			Above	Below
4	20	Downcomer - Broken Quarter	29	11
	21	Downcomer - Intact Quarter	30	12
	22	Downcomer - Intact Quarter	31	13
	23	Downcomer - Intact Quarter	32	14
	24	Global Volume Below UCP, Not Within Fuel Region	--	--
	25	CCFL Region Above Low Power/Periphery Assemblies	34	16
	26	CCFL Region Below Support Columns/Open Holes/Free-Standing Mixers	35	17
	27	CCFL Region Below Guide Tubes	36	18
	28	CCFL Region Below A Free-Standing Mixer and Above Hot Assembly	37	19
5	29	Downcomer - Broken Quarter	38	20
	30	Downcomer - Intact Quarter	39	21
	31	Downcomer - Intact Quarter	40	22
	32	Downcomer - Intact Quarter	41	23
	33	Inner Global Region Above UCP	43	--
	34	Upper Plenum Support Columns/Open Holes/Free-Standing Mixers in Outer Ring Above Low Power Assemblies	43	25
	35	Upper Plenum Support Columns/Open Holes/Free-Standing Mixers	44	26
	36	Upper Plenum Guide Tubes	45	27
	37	Upper Plenum Free-Standing Mixer Above the Hot Assembly	44	28
	62	Outer Global Region Above UCP	43	--

Table 3-1 (Cont'd)
Channel Descriptions for WCOBRA/TRAC IP2 Vessel Model

Section	Channel	Description	Connections to Channels	
			Above	Below
6	38	Downcomer - Broken Quarter	50	29
	39	Downcomer - Intact Quarter	51	30
	40	Downcomer - Intact Quarter	52	31
	41	Downcomer - Intact Quarter	53	32
	42	Upper Plenum Inner Global Region	54	42
	43	Upper Plenum Outer Global Region	55	43
	44	Upper Plenum Support Columns/Open Holes/Free-Standing Mixers	56	35
	45	Upper Plenum Guide Tubes	57	36
	46	Hot Leg Inlet - Broken Quarter	--	--
	47	Hot Leg Inlet - Intact Quarter	--	--
	48	Hot Leg Inlet - Intact Quarter	--	--
	49	Hot Leg Inlet - Intact Quarter	--	--
7	50	Downcomer - Broken Quarter	58	38
	51	Downcomer - Intact Quarter	58	39
	52	Downcomer - Intact Quarter	63	40
	53	Downcomer - Intact Quarter	63	41
	54	Upper Plenum Inner Global Region	--	42
	55	Upper Plenum Outer Global Region	--	43
	56	Upper Plenum Support Columns/Open Holes/Free-Standing Mixers	--	44
	57	Upper Plenum Guide Tubes	60	45

Table 3-1 (Cont'd)
Channel Descriptions for WCOBRA/TRAC IP2 Vessel Model

Section	Channel	Description	Connections to Channels	
			Above	Below
8	58	Lower Upper Head Outer Region Above Spray Nozzles - Broken/Intact Quarter Side	--	50,51
	63	Lower Upper Head Outer Region Above Spray Nozzles - Intact/Intact Quarter Side	--	52,53
	59	Lower Upper Head Inner Region	61	--
	60	Upper Guide Tube	61	57
9	61	Upper Head Top Region	--	59,60

Table 3-2
Gap Connections for WCOBRA/TRAC IP2 Vessel Model

Section	Gap	From Channel	To Channel
1	1	1	4
	2	1	2
	3	2	3
	4	3	4
	5	1	5
	6	2	5
	7	3	5
	8	4	5
2	9	6	9
	10	6	7
	11	7	8
	12	8	9
	13	6	10
	14	7	10
	15	8	10
	16	9	10
3	17	11	14
	18	11	12
	19	12	13
	20	13	14
	21	11	15
	22	12	15
	23	13	15
	24	14	15
	25	16	17
	26	16	18
	27	17	18
	28	17	19
4	29	20	23
	30	20	21
	31	21	22
	32	22	23
	33	24	25
	34	24	26
	35	24	27
	36	24	28

Table 3-2 (Cont'd)
Gap Connections for WCOBRA/TRAC IP2 Vessel Model

Section	Gap	From Channel	To Channel
5	37	29	32
	38	29	30
	39	30	31
	40	31	32
	41	33	62
	42	33	35
	43	33	36
	44	33	37
	64	34	62
6	45	38	41
	46	38	39
	47	39	40
	48	40	41
	49	42	43
	50	42	44
	51	42	51
	52	43	46
	43	43	67
	54	43	68
	55	43	49
7	56	50	53
	57	50	51
	58	51	52
	59	52	53
	60	54	55
	61	54	56
	62	54	57
8	63	58	59
	65	58	63
	66	63	59

Loop Model

As with the vessel inputs, each component in the one-dimensional loop can have various cells to allow for changes in geometry to be modeled along the component. In the input structure each component was identified by a module title, a unique component number, and connections to numbered junctions between components. In addition, a descriptive text title can be used to uniquely identify each components. The four loops for IP2 were defined using 53 components and 57 junctions. A total of 56 one-dimensional components and 63 junctions were employed in the loop model. The interface junction numbers between one-dimensional component and the vessel were defined in the vessel input. Figure 3-11 presents the IP2 WCOBRA/TRAC loop noding diagram, with component numbers indicated by rectangular boxes and junctions by circular boxes.

As seen in Figure 3-11, component 41 was the intact loop (Loop 4, which is opposite to Loop 1, the assumed broken loop) hot leg and was modeled as a TEE module. Component 54, the pressurizer (PRIZER module), was connected to the secondary branch of the hot leg TEE. Component 42 was the steam generator of this loop (STGEN module). Component 45 was the crossover leg of this intact loop and was modeled using a PIPE module. Component 46 was the reactor coolant pump (PUMP) module. Component 47 was the loop-side cold leg modeled by a TEE with its secondary branch connecting the accumulator/safety injection (SI) components. Component 48 was the vessel-side cold leg. Component 92 was the accumulator line SI TEE. Component 94 was the accumulator line check valve (VALVE module). Component 93 was the SI fill (FILL module) and component 95 was the accumulator (ACCUM module) of this loop. This sampling allows one to infer the remainder of the modeling.

Components 55, 56 and 57 modeled the thimble bypass flow of the low power assemblies, the support column/open hole/free-standing mixer assemblies and the guide tube assemblies, respectively, using the PIPE module. This bypass flow, while small, must be modeled to accurately predict steady-state fluid temperatures:

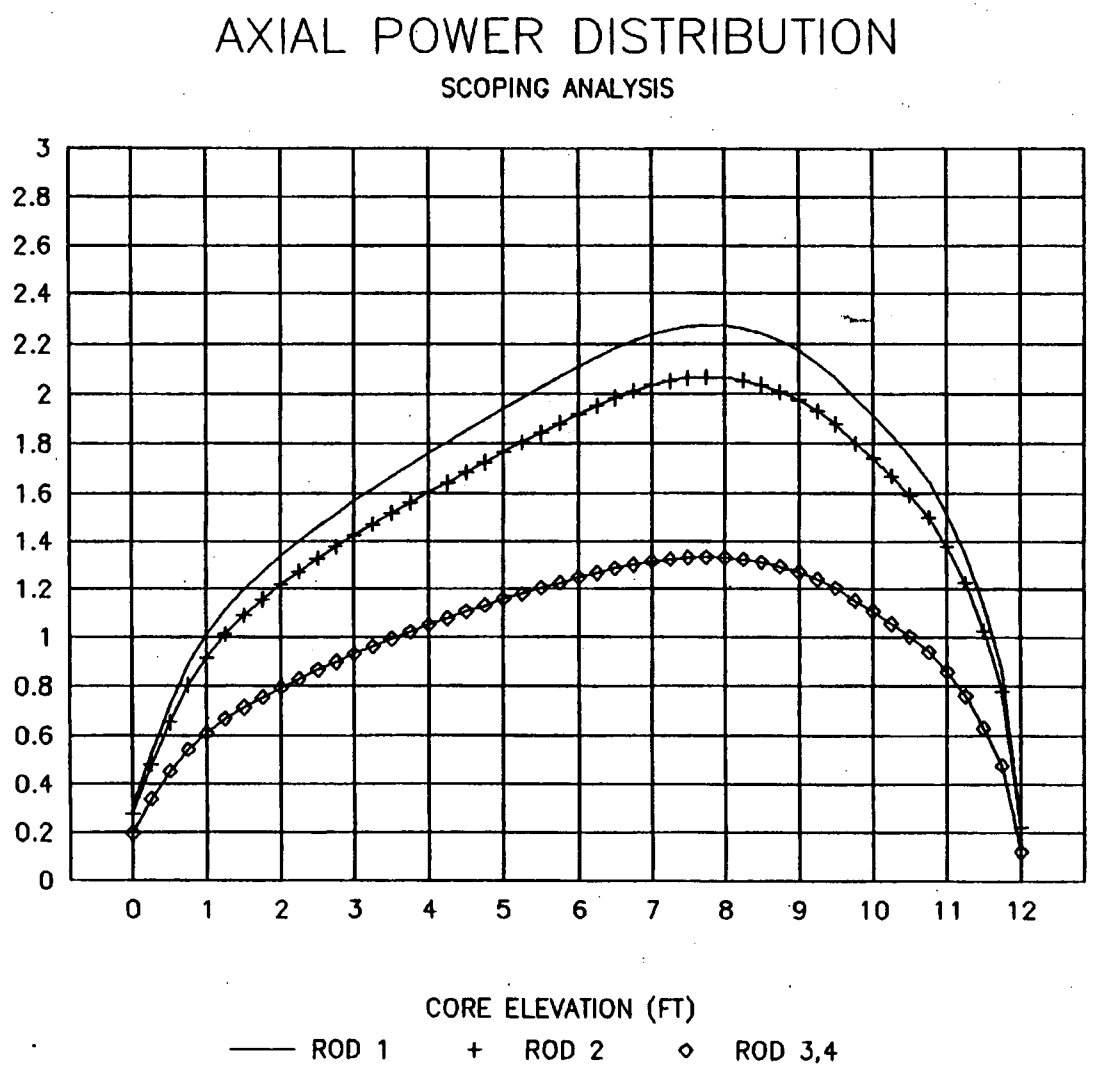

Figure 3-10. Axial Power Distribution Used in Scoping Analysis

Emergency Core Cooling (ECC) and Safety Injection (SI) Model

The Safety Injection System (SIS) for IP2 consists of four accumulator tanks, three high head safety injection pumps (HHSI) and two low head safety injection pumps (LHSI). All pumps are connected to injection lines which emerge into either the accumulator injection lines connected to the cold legs or the cold legs. The former arrangement was modeled for all four loops, as can be seen in Figure 3-11. This arrangement is judged to be more conservative, because SI injection is reduced while accumulators are injecting, due to the large pressure drop through the line. It was assumed that one of the three HHSI pumps would fail and the other two remained in operation. For the LHSI it was assumed that one of the two pumps failed (single failure) and one remained in operation. While the failure of one LHSI and one HHSI pump is more conservative than required, it simplifies the analysis for the following reason. The limiting single failure must take into account the effect on containment pressure. Failure of an entire safety train would result in the loss of one or several containment spray and fan cooling units, reducing containment cooling, and increasing containment pressure, which is expected to reduce PCT. Failure of one LHSI maintains all containment cooling systems to minimize pressure. On the other hand, this failure results in slightly greater SI flow, also expected to be a benefit. Assuming loss of one HHSI and one LHSI bounds both situations. Minimum injection flows were assumed. To provide for future plant margin, only 85 percent of the resulting HHSI flow and 90 percent of the resulting LHSI flow were counted for as the available safety injection flow which was equally distributed among the three intact loops.

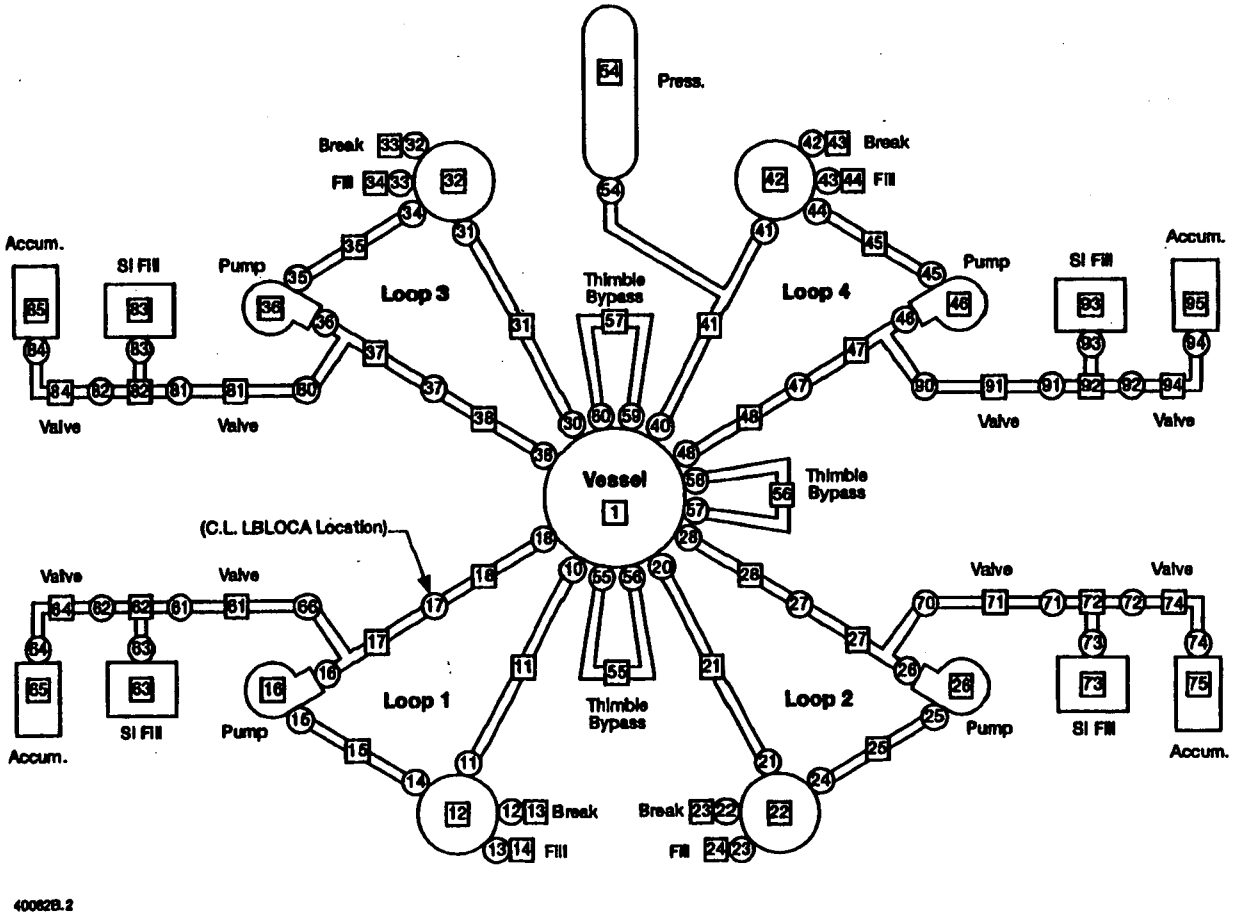

Figure 3-11. IP2 WCOBRA/TRAC Model Vessel/Loop Layout (Steady-State)

SECTION 4
BASE CASE LOCA PARAMETERS

An important part of the best estimate methodology is the identification and ranking of processes and initial conditions which affect the PCT. As a result of the evaluation performed in the Code Qualification Document (CQD), a list of key LOCA parameters was developed. These parameters are described below. The values for the parameters are such that they represent a more likely initial condition for the plant than was typically assumed in prior analyses. However, in some cases the assumption is still a conservative one. The general rule applied was to use limiting assumptions in cases where the parameter effect was small, or where the parameter was difficult to quantify statistically. The assumed values for the parameters described below are those used in the base case, which defines the value of PCT_j^B in Equation (2-1).

1.0 Plant Physical Description

1.0a Dimensions: Nominal geometry is assumed. Nominal geometry input is accounted for in the code uncertainty, since experiments were also subject to thermal expansion and dimensional uncertainty effects. The effect of seismic and LOCA forces on core coolability is included in the PCT uncertainty evaluation, if necessary, as described in Section 7.

1.0b Flow Resistance: Best estimate values of loop flow resistance are assumed. Variations in this parameter are accounted for in the break flow uncertainty as described in Section 5.

1.0c Pressurizer Location: The loop opposite of (two- and four- loop plants) or adjacent to (three-loop plants) the pressurizer will be assumed for the broken loop. This places the pressurizer on an intact loop, which is the more likely location, and was confirmed to also be the limiting location, or to have a small effect on the results.

1.0d Hot Assembly Location: The location assumed for the hot assembly is that which reduces the direct flow of water from the upper head or upper plenum. This location is described in detail in Section 3.

1.0e Hot Assembly Type: The hot assembly is a fresh reload assembly, since it exhibits the highest linear heat rates and stored energy, which have been confirmed to result in the highest PCT.

1.0f Steam Generator Tube Plugging Level: The highest average tube plugging likely to be present during the next several cycles is assumed. This is the limiting condition, based on the scoping studies.

2.0 Plant Initial Operating Conditions

2.1 Reactor Power

2.1a Initial Core Average Linear Heat Rate: Maximum licensed power without measurement uncertainties is assumed. Uncertainties are accounted for as part of the power distribution uncertainty.

2.1b Rod Peak Linear Heat Rate: The hot rod peak linear heat rate is assumed to be a value mid-point between the expected baseload value and the Technical Specification value. The reason for this choice is described in CQD Volume V, Section 26. The value of F_Q assumed in the base case is therefore higher than the value likely to be measured during normal scheduled surveillance early in the fuel cycle. The basis for the hot rod bias and the treatment of uncertainties were discussed in Section 21 of CQD Volume IV and are further discussed in Section 26.

2.1c Hot Rod Average Linear Heat Rate: The highest expected value during normal operation throughout the cycle is assumed, not including calculational uncertainties. The value of $F_{\Delta H}$ assumed in the base case is therefore higher than the value likely to be measured during most of the

fuel cycle. Variations in this parameter are included in the overall uncertainty as described in CQD Section 26.

2.1d Hot Assembly Average Linear Heat Rate: The power generated in the hot assembly rod is several percent lower than that generated in the hot rod. Calculational uncertainties associated with the hot assembly power and with its redistribution are included in the power distribution uncertainty.

2.1e Hot Assembly Peak Linear Heat Rate: Consistent with the average linear heat rates, the peaking factor used to calculate the peak nuclear energy generated in the hot assembly average rod is several percent lower than the value assumed in the hot rod. Uncertainties are included in the power distribution uncertainty.

2.1f Axial Power Distribution: A shape with a skewed power distribution within the expected range is assumed. Variations in axial power distribution due to transient operation are accounted for in the power distribution uncertainty.

2.1g Low Power Region (PLOW): A relative power approximately half of the core average is assumed for the low power region. This value is typical of current and future low leakage loading patterns. Variations in this parameter were found to have a relatively small effect. The uncertainty resulting from this parameter is included in the initial condition uncertainty.

2.1h Hot Assembly Burnup: Beginning of Life (BOL) conditions in the hot assembly have been confirmed to be conservative and are assumed in the base case. The core average rods are assumed to be at an average burnup representative of typical reload cycles.

2.1i Prior Operating History: The reactor is assumed to have been operating, since fuel cycle startup, at 100 percent power. When a given axial power distribution is considered, it is assumed to have existed since this startup time. This means that the distribution of fission products coincides with the steady-state fission rate distribution. This assumption conservatively places both the initial fission rate and stored energy, and the subsequent decay heat production, at the same axial location.

2.1j Moderator Temperature Coefficient: The maximum value specified in the Technical Specifications is assumed, to conservatively estimate core reactivity and fission power.

2.1k Hot Full Power (HFP) Boron Concentration: A value typical of those used in current cores at BOL conditions is assumed.

2.2 Fluid Conditions

2.2a Average Fluid Temperature (T_{avg}): T_{avg} is assumed at the maximum expected value during normal full power operation. Scoping studies indicated that higher T_{avg} resulted in higher PCT for all plants. The effect of uncertainties in this parameter are accounted for in the initial condition uncertainty.

2.2b Pressurizer Pressure: The maximum expected value of pressurizer pressure is assumed. Scoping studies indicated that higher pressure resulted in higher PCT for all plants. The effect of uncertainties in this parameter are accounted for in the initial condition uncertainty.

2.2c Loop Flowrate: The minimum expected loop flowrate is assumed. This assumption is made to be consistent with other safety analyses. In some plants a low flow results in a small PCT reduction. Uncertainty related to this parameter is accounted for in the break flow uncertainty.

2.2d Upper Head Temperature (T_{UH}): The appropriate best estimate value of T_{UH} is assumed. Since variation in this parameter is quite small, uncertainties are not included.

2.2e Pressurizer Level: The nominal value of pressurizer level is assumed. Because the pressurizer level is automatically controlled and the effect on PCT is small, uncertainties are not included.

2.2f Accumulator Water Temperature: A nominal (mid-point) value is assumed, with variations treated as part of the initial condition uncertainty.

2.2g Accumulator Pressure: A nominal (mid-point) value of accumulator pressure is assumed in the base case. Variations in pressure are included in the initial condition uncertainty.

2.2h Accumulator Water Volume: A nominal (mid-point) value of accumulator water volume is assumed in the base case. Variations in volume are included in the initial condition uncertainty.

2.2i Accumulator Line Resistance: A best estimate value of accumulator line resistance is assumed in the base case. Variations in line resistance are included in the initial condition uncertainty.

2.2j Accumulator Boron Concentration: The Technical Specification minimum value is assumed.

3.0 Accident Boundary Conditions

3.0a Break Location: A break near the mid-point in the cold leg is assumed. Scoping studies have confirmed that the cold leg remains the limiting location for large LOCA.

3.0b Break Type: The cold leg guillotine break is assumed in the base case. The effect of variations in break type are accounted for in the break flow uncertainty component.

3.0c Break Size: For a double-ended guillotine break, a nominal cold leg area is assumed. For split breaks, a wide range of break sizes were considered, and the limiting break size is used in the uncertainty evaluation.

3.0d Offsite Power: No loss of offsite power, consistent with the limiting case from the scoping results, is assumed.

3.0e Safety Injection (SI) Flow: Minimum SI flow is assumed, calculated using methods consistent with those currently employed for Appendix K analysis. Scoping studies indicate that increased SI flow reduces PCT. This parameter is therefore bounded. The primary reason for this choice is that using best estimate values for this important parameter, while producing more realistic results, may also require additional testing and surveillance to verify the assumed flow uncertainty.

3.0f Safety Injection Temperature: Nominal (mid-point) values are assumed. Variations are accounted for in the initial condition uncertainty.

3.0g Safety Injection (SI) Delay: Maximum values consistent with the limiting offsite power assumption (offsite power available) are used.

3.0h Containment Pressure: A conservatively low value calculated using currently approved containment codes (Bordelon, 1974) and mass and energy release from the WCOBRA/TRAC calculation, is assumed.

3.0i Single Failure Assumption: In order to simplify the analysis, the loss of a train will be assumed for the determination of pumped Emergency Core Cooling System (ECCS) flow during the LOCA, while the train will be assumed to

operate in the calculation of containment backpressure. This will conservatively bound the possible single failures.

3.0j Rod Drop Time: Consistent with the current design basis for this plant, control rods are assumed not to drop during the LOCA.

4.0 Model Parameters

All model parameters, with the exception of several biases applied to the hot rod, are used at their best estimate values in the base case. In addition, all models with the exception of the break type and break discharge coefficient are accounted for through the code uncertainty.

Table 4-1 summarizes the base case assumptions described above. For those parameters where a best estimate or mid-point (nominal) value was used, the corresponding uncertainty treatment is also given.

The base case, while it includes several best estimate assumptions, still represents a conservative set of conditions. Based on the scoping study results, the assumed guillotine break and high linear heat rates alone, result in a level of conservatism estimated at several hundred degrees F.

Table 4-1
Key LOCA Parameters and Base Case Assumptions

Parameter	Base Case	Uncertainty or Bias
1.0 Plant Physical Description		
a. Dimensions	Nominal	U1[1]
b. Flow resistance	Best Estimate	U3[3]
c. Pressurizer location	Opp. broken loop	Conservative
d. Hot assembly location	Under limiting location	Conservative
e. Hot assembly type	Fresh assembly	Conservative
f. SG tube plugging level	High	Conservative
2.0 Plant Initial Operating Conditions		
2.1 Reactor Power		
a. Core average linear heat rate (AFLUX)	Nominal	U2[2]
b. Peak linear heat rate (PLHR)	Nominal	U2
c. Hot rod average linear heat rate (HRFLUX)	Nominal	U2
d. Hot assembly average heat rate (HAFLUX)	Nominal	U2
e. Hot assembly peak heat rate (HAPHR)	Nominal	U2
f. Axial power distribution (PBOT, PMID)	Nominal	U2
g. Low power region relative power (PLOW)	Nominal	U4

Table 4-1 (Cont'd)
Key LOCA Parameters and Base Case Assumptions

Parameter	Base Case	Uncertainty or Bias
h. Hot assembly burnup	BOL	Conservative
i. Prior operating history	Equilibrium decay heat	Conservative
j. MTC	Max full power (0)	Conservative
k. HFP boron	Nominal BOL (800)	Typical
2.2 Fluid Conditions		
a. T_{avg}	Maximum	U4
b. Pressurizer pressure	Maximum	U4
c. Loop flow	Minimum	U3
d. T_{UH}	Nominal	0
e. Pressurizer level	Nominal	0
f. Accumulator temperature	Nominal	U4
g. Accumulator pressure	Nominal	U4
h. Accumulator volume	Nominal	U4
i. Accumulator fL/D	Nominal	U4
j. Accumulator boron	Minimum	Conservative

Table 4-1 (Cont'd)
Key LOCA Parameters and Base Case Assumptions

Parameter	Base Case	Uncertainty or Bias
3.0 Accident Boundary Conditions		
a. Break location	Cold leg	U3
b. Break type	Guillotine	U3
c. Break size	Nominal	U3
d. Offsite power	On	Conservative
e. Safety injection flow	Minimum	Conservative
f. Safety injection temperature	Nominal	U4
g. Safety injection delay	Max delay	Conservative
h. Containment pressure	Minimum based on WC/T M&E	Conservative
i. Single failure	ECCS: (N-1) trains Containment press: all trains	Conservative
j. Control rod drop time	No control rods	Conservative
4.0 Model Parameters		
a. Break flow model (C_D)	Best estimate	U3
b. Pump model (two-phase performance)	Best estimate	U3
c. Accumulator nitrogen model (effect on RCS pressure)	Best estimate	U1

SECTION 5
PLANT SENSITIVITY STUDIES

5-1 Indian Point Unit 2 Scoping Studies

A series of WCOBRA/TRAC calculations was performed using the Indian Point 2 (IP2) plant input model, to determine the effect on peak cladding temperature (PCT) of variations in several key LOCA parameters. From these studies, an assessment was made of the parameters which had a significant effect.

The sensitivity studies are performed in three parts. The first part is a scoping study in which several of the key LOCA parameters are varied one-at-a-time. To perform this study, a set of initial conditions which is more conservative than those described in the previous section is employed, to assure that the sensitivity to the parameter change is conservatively quantified, at a relatively high PCT level. Several of the results from these scoping studies will be used to estimate the uncertainty resulting from the plant initial conditions, ΔPCT_4. The second part consists of sensitivity studies in which several power distribution parameters are varied singly and in combination in order to develop a response surface to describe the effect of these parameters on the PCT. The third part is similar to the second, where the parameters varied are those which affect the break flowrate.

5-2 IP2 Reference Transient Description

The IP2 reference transient used the conditions listed in Table 5-1. Many of these conditions represent conservative or limiting plant operating points. Consequently, the PCT generated by the reference transient is expected to be relatively high. The LOCA transient can be divided into time periods in which specific phenomena are occurring. A convenient way to divide the transient is in terms of the various heatup and cooldown transients that the hot assembly undergoes. For each of these phases, specific phenomena and heat transfer regimes are important, as discussed below. Results are shown in Figures 5-1 to 5-14. In these figures, the transient starts at 30 seconds. (The first 30 seconds were used to establish steady-state conditions.)

I. Critical Heat Flux (CHF) Phase

In this phase, the break discharge rate is subcooled and high, the core flow reverses, the fuel rods go through departure from nucleate boiling (DNB) and the cladding rapidly heats up while core power shuts down. Figure 5-1 shows the maximum cladding temperature in the core, as a function of time. The hot water in the core and upper plenum flashes during this period. This phase is terminated when the water in the lower plenum and downcomer begin to flash. The mixture swells and the intact loop pumps, still rotating in single-phase liquid, push this two-phase mixture into the core.

II. Upward Core Flow Phase

Heat transfer is improved as the two-phase mixture is pushed into the core. This phase may be enhanced if the pumps are not degraded, and the break discharge rate is low because the fluid is saturated at the break. Figures 5-2 and 5-3 show the break flowrate from the vessel and loop sides of the break. In Figure 5-2 the negative flow is flow from the vessel into the break. This phase ends as lower plenum mass is depleted, the loops become two-phase, and the pump head degrades. If pumps are highly degraded or the break flow is large, the cooling effect due to upward flow may not be significant. Figures 5-4 and 5-5 show the void fraction at the pump inlet for one intact loop pump and the broken loop pump. The intact loop pump remains in single-phase liquid flow for several seconds, while the broken loop pump is in two-phase and steam flow soon after the break.

III. Downward Core Flow Phase

The loop flow is pushed into the vessel by the intact loop pumps and decreases as the pumps become two-phase. The break flow begins to dominate and pulls flow down through the core. Figures 5-6 and 5-7 show the liquid flow into the top of channels 17 and 19 on a per channel basis. While entrained liquid and steam flow also provide cooling, the amount of liquid entering the core was found to be the best indicator of core cooling. For some plants, this period is enhanced by flow from the upper head.

For IP2, the upper head flashed earlier and therefore has a minor impact. As the system pressure continues to fall, the break flow and consequently the core flow, are reduced. The core begins to heat up as the system reaches containment pressure and the vessel begins to fill with Emergency Core Cooling System (ECCS) water.

IV. Refill Phase

The core continues to heat up as the lower plenum fills with ECCS water. Figure 5-8 shows the lower plenum liquid level. This phase ends when the ECCS water enters the core and entrainment begins, with a resulting improvement in heat transfer. Figures 5-9 and 5-10 show the liquid flows from the accumulator and the safety injection on the intact loop opposite to the broken loop. In Figure 5-10, negative flow is flow into the RCS. The repressurization, which occurs as reflood begins, can be seen in the slight reduction in pumped flow.

V. Early Reflood Phase

Reflood oscillations occur as the core begins to fill. The accumulators begin to empty and nitrogen enters the system. Figure 5-11 and 5-12 show the core and downcomer liquid levels, and Figure 5-13 shows the vessel fluid mass. For IP2, the cladding temperature reaches a maximum during this phase.

VI. Late Reflood Phase

The accumulators have emptied and the core is filling via pumped injection. A second heatup and cooldown period may occur. For IP2, cladding temperatures remain steady for a while then decrease at higher elevations, as seen in Figure 5-14.

5-3 IP2 Scoping Study Results

A number of sensitivity calculations were carried out to investigate the effect of the key LOCA parameters (Table 5-1). The results of those studies are discussed in this section. In the figures presented in this section (Figures 5-15 to 5-44), the transient starts at time = 0.

The first 30 seconds which were used for steady-state conditions are not shown in these figures.

In the sensitivity studies performed, LOCA parameters were varied one at a time. For each sensitivity study, a comparison between the base case and the sensitivity case transient results was made. In the figures presented, the reference case is shown as a solid line, and the results, with the parameter varied, are shown as a dotted line.

During the course of these scoping studies, some changes were made to the reference case. These primarily involved changes in input to correct minor errors, or changes in timestep size. These changes resulted in some variation in the PCT, but were not considered significant enough to require recalculating previous sensitivities. The parameter variations described below always present the effect of the single parameter; that is, both runs included the input corrections. In addition, several cases included variations both above and below the nominal value of the parameter. If the effect was small, only one case is discussed. Both cases are presented in the overall summary of results shown in Table 5-2.

Case 1.0 a) — Dimensions

This effect was investigated during the scoping studies for another four-loop PWR (CQD Section 22-3), and was found to be on the order of 10°F.

Case 1.0 b) — Reduced Broken Loop Nozzle Resistance (Figures 5-15 and 5-16)

This case was modeled by replacing the form loss coefficient of the broken cold leg nozzle, from the base case value to a reduced value. A reduced resistance in the vessel nozzle of the broken loop increases the mass discharge from the vessel side of the break. As a result of the increased break flow, more mass is pulled through the core, improving the core heat transfer during blowdown. During reflood, a two-phase mixture flows through the nozzle as steam flows through the intact loops, along with entrained Safety Injection (SI) water. This results in a pressure drop at the nozzle which increases the downcomer pressure, resulting in improved flooding rates. Consequently, during reflood a lower nozzle resistance would be expected to reduce

core heat transfer. As discussed in the introduction, the reflood transient calculation by the best estimate model does not exhibit the high loop steam flows found in the older models. For IP2, the blowdown effect is more important than the reflood effect, resulting in a PCT reduction.

Case 1.0 c) — Moving Pressurizer from Intact Loop to Broken Loop (Figures 5-17 and 5-18)

This case was modeled by attaching the pressurizer to the hot leg of the broken loop instead of the intact loop during steady-state initiation. The pressurizer injects a significant amount of mass into the loop to which it is connected during blowdown. When this mass is injected into the broken loop, its effect is to reduce the flow from the vessel to the broken loop. As a result, vessel mass preferentially flows through the core to the vessel side of the break, improving core cooling along the way and reducing PCT.

Case 1.0 f) — Decreasing Steam Generator Tube Plugging (Figures 5-19 and 5-20)

A reduction in the steam generator tube plugging level was modeled by changing the following primary side parameters to values consistent with an increased number of active tubes: volume and flow area within tube region, and total tube inner surface heat transfer area. The total tube outer surface heat transfer area was modified accordingly, on the steam generator secondary side. Additionally, the steam generator secondary side pressure was increased, to offset the effect of increased heat transfer area on primary fluid temperature. The loop flowrate was allowed to increase consistent with the lower loop resistance. With reduced tube plugging, during blowdown the steam generated in the core has an alternate path through the vessel side of the break. This may induce increased upward flow through the hot assembly and the assemblies around it, and results in slightly improved core cooling for IP2, when tube plugging is reduced from 25 to 5 percent.

Case 2.1 a to f)

These effects are examined in detail in Section 5-5.

Case 2.1 g) — Reduced Low Power Region Relative Power (Figure 5-21)

This effect was modeled by readjusting the radial power factors of the average rods with the low power factor set at a reduced value. Reducing the low power region relative power requires an increase in power in the other average power channels. The change would be expected to have some effect on the core transverse flows during blowdown and reflood. Calculation results showed that when the low power region power is reduced from 0.7 to 0.4, a small reduction in PCT results.

Case 2.2 a) — Reduced Core Average Fluid Temperature (Figure 5-22)

This case was modeled by reducing the initial primary side fluid and structural temperatures. The steam generator secondary side pressure was also reduced to maintain the desired primary side temperatures during the steady-state initialization. A lower T_{avg} improves core cooling during blowdown, because it delays DNB, and because flashing mixtures generally contain more liquid. On the other hand, lower cold leg temperature may increase subcooled break flows, causing a more rapid flow reversal and earlier DNB. A 10°F reduction in T_{avg} caused only a slight change in PCT.

Case 2.2 b) — Reduced Initial System Pressure (Figure 5-23)

This effort was modeled by reducing the initial pressure in the reactor system and setting the temperature in the pressurizer close to the saturation temperature at the desired system pressure. Reducing the initial system pressure causes earlier occurrences of flashing, accumulator injection, and end of ECCS bypass. For IP2, a small PCT penalty was observed.

Case 2.2 c) — Increased Loop Flowrate (Figure 5-24)

Increased loop flow was simulated by increasing Reactor Coolant System (RCS) pump speed. The increase in pumping capability causes mass to flow through the loops, preferentially to the break on the vessel side. This effect is equivalent to reducing the loop resistance, which would also increase loop flow. Consequently, less fluid mass is drawn through the core, and the heat transfer is reduced. The increase in pump capability may also induce some upward core flow which improves core cooling as in the steam generator tube plugging reduction case. However, for IP2 the latter effect is smaller. This results in a small PCT penalty, which is accounted for in the break flow uncertainty (Section 5-7).

Case 2.2 d) — Decreased Upper Head Fluid Temperature (Figures 5-25 and 5-26)

This effect was modeled by reducing the initial metal and fluid temperature in the upper head region. The fluid in the upper head represents a significant fluid mass which can flow down into the upper plenum and core through the guide tubes during blowdown. The driving force is primarily the pressure generated as a result of flashing. If the initial temperature is high, it will flash early in the transient, when the core flow is still upward. Colder fluid temperature will delay flashing until the core flow is reversed (downward). Consequently core cooling is increased with lower upper head temperature. Small variations in T_{UH} during normal operation were found to have a small effect on PCT. Large change in T_{UH} such as changing T_{UH} from T_{hot} to T_{cold} results in a large change in PCT as shown in Figure 5-25.

Case 2.2 e) — Variation in Pressurizer Level

This effect was modeled by first increasing the pressurizer water level by 5 percent, then decreasing by 5 percent. The range is consistent with the maximum range of variation expected for short periods of time during normal operation. In both cases, the variation was found to have a small effect on PCT.

Case 2.2 f) — Increased Accumulator Water Temperature (Figure 5-27)

This effect was modeled by setting the liquid temperature in the accumulators at a higher level. Higher accumulator fluid temperature has a small effect during blowdown, possibly due to the effect of a higher gas temperature on the accumulator flowrate. During reflood, the expected effect is found, as a higher fluid temperature leads to earlier ECCS water boiling and a slightly lower vessel mass inventory. However, the effect on PCT is small.

Case 2.2 g) — Increased Accumulator Pressure (Figure 5-28)

This effect was modeled by increasing the initial accumulator pressure to a desired value. Increasing the accumulator pressure affects the injection initiation time and injection rate slightly. The effect on PCT is small.

Case 2.2 h) — Reduced Accumulator Water Volume (Figure 5-29)

This effect was modeled by decreasing the initial accumulator water volume to a desired value. Reducing accumulator water volume results in higher nitrogen volume, faster depletion of accumulator water, and earlier nitrogen injection. Earlier nitrogen injection pressurizes the top of the downcomer and pushes the liquid into the core earlier (a PCT benefit). However, further reductions in water volume result in lower mass inventory at the onset of reflood (a PCT penalty).

Case 2.2 i) — Decreased Accumulator Line fL/D (Figures 5-30 and 5-31)

This case was modeled by using a reduced frictional factor in the accumulators/SI lines. Decreasing the accumulator line resistance increases the water delivery rate to the vessel, and helps to pressurize the top of the downcomer pushing the liquid into the core. For IP2, a 20 percent line resistance reduction results in a PCT reduction, and a 20 percent line resistance increase results in a PCT increase.

Case 3.0 a) — Pump Suction Break (Figures 5-32 to 5-34)

This case was modeled by placing the breaks (BREAK components 4 and 6) at the mid-point of the crossover pipe (component 15, Figure 3-11), instead of the cold leg. In the pump suction break case, the accumulator/SI line on the broken loop was assumed to be intact. This accumulator provides early injection into the cold leg of the broken loop (the cold leg itself is intact), preventing liquid depletion in the lower plenum. Flow through the core remains positive (upward) providing continuous cooling and resulting in a PCT substantially below the cold leg break.

Case 3.0 d) — Pump Behavior due to Offsite Power (Figures 5-35 and 5-36)

This case was modeled by setting the pumps to be tripped at the beginning of the transient, and the coastdown pump speed to be calculated by the code. The most significant effect of the availability, or lack of, offsite power on the LOCA is the effect on the reactor coolant pump, which will lose power and begin to coast down if offsite power sources are not available. It is possible that, were a LOCA to occur, the effect of the reactor trip on the external power grid, or vibration in the pump, will cause the pump to lose power and begin coasting down. However, such an event cannot be guaranteed, so a study of the effect of the pump, if kept operating during the LOCA, was performed. It was found that operating pumps resulted in higher PCT. This is a result of the effect that the pumps have on loop flow during the blowdown transient. If the pumps continue to operate, they maintain significant pumping capacity for several seconds, while the flow through them is still single-phase. Mass flows preferentially through the intact loops rather than the vessel. Consequently, less mass is drawn through the core and heat transfer is reduced. The effect also explains the penalty observed when the loop flowrate was increased by increasing the pump speed, as was discussed in Case 2.2c.

Case 3.0 e) — Safety Injection Flow

For IP2, the effect of variations in safety injection flow are expected to be minor. This is because the cladding temperature reaches a maximum shortly after the

beginning of reflood, before pumped safety injection can have a significant effect. Naturally, safety injection is important in maintaining core cooling after PCT has been reached. The reference case assumes a low injection flow as discussed in Section 3. This flow is sufficient to maintain core cooling after the PCT has been reached. Increasing the flow by 10 percent was found to have a small effect on the PCT, as expected.

Case 3.0 f) — Safety Injection Temperature (Figure 5-37)

This case was modeled by setting the SI FILL temperature at a specified value. The PCT usually occurs around 41 to 45 seconds in the transient, before pumped safety injection can provide the vessel a significant amount of cooling water. Consequently, the SI injection temperature has little effect on the PCT.

Case 3.0 g) — Safety Injection Delay (Figure 5-38)

This case was modeled by specifying an increased delay time in the SI initiation signal. In the IP2 scoping simulation, the assumed SI delay time was quite long: 45 seconds if offsite power is off, and 38 seconds if offsite power is on. (These delay times are 20 seconds longer than the actual times currently established for the plant.) For the same reason as Case 3.0f, further SI injection delay has no impact on the PCT for IP2.

Case 3.0 h) — Increased Containment Pressure (Figure 5-39)

This case was modeled by setting the pressures in the break's time/pressure table at higher values. Increased containment pressure has a beneficial effect during reflood. However, the reason for the improved results is different than that usually identified for the older models. In the older models, higher containment pressure would increase reactor pressure, increasing fluid density and somewhat mitigating the steam binding caused by calculated high entrainment rates. In the best estimate calculation, the higher containment pressure results in more ECCS water in the vessel during reflood. For reasons discussed previously, this has a beneficial effect on the reflood transient.

Case 4.0 a) — Variations in Break Model Discharge Coefficient (Figures 5-40 to 5-43)

These cases were modeled by increasing or decreasing the broken pipe/break interface area by a factor equal to the specified discharge coefficient. Because the effective broken cold leg nozzle loss coefficient used in the code is affected by the downstream area changes, the corresponding loss coefficient input value also has to be changed. The best estimate value of the discharge coefficient for the WCOBRA/TRAC break flow model is 1.0, with an uncertainty range of 20 percent. The appropriate variation in discharge coefficient to consider is therefore 1.2 and 0.8. Use of CD=1.2 (Figures 5-40 and 5-41) reduces the vessel side broken leg resistance, increases downward flow through the core. This improves core cooling. Use of CD=0.8 (Figures 5-42 and 5-43) reduces the break flow, resulting in a more effect upward core flow cooling. Additional detail on break flow modeling is provided in Section 5-7.

Case 4.0 b) — Pump Two-Phase Performance (Figure 5-44)

The pump two-phase head multiplier curves used in this analysis are described in the CQD. The values of these curves (head multiplier as function of vapor fraction) are included in the pump model of the code. The pump performance sensitivity cases were modeled by using these curves (the best-estimate, the lower bound or the upper bound curves). This case was modeled by using the lower-bound head multiplier (MLL) for the broken loop pump during transient. Because the broken loop pump was less degraded than the reference case, there was a slight increase in the upward core flow. This resulted in a small improvement in PCT as shown in Figure 5-44.

Case 4.0 c) — Accumulator Nitrogen Model

The base case includes the effect of nitrogen injection. The effect of removing nitrogen injections was modeled by replacing the intact leg accumulators by FILL components when the water level in the accumulators dropped down to about 1.8 feet. A velocity-time table is provided to each FILL such that the water still contained in the accumulator will be drained (with a constant velocity) within the first 10 seconds.

For the remaining time, the velocities are specified as zero. Results showed that for IP2 nitrogen injection had no effect on PCT.

5-4 Conclusions from the Scoping Studies

From the results obtained we may conclude the following:

1. A cold leg guillotine break with a discharge coefficient of 1.0 results in the highest PCT for IP2.

2. No loss of offsite power, with the assumption that the RCS pumps continue to run during the LOCA, results in the highest PCT.

3. In most of the cases studied, PCTs all occurred around 41 to 45 seconds during the LOCA transient. By this time the accumulators were nearly empty; because of the long SI injection delay, only a very small amount of SI water (or no SI water) had entered the vessel. Consequently, the SI has little impact on the PCT for IP2.

4. Results indicated that cooling of the hot assembly was mainly provided by the transverse flows from its surrounding assemblies. LOCA parameters that can increase the upward or the downward axial flows through the hot assembly, or increase the core transverse flow, can be expected to have a significant impact on the PCT.

5. A number of parameters have been identified which have a small effect on PCT. The PCT uncertainty due to uncertainty in the values of these parameters can be treated in a simple manner, as described in Volume V of the CQD.

6. The scoping study has provided the needed information to determine which key LOCA parameters should be set to nominal values, and which should be bounded, for the base case and response surface calculations. The appropriate values to use for each parameter is discussed in Section 4.

Table 5-2 summarizes the sensitivity calculations performed for IP2. Not all the LOCA parameters were evaluated; some parameters, such as physical dimensions, were confirmed to have a small effect on PCT using results from similar PWR's, while other parameters such as hot assembly location, were shown to be at their limiting values in the base case. The uncertainty arising from many of the model parameters are covered by the code uncertainty derived in Section 18 of CQD Volume IV. The final treatment of the parameter in the overall uncertainty evaluation is also summarized in the table.

Table 5-1
Key LOCA Parameters and Scoping Study Values (IP2)

Parameter	Values
1.0 Plant Physical Description	
a) Dimensions	Nominal + 3%
b) Flow resistance	Nominal
c) Pressurizer location	Intact loop
d) Hot assembly location	Location with least water delivery
e) Hot assembly type	15x15 OFA, fresh
f) SG tube plugging level	25%
2.0 Plant Initial Operating Conditions	
2.1 Reactor Power	
a) Core avg linear heat rate (AFLUX)	Based on 102% of 3216 MWt
b) Peak linear heat rate (PLHR)	Derived from Tech Spec FQ/1.1
c) Hot rod avg linear heat rate (HRFLUX)	Derived from Tech Spec $F_{\Delta H}$
d) Hot assembly avg heat rate (HAFLUX)	HRFLUX/1.1
e) Hot assembly peak heat rate (HAPHR)	PLHR/1.1
f) Axial power dist (PBOT, PMID)	"Nominal" 8-foot peak distribution
g) Low power region rel pwr (PLOW)	Maximum expected
h) Hot assembly burnup	BOL
i) Prior operating history	Equilibrium fission product distribution
j) MTC	Tech Spec Maximum (0)
k) HFP boron	Minimum at BOL
2.2 Fluid Conditions	
a) T_{avg}	Tech Spec Maximum
b) Pressurizer pressure	Tech Spec Maximum
c) Loop flow	Tech Spec Minimum
d) T_{UH}	Nominal
e) Pressurizer level	Nominal
f) Accumulator temperature	Nominal
g) Accumulator pressure	Nominal
h) Accumulator liquid volume	Nominal
i) Accumulator line resistance	Nominal
j) Accumulator boron	Tech Spec Minimum

Table 5-1 (Cont'd)
Key LOCA Parameters and Scoping Study Values (IP2)

Parameter	Values
3.0 Accident Boundary Conditions	
a) Break location	Cold leg
b) Break type	Guillotine
c) Break size	Nominal (cold leg area)
d) Offsite power	On (RCS pumps running)
e) Safety injection flow	Minimum
f) Safety injection temperature	Nominal
g) Safety injection delay	Max delay
h) Containment pressure	Minimum (use latest Appendix K transient)
i) Single failure	ECCS: (N-1) SI trains/Cont p: all SI trains
j) Control rod drop time	No control rods
4.0 Model Parameters	
a) Break flow model (C_D)	Best estimate (C_D=1.0)
b) Pump model (two-phase performance)	Best estimate
c) Accumulator nitrogen model (effect on RCS pressure)	Best estimate
d) Condensation model (hA)	Best estimate
e) Entrainment model	Best estimate
f) ECC bypass model (end of bypass)	Best estimate
g) Core heat transfer model (h, DNB)	Best estimate
h) Fuel rod model (fuel temperature, decay heat, cladding reaction, rewet temperature)	Best estimate except hot rod

Table 5-2
Summary of Scoping Study Results (IP2)

1.0 Plant Physical Configuration						
Parameter	**Scoping Base Value**	**Variation (Ref)**	**Δ= PCT-PCT$_{BASE}$**			**Generic Conclusions**
			Δ1	**Δ2**	**Δ3**	
(a) dimensions	+2-3%	Generic results indicate small effect				Base: Nominal Value Small Effect, Included in Code Uncertainty
(b) flow resistance 1) Cold leg nozzle K_{CL} 2) Hot leg nozzle K_{HL}	nominal (A816F)	K_{CL} -40% (A923B)	-10	-108	—	Base: Nominal Value Include Effect in Break Flow Uncertainty
		K_{HL} +50% (C012B)	-43	-118	—	
(c) pressurizer location	intact loop (A816F)	Broken loop (B816D)	0	-28	—	Base: Intact Loop No Uncertainty
(d) hot assembly location	under FSM	Limiting location	—	—	—	Base: Location Minimizes Direct Flow From UP and UH No Uncertainty
(e) hot assembly type: IFM's	15X15OFA with IFM resistance	+IFM heat transfer (A925B)	-15	-17	—	Base: Plant Specific Input No Uncertainty
(e) BOL fuel, variations in rod internal pressure (Rods 1,2)	nominal internal pressure	To 300 psia	—	-50	—	Base: BOL, Non-IFBA Fuel at Nominal Pressure. Include Uncertainty in Initial Condition Uncertainty
		To 1500 psia	—	+80	—	

Table 5-2 (Cont'd)
Summary of Scoping Study Results (IP2)

2.1 Reactor Power Parameters						
Parameter	**Scoping Base Value**	**Variation (Ref)**	**Δ=PCT-PCT$_{BASE}$**			**Generic Conclusions**
			Δ1	**Δ2**	**Δ3**	
(a) AFLUX (kW/ft) (% FULL POWER)	maximum	-5% (A903C)	0	-46	—	Base: 100% Power Include in Power Uncertainty
(b) PLHR (kW/ft) (FQ)	nominal	See Section 5-5	—	—	—	Base: Nominal Value Include in Power Uncertainty
(c) HRFLUX (kW/ft) (FΔH)	maximum	See Section 5-5	—	—	—	Base: Best Estimate Maximum Value Include in Power Uncertainty
(d) HAFLUX (kW/ft) (FΔH$_{HA}$)	nominal	See Section 5-5	—	—	—	Base: Best Estimate Maximum Value Include in Power Uncertainty
(e) HAPHR (kW/ft) (FQ$_{HA}$)	maximum	See Section 5-5	—	—	—	Base: Nominal Value Include in Power Uncertainty

Table 5-2 (Cont'd)
Summary of Scoping Study Results (IP2)

2.2 Reactor Fluid Conditions						
Parameter	**Scoping Base Value**	**Variation (Ref)**	**Δ=PCT-PCT$_{BASE}$**			**Generic Conclusions**
			Δ1	**Δ2**	**Δ3**	
(a) T_{AVG} (Degrees F)	586.7(A816F)	-11/-1.9%(AN17C)	0	-3	—	Base: Maximum Initial Condition Uncertainty
(b) RCS pressure (psia)	2310	-100/-4.4%(AN16C)	+11	+23	—	Base: Nominal Initial Condition Uncertainty
(c) Loop flow (gpm/loop)	80600	+ 5% (F816B)	-20	+16	—	Base: Minimum Include in Break Flow Uncertainty
(d) T_{UH} (Degrees F)	620.5 (T_{hot})	-10/-1.5%(B016C)	0	-14		Base: Best Estimate No Uncertainty
		-70/-10.8%(AN11C)	-25	-139	—	
(e) Pressurizer level (percent of span)	60%	+5% (ADO3B)	-4	-14	—	Base: Normal Level No Uncertainty
		-5% (BDO3B)	0	+21	—	
(f) Accumulator Temperature (Degrees F)	105	+25/24% (D909D)	-1	-27	—	Base: Nominal Initial Condition Uncertainty
		+45/43% (E816E)	+2	>+100	—	

Table 5-2 (Cont'd)
Summary of Scoping Study Results (IP2)

2.2 Reactor Fluid Conditions						
Parameter	**Scoping Base Value**	**Variation (Ref)**	**Δ=PCT-PCT$_{BASE}$**			**Generic Conclusions**
			Δ1	**Δ2**	**Δ3**	
(g) Accumulator pressure (psia)	655	+45/7% (B916B)	0	+9	—	Base: Nominal Initial Condition Uncertainty
		-45/-7% (B1202)	-7	-15	—	
(h) Accumulator water volume (cubic feet)	800	+10% (A904B)	-11	-14	—	Base: Nominal Initial Condition Uncertainty
		-10% (J816B)	-11	-47	—	
		-20% (A905B)	+7	+8	—	
(i) Accumulator line resistance (Fl/D)	nominal	+20% (K1202)	+5	+16	—	Base: Best Estimate Initial Condition Uncertainty
		-10% (K816B)	-8	-21	—	
		-20% (K905B)	-12	-83	—	
(i) Accumulator boron concentration (PPM)	minimum	limiting value				Base: Minimum

Table 5-2 (Cont'd)
Summary of Scoping Study Results (IP2)

3.0 Accident Boundary Conditions						
Parameter	**Scoping Base Value**	**Variation (Ref)**	**Δ=PCT-PCT$_{BASE}$**			**Generic Conclusions**
			Δ1	**Δ2**	**Δ3**	
(a) break location	cold leg	see Table 5-2a	—	—	—	Base: Middle of Cold Leg Include in Break Flow Uncertainty
(b) break type	guillotine (SS99B)	see Table 5-2a	-280	-276	—	Base: Guillotine Break Flow Uncertainty
(c) break area (fraction of cold leg area)	1.0*CL SPLIT (S415B)	see Table 5-2a	—	—	—	Base: 1.0*CL Break Flow Uncertainty
(d) offsite power (pump on or off)	pump on (A816F)	pump off (A824D)	-50	-62	—	Base: Pump On No Uncertainty
(e) SI flow	minimum flow	+10%	—	-15	—	Base: Minimum Flow No Uncertainty
(f) SI temp (degrees F)	40	+50 (I816D)	0	0	—	Base: Nominal Initial Condition Uncertainty

Table 5-2 (Cont'd)
Summary of Scoping Study Results (IP2)

3.0 Accident Boundary Conditions						
Parameter	**Scoping Base Value**	**Variation (Ref)**	**Δ=PCT-PCT$_{BASE}$**			**Generic Conclusions**
			Δ1	**Δ2**	**Δ3**	
(g) SI delay	max, pmp on	+15s	0	0+		Base: Maximum Delay with Offsite Power
(h) contnmnt pressure (psia)	minimum	+10 (D816C)	-8	-18	—	Base: Minimum Calculated Using Approved Codes No Uncertainty
(i) single failure	1 RHR	see item 3.0 (e)	-	-	-	Base: 1 RHR, 1 HSI Limiting Due to 3.0(e) And 3.0(h)

Table 5-2 (Cont'd)
Summary of Scoping Study Results (IP2)

4.0 Models						
Parameter	**Scoping Base Value**	**Variation (Ref)**	**Δ=PCT -PCT$_{BASE}$**			**Generic Conclusions**
			Δ1	**Δ2**	**Δ3**	
(a) break model	CD=1	See Table 5-2a	—	—	—	Base: CD=1.0. Include CD in Break Flow Uncertainty
(b) pump model	Best estimate (ID04B)	MAX (BL pump) (IF04B)	+2	-35		Base: Best Estimate Include in Break Flow Uncertainty
		MAX (BL pump) (IE04B)	+1	-30	—	
(c) Accumulator nitrogen model	Best estimate	no N2 injection (M816E)	—	0	—	Base: Best Estimate Include in Code Uncertainty
(d) condensation model	Best estimate	validated against experiments	—	—	—	Base: Best Estimate Include in Code Uncertainty
(e) ECC bypass model	Best estimate	validated against experiments	—	—	—	Base: Best Estimate Include in Code Uncertainty
(f) core heat transfer model	Best estimate	validated against experiments	—	—	—	Base: Best Estimate Include in Code Uncertainty
(g) fuel rod model	Best estimate	validated against experiments	—	—	—	Base: Best Estimate Except Hot Rod

Table 5-2 (Cont'd)
Summary of Scoping Study Results (IP2)

Other Sensitivity Studies					
Plant	**Variation**	**Δ=PCT-PCT$_{BASE}$**			**Comments**
		Δ1	**Δ2**	**Δ3**	
IP2	Increase TACC to 130 and SI to 90(c909b)	-10	-24	—	
IP2	Increase # LP levels(A013C)	-19	-26	—	
IP2	Reduce inner/outer channel gap k's(005b)	-7	-37	—	
IP2	PLOW=0.4 and pumps off (c928b)	-49	-92	—	

Table 5-2a
Break Spectrum Results (IP2)

Break Type	Break Area Fraction or (C_D)[1]	PCT_1	PCT_2
Cold Leg Split	1.0 (0.5) (S415B)	1540	1641
	1.2 (0.6) (T415B)	1650	1761
	1.4 (0.7) (U415B)	1750	1823
	1.6 (0.8) (V415B)	1810	1861
	1.8 (0.9) (W415B)	1810	1844
	2.0 (1.0) (X415B)	1805	1817
Cold Leg Guillotine	1.6 (0.8) (X816C)	1720	1892
	2.0 (1.0) (BU01)	1838	1935
	2.4 (1.2 (H816B)	1801	1806
Pump Suction Guillotine	(1.0) (A915B) Pumps On	1070	<1100
	(1.0) (B915B) BL Pump Off	1230	1230

[1]Break area fraction is the ratio of total break area to cold leg area. C_D is the ratio of effective break area to nominal break area.

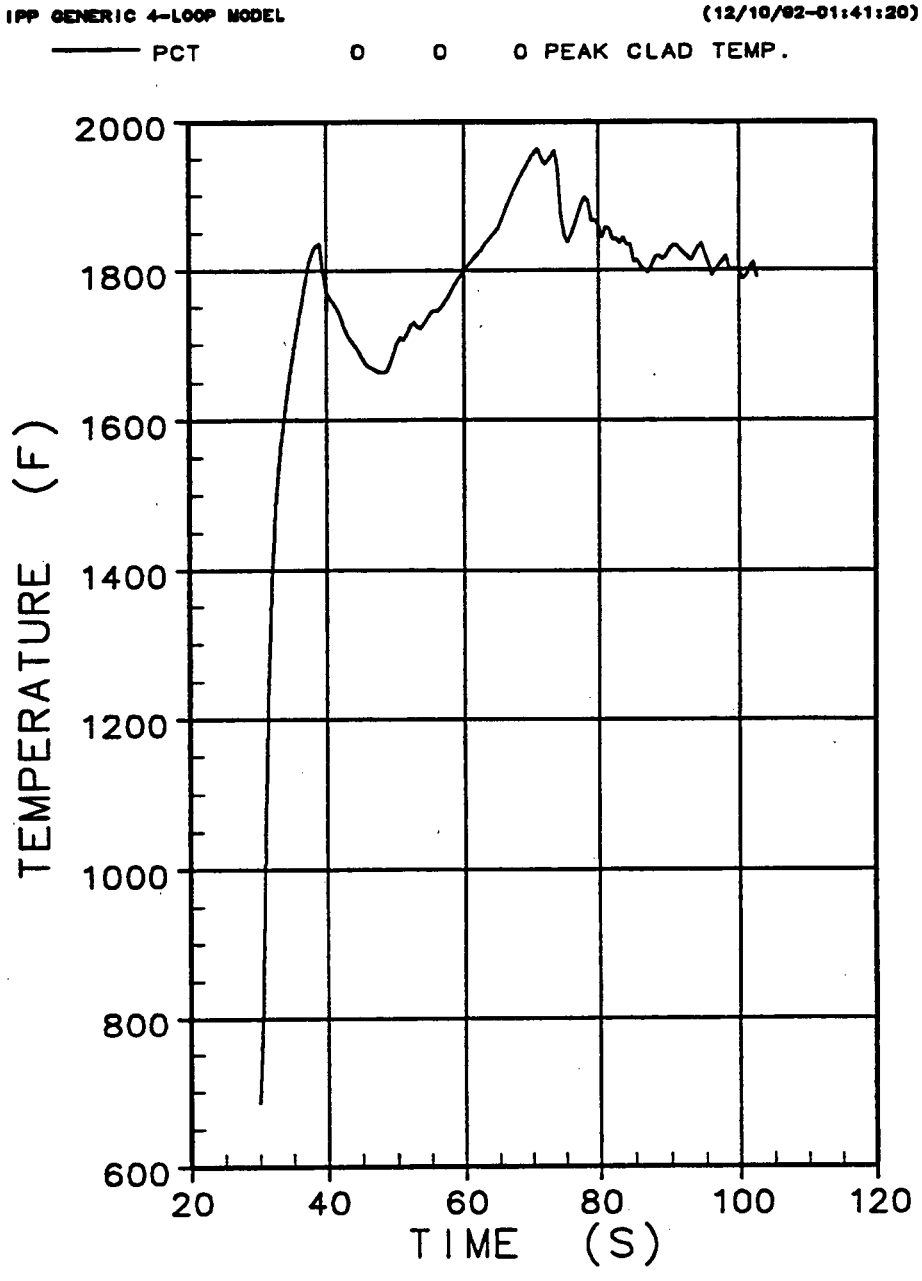

Figure 5-1. Peak Cladding Temperature (Base Case)

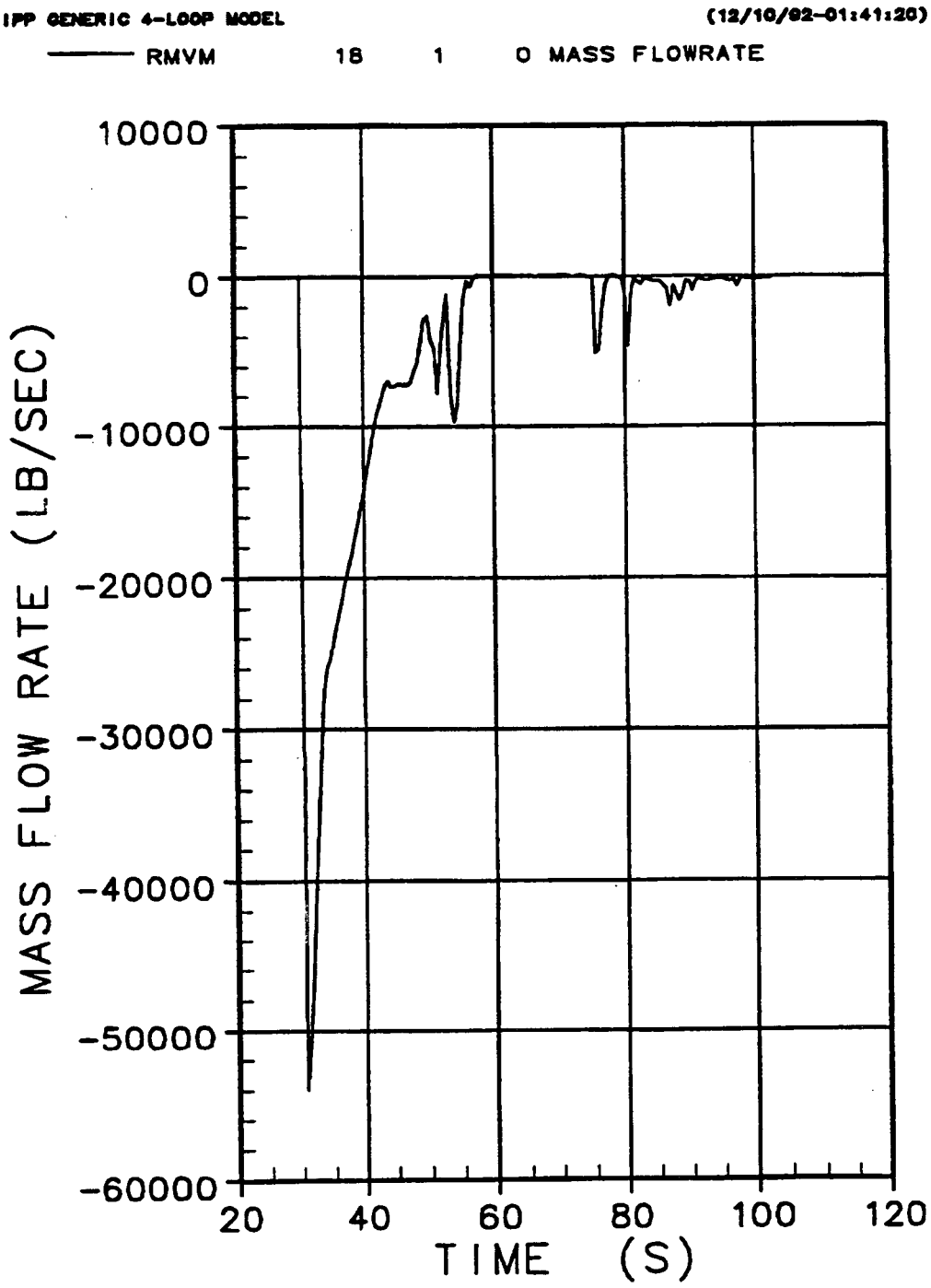

Figure 5-2. Break Flow (Vessel Side)

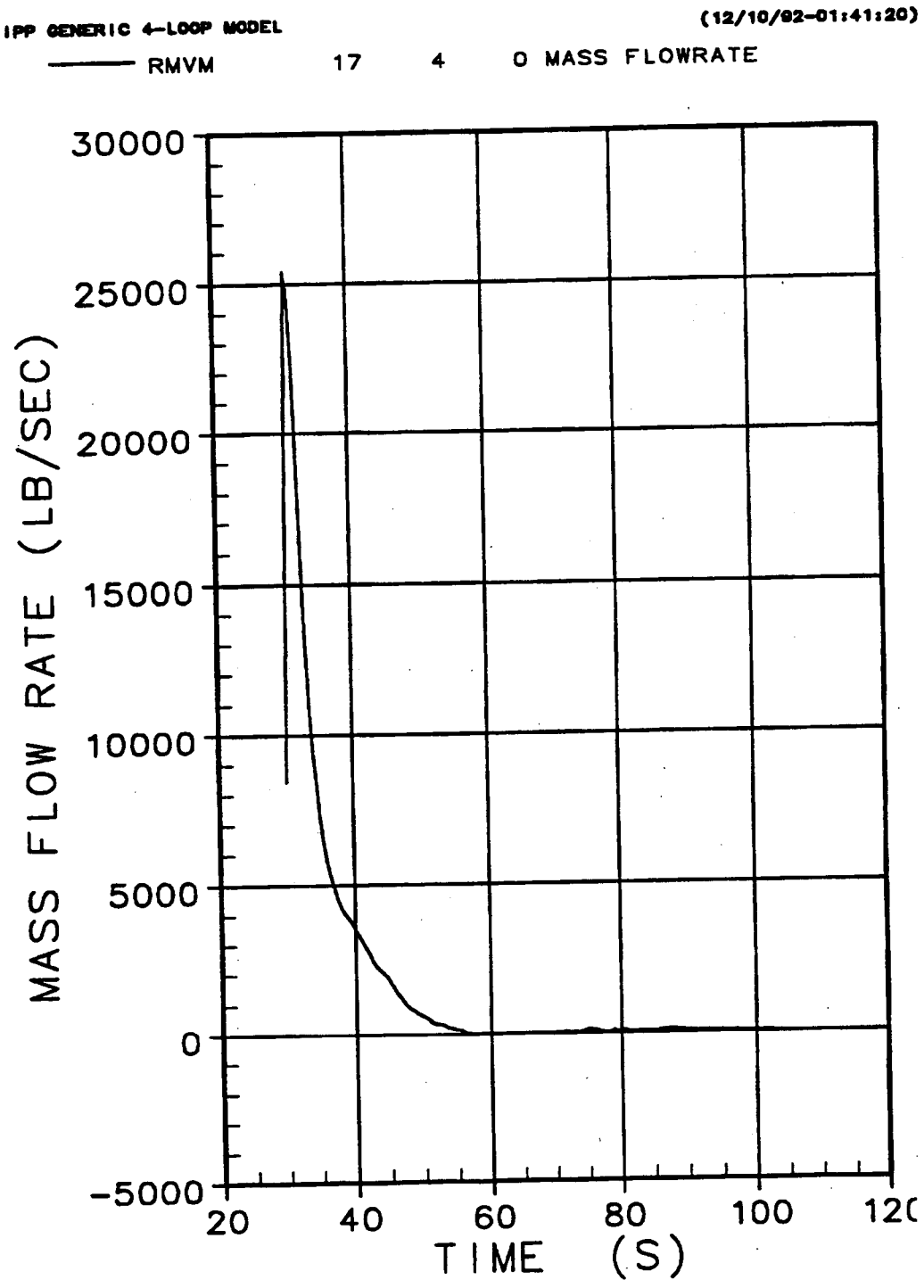

Figure 5-3. Break Flow (Loop Side)

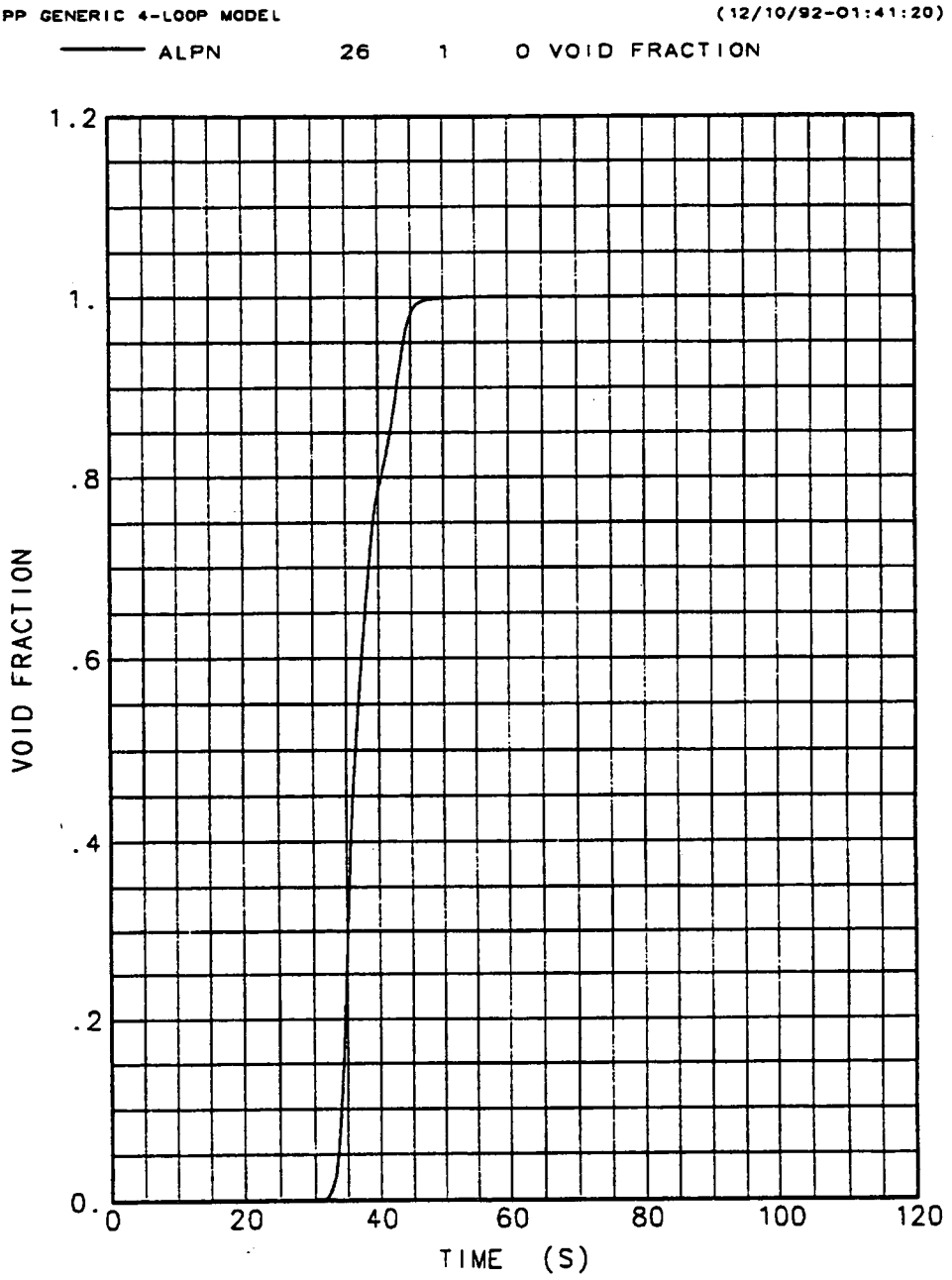

Figure 5-4. Intact Loop Pump Inlet Void Fraction

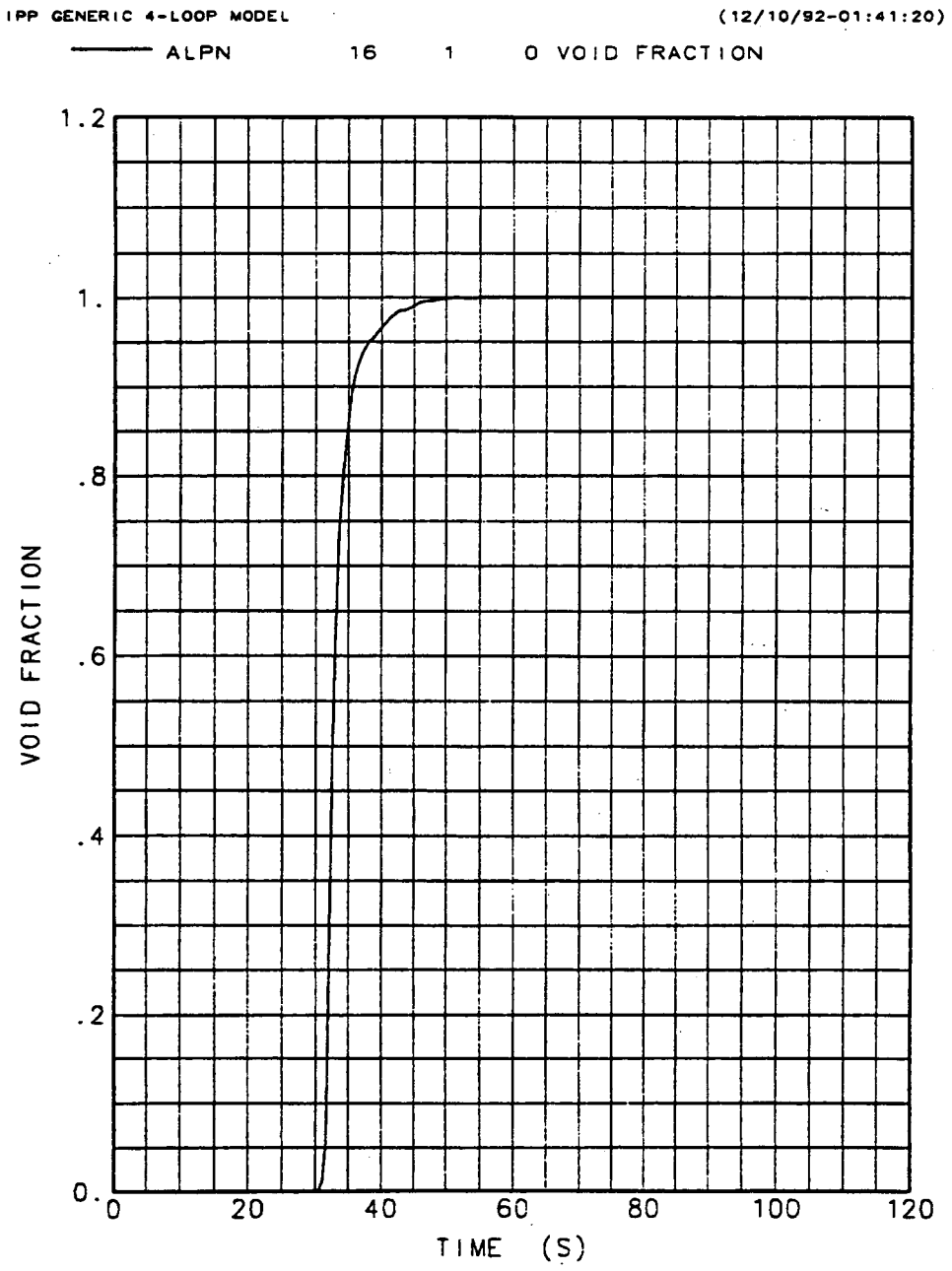

Figure 5-5. Broken Loop Pump Inlet Void Fraction

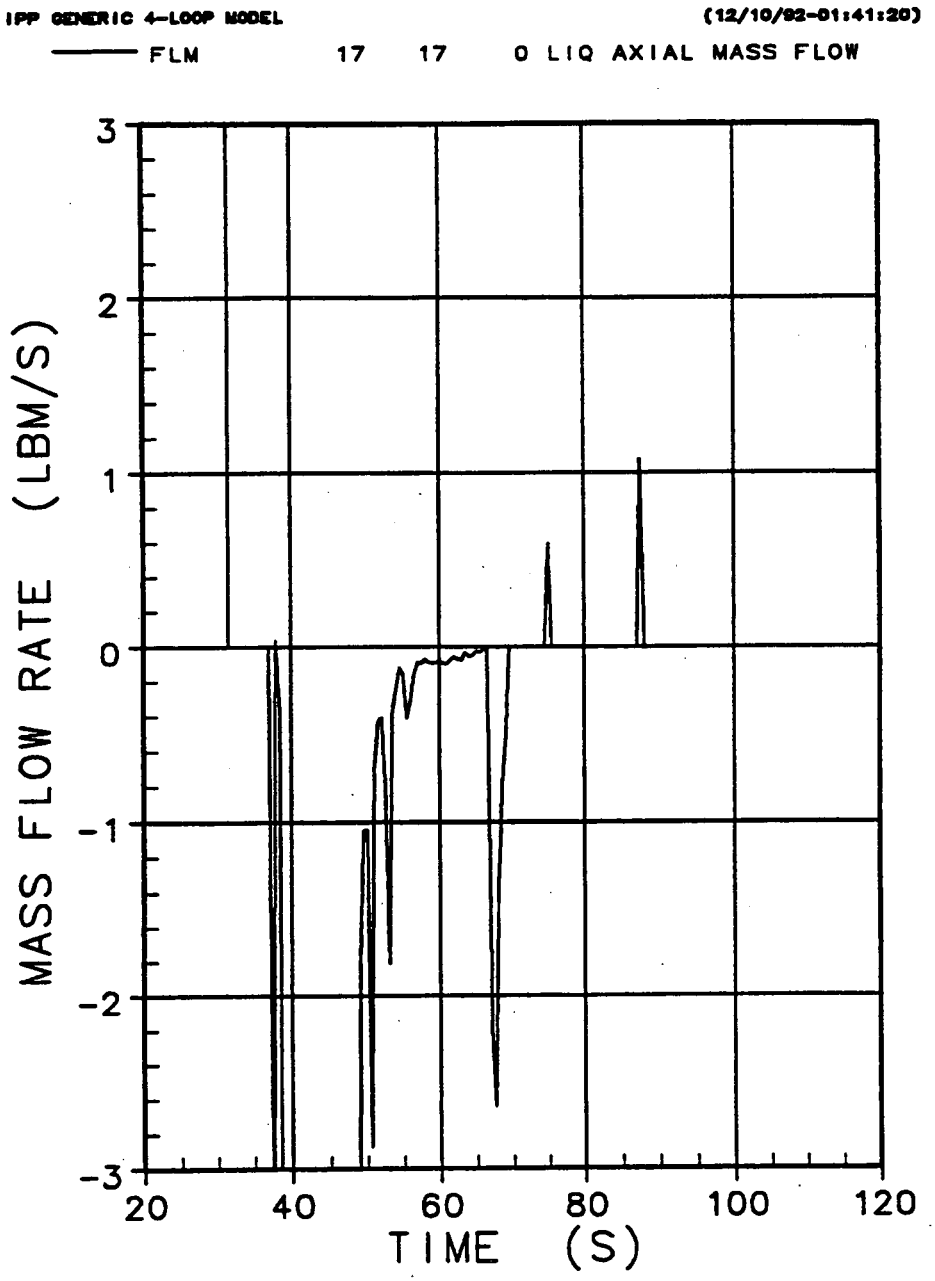

Figure 5-6. Liquid Flow at Top of Channel 17 (SC/OH/FSM Channel)

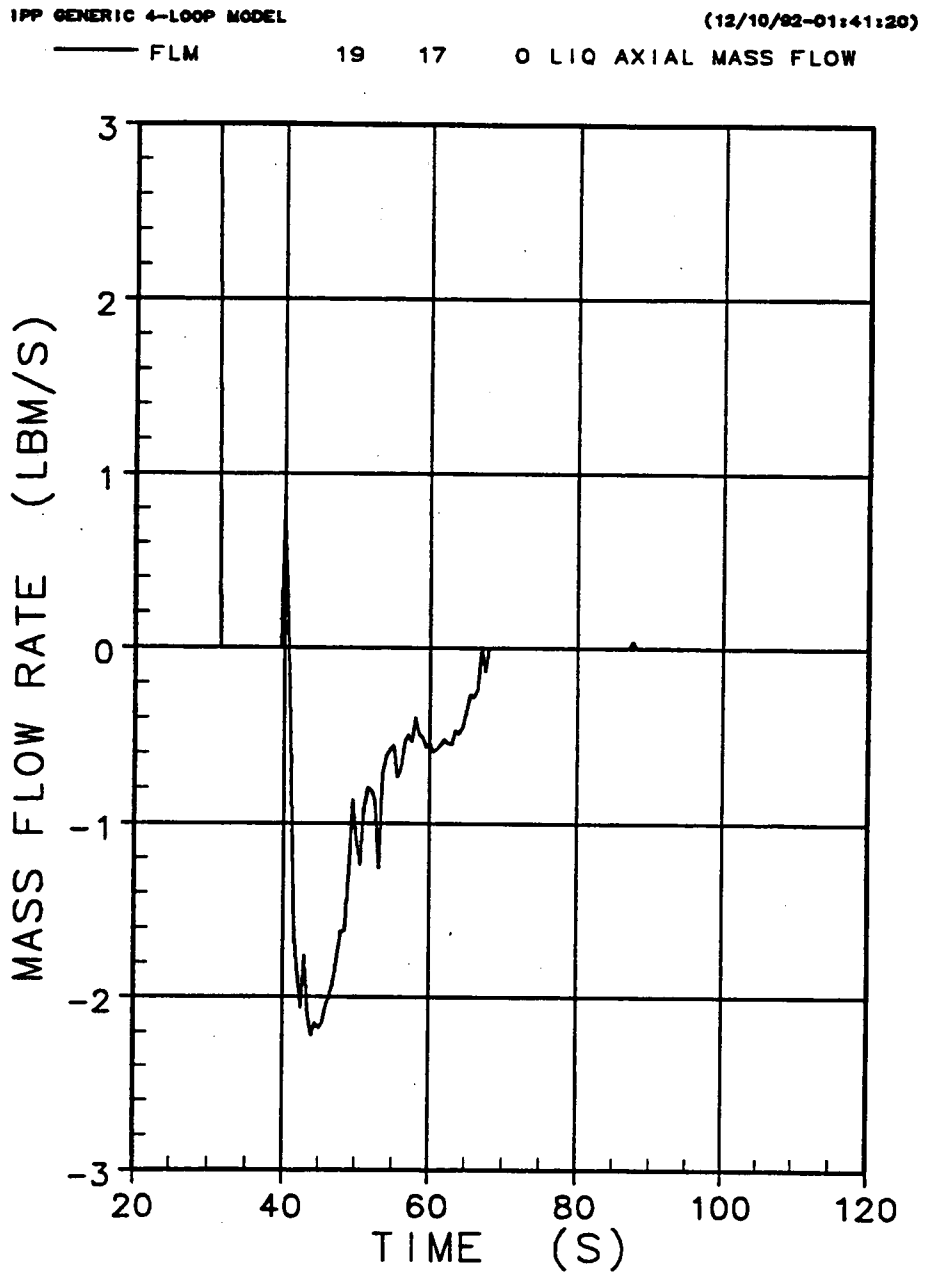

Figure 5-7. Liquid Flow at Top of Channel 19 (Hot Assembly Channel)

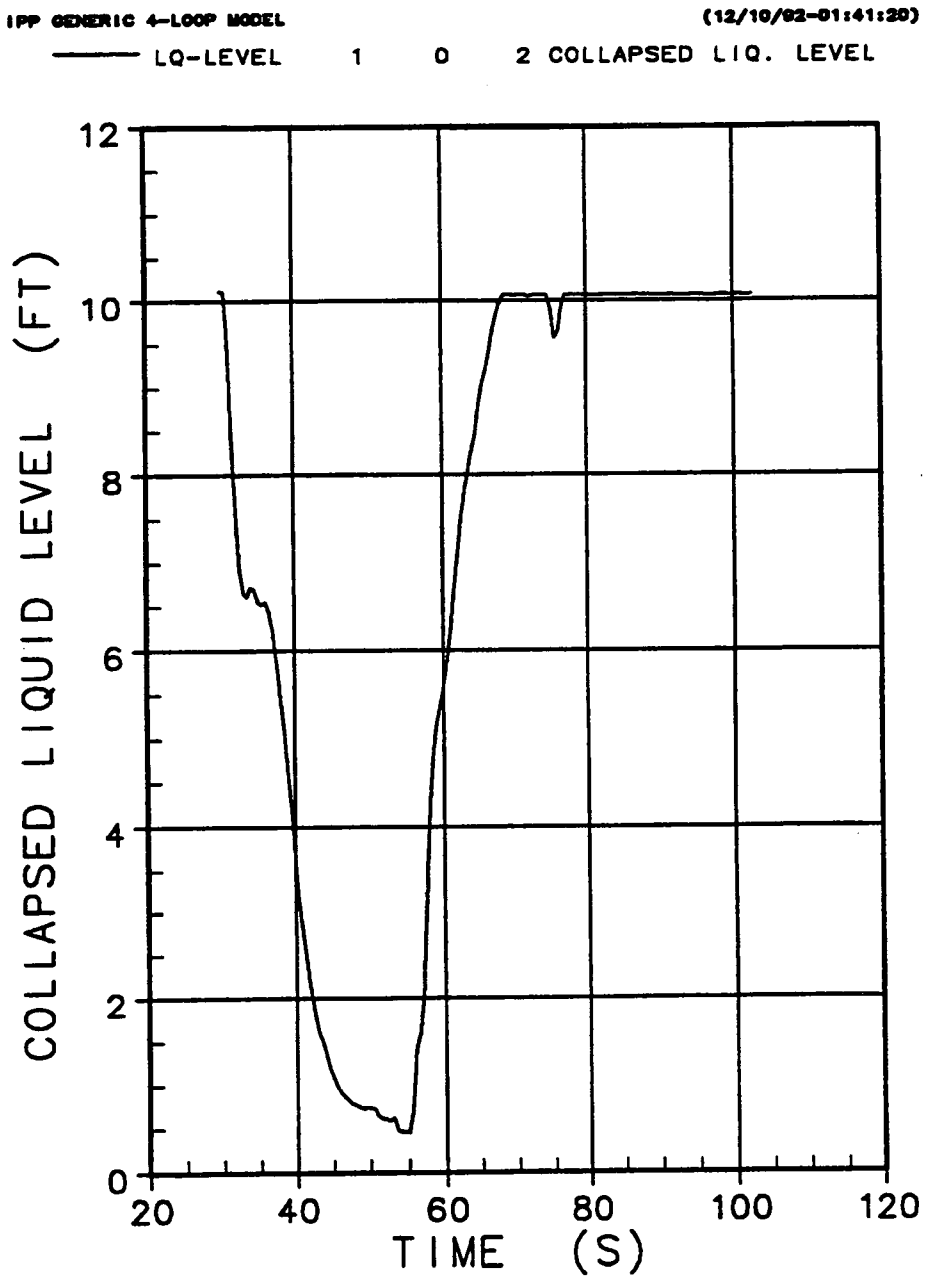

Figure 5-8. Lower Plenum Collapsed Liquid Level

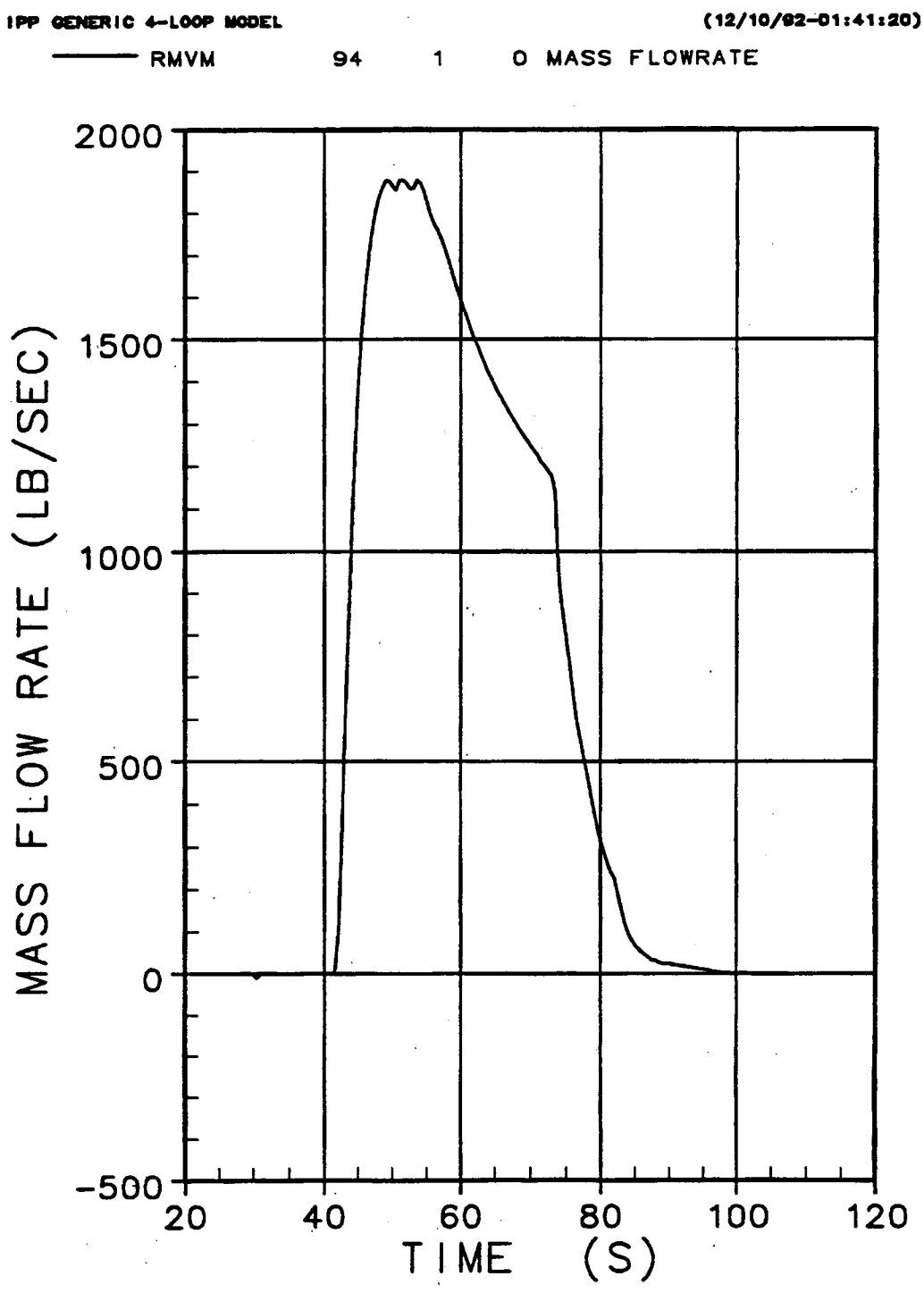

Figure 5-9. Accumulator Liquid Flow

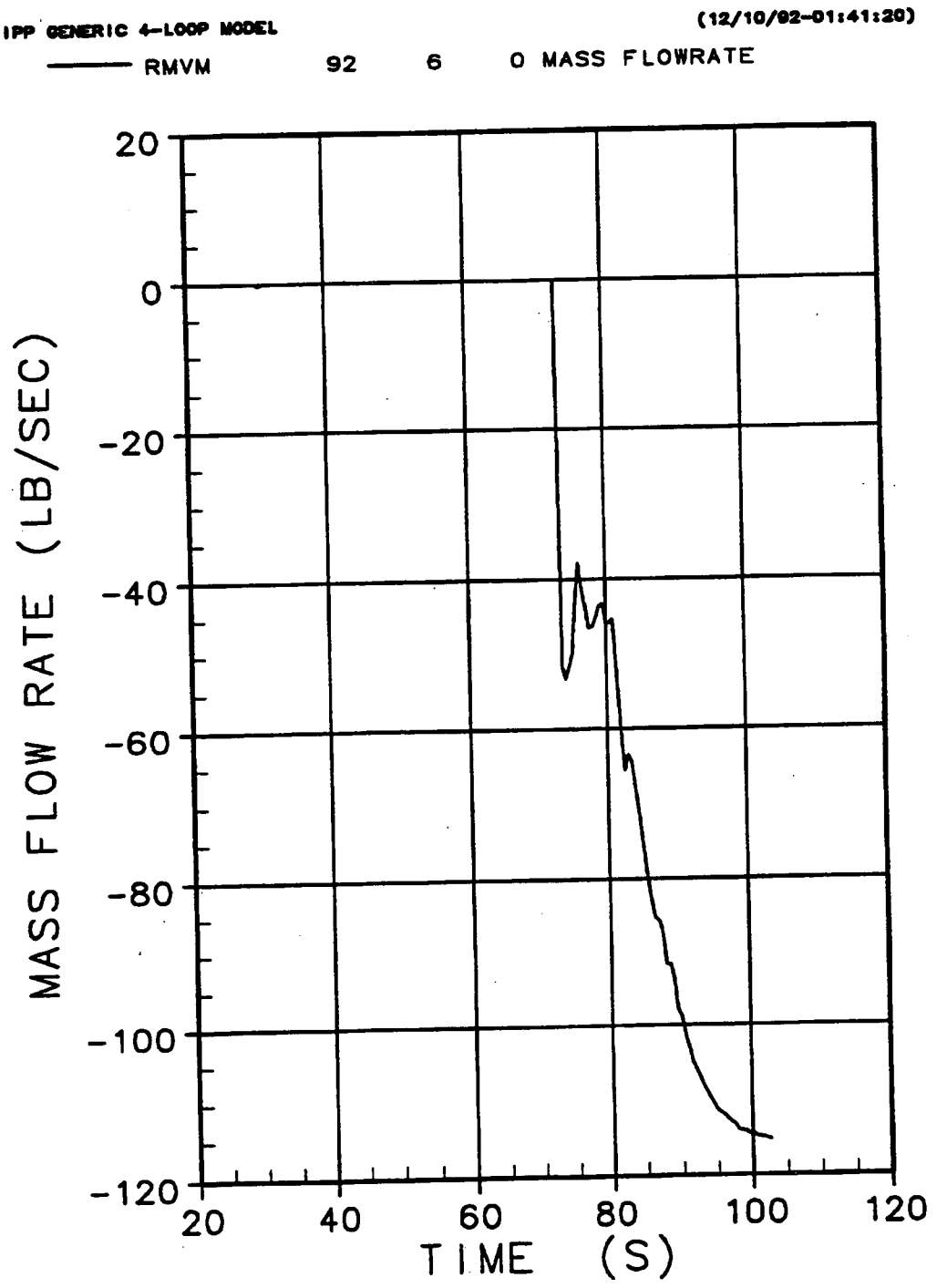

Figure 5-10. Safety Injection Flow (38 Second Delay)

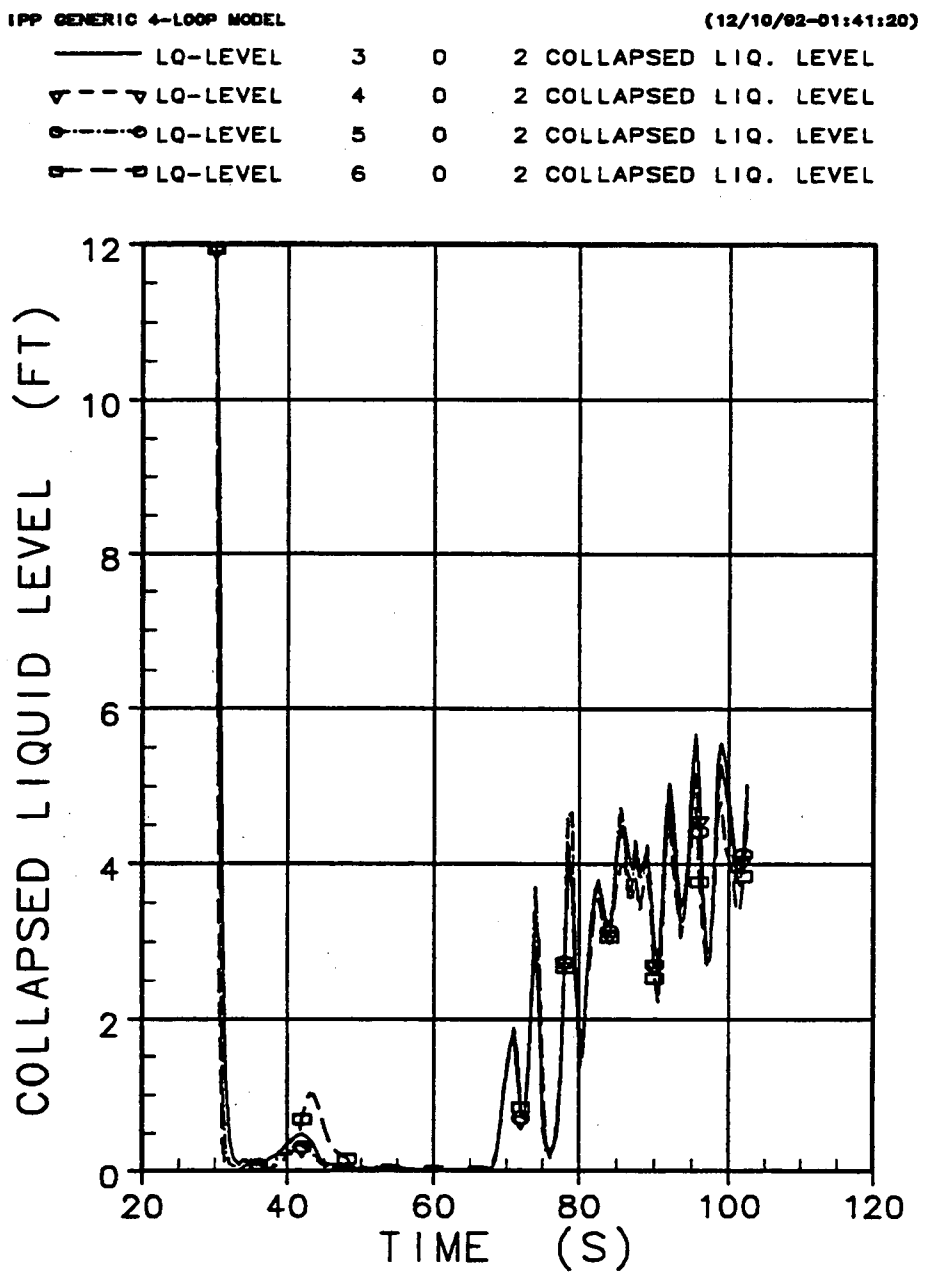

Figure 5-11. Core Channels Collapsed Liquid Level

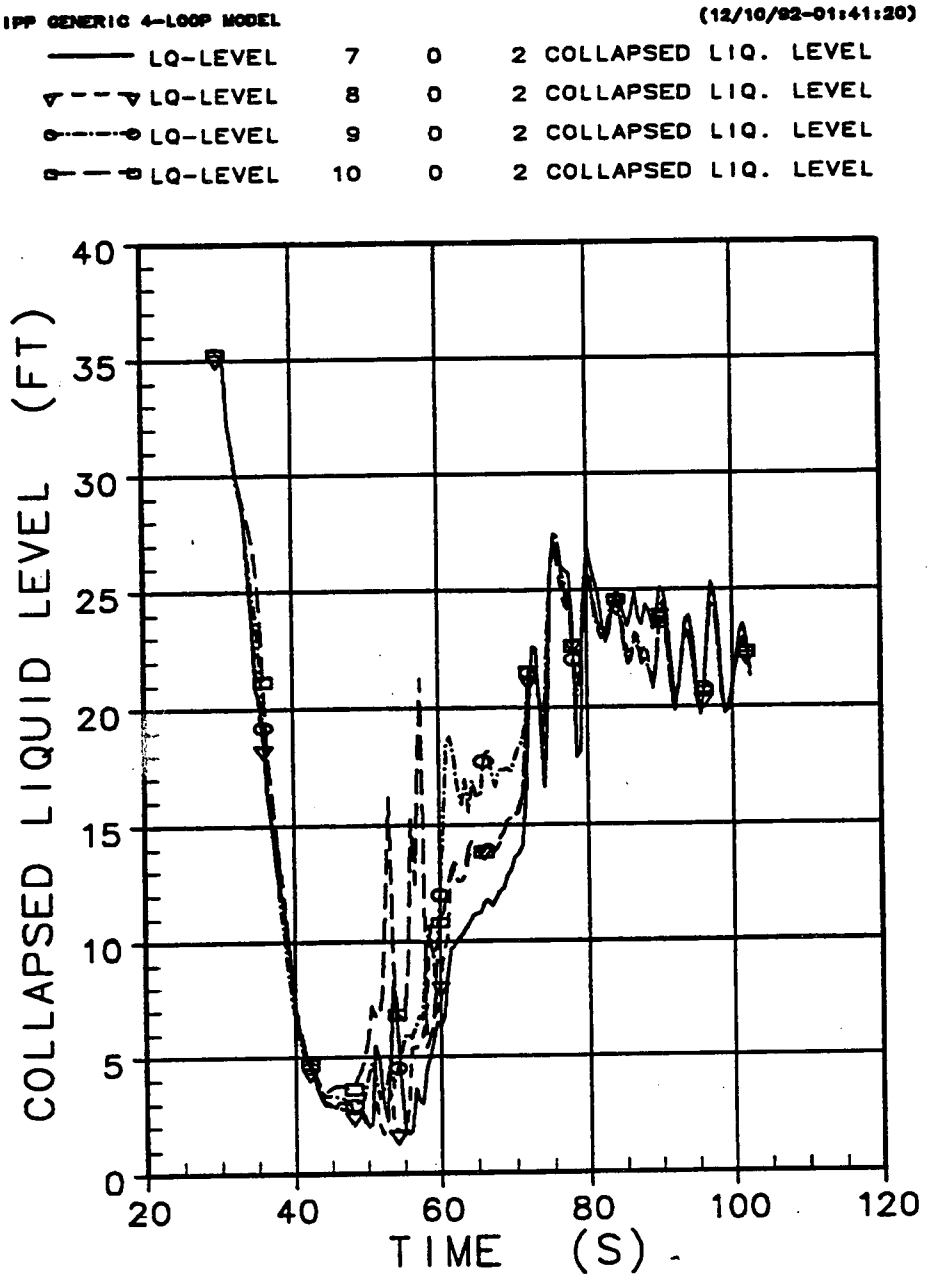

Figure 5-12. Downcomer Channels Collapsed Liquid Level

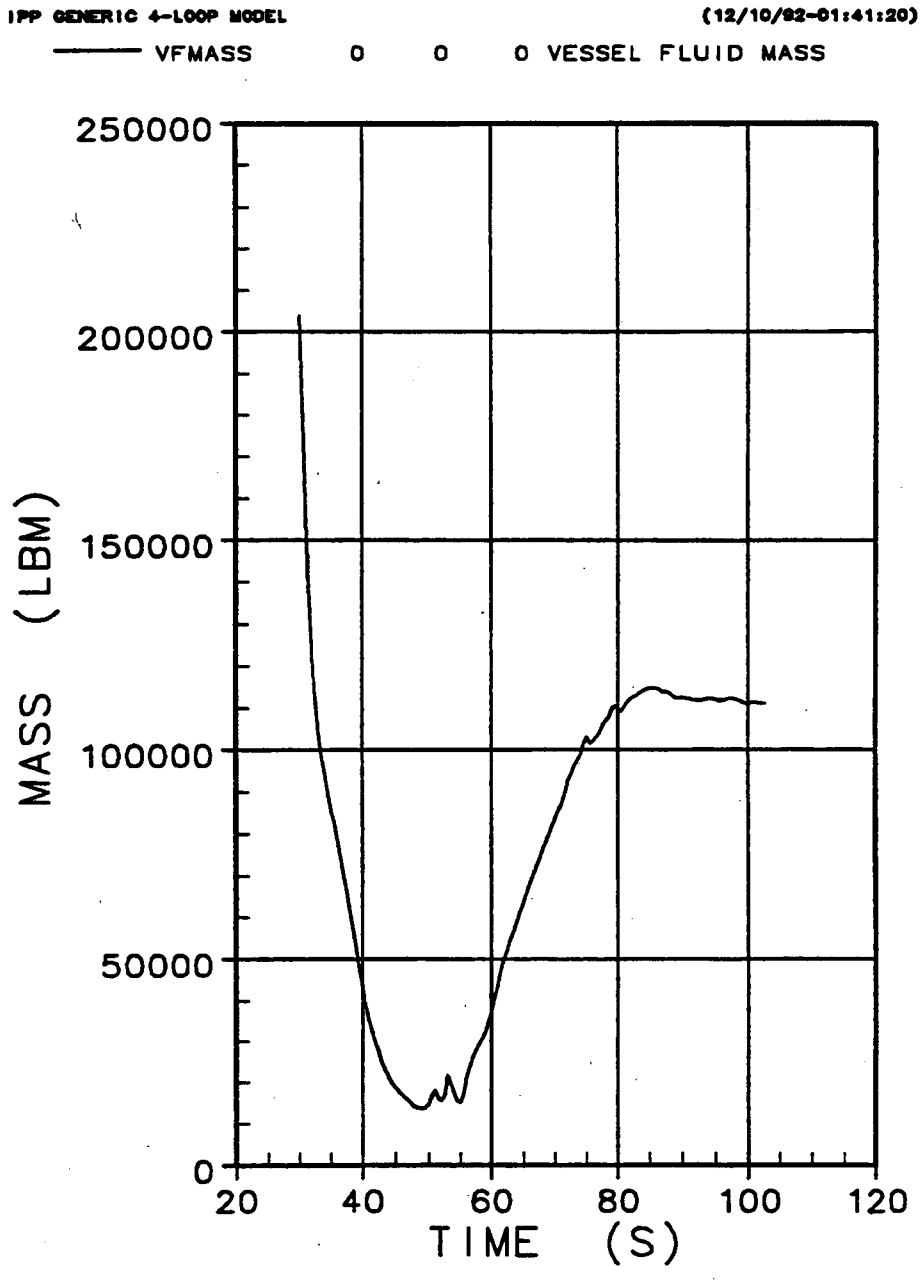

Figure 5-13. Vessel Fluid Mass

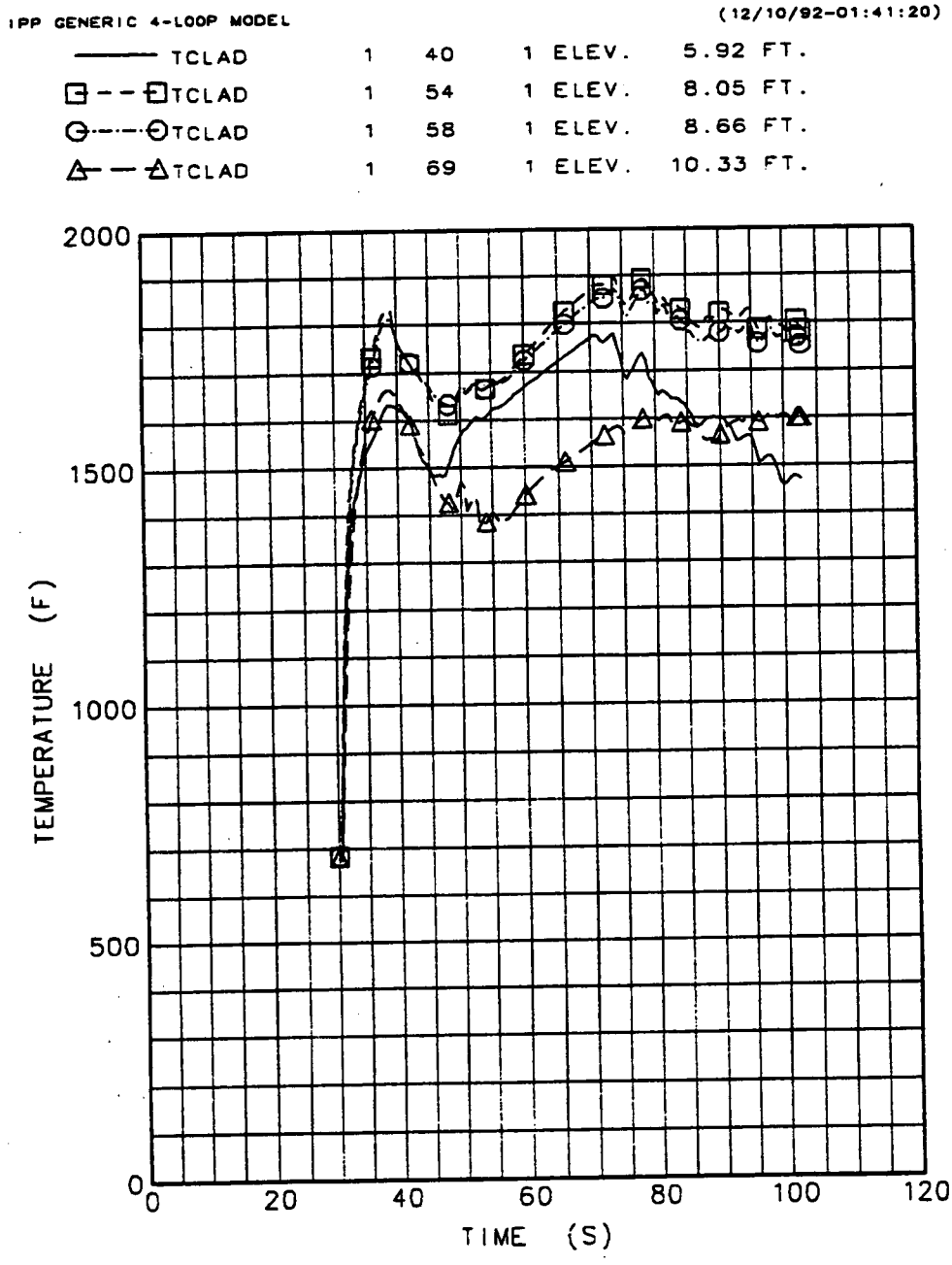

Figure 5-14. Cladding Temperature at Various Elevations (Hot Rod)

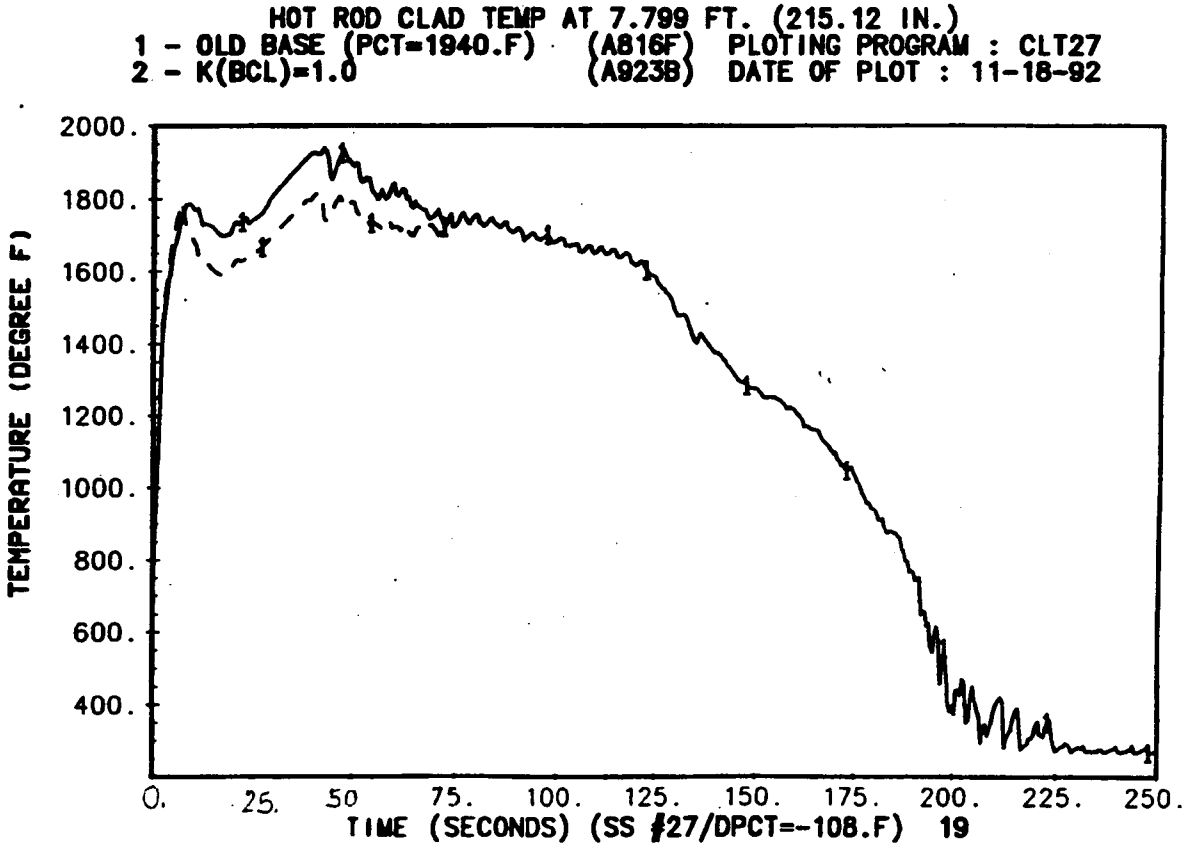

Figure 5-15. PCT Overlay (Case 1.0b)

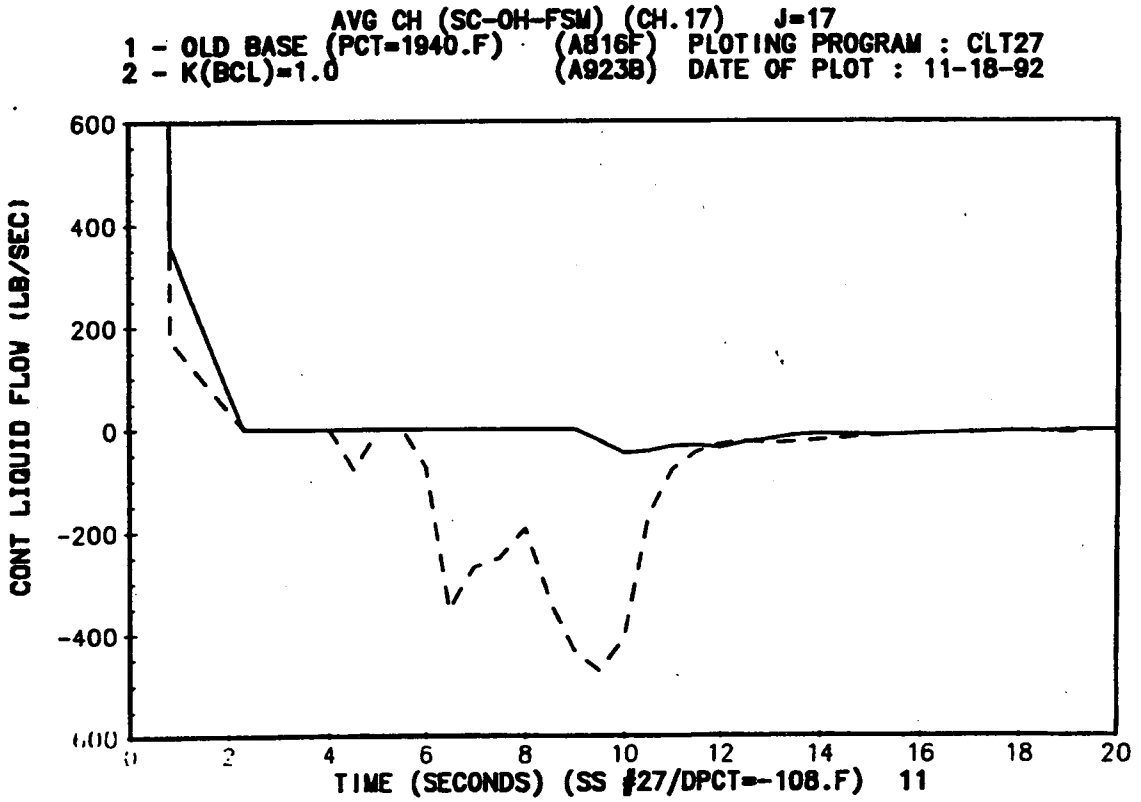

Figure 5-16. Liquid Flow at Top of Core Average Channel (Case 1.0b)

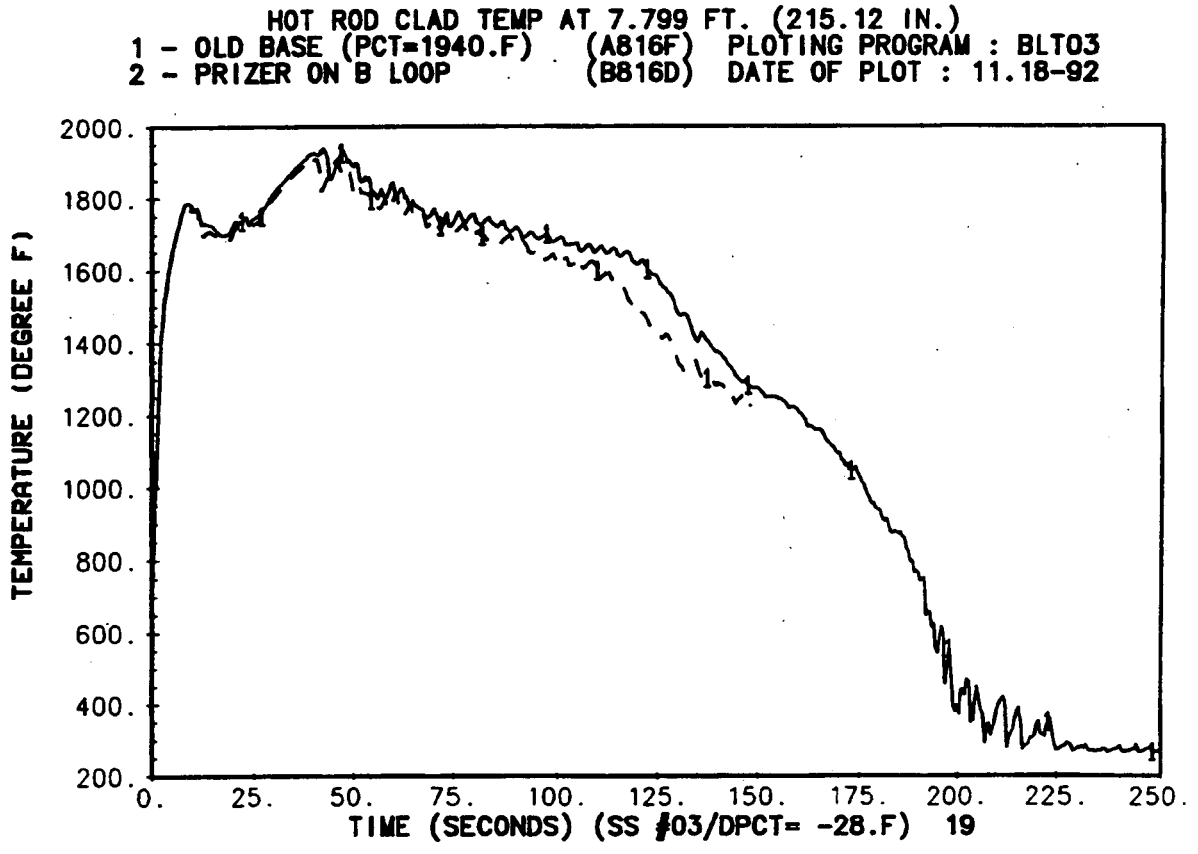

Figure 5-17. PCT Overlay (Case 1.0c)

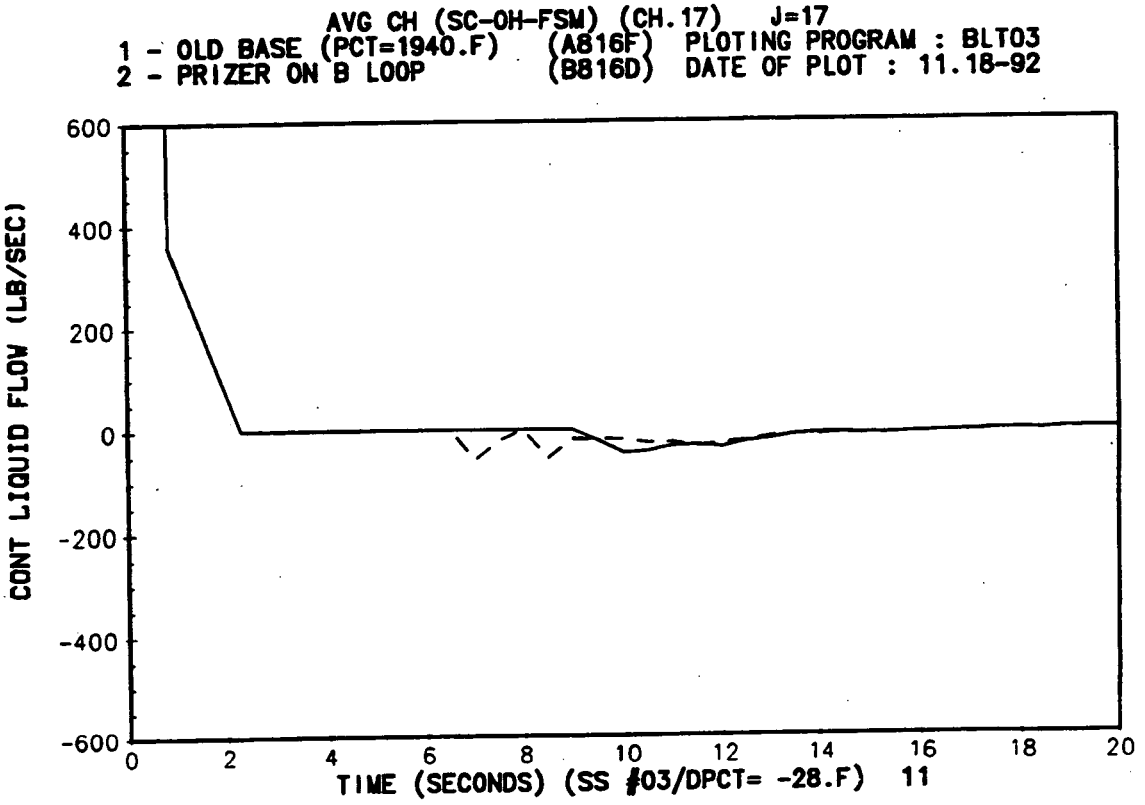

Figure 5-18. Liquid Flow at Top of Core Average Channel (Case 1.0c)

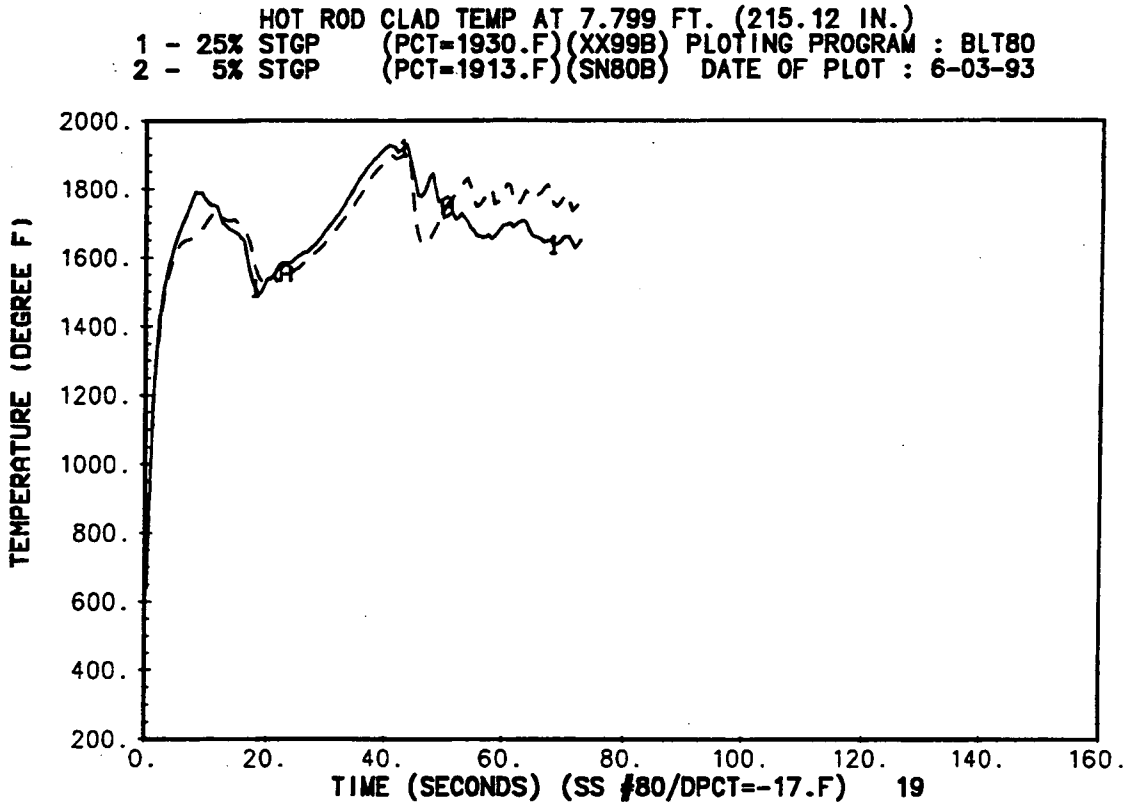

Figure 5-19. PCT Overlay (Case 1.0f)

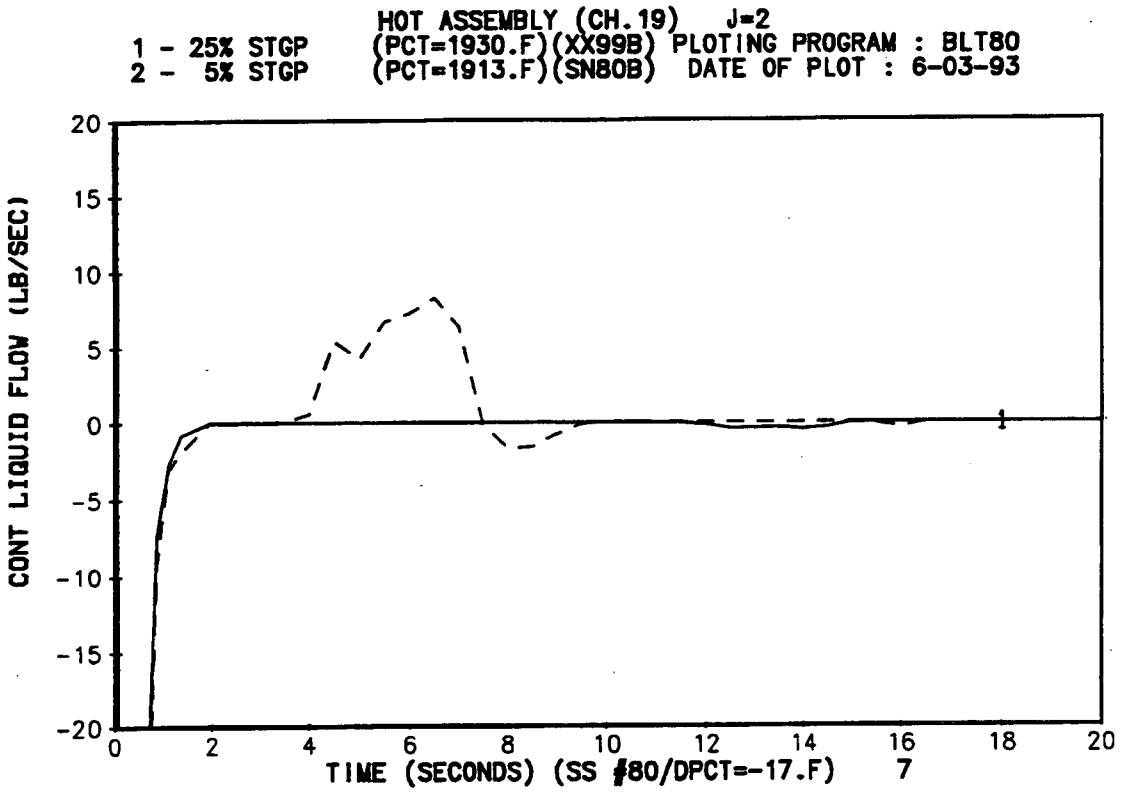

Figure 5-20. Liquid Flow at Top of Hot Assembly Channel (Case 1.0f)

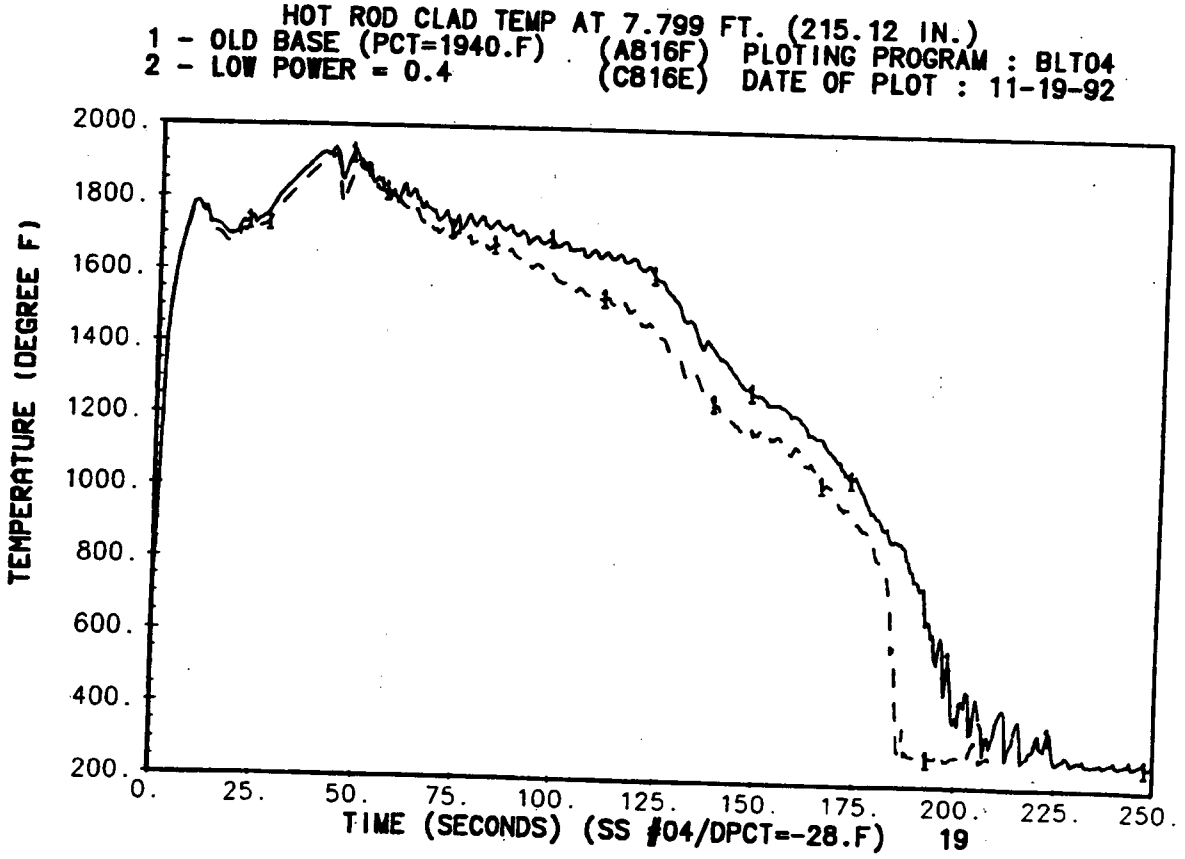

Figure 5-21. PCT Overlay (Case 2.1g)

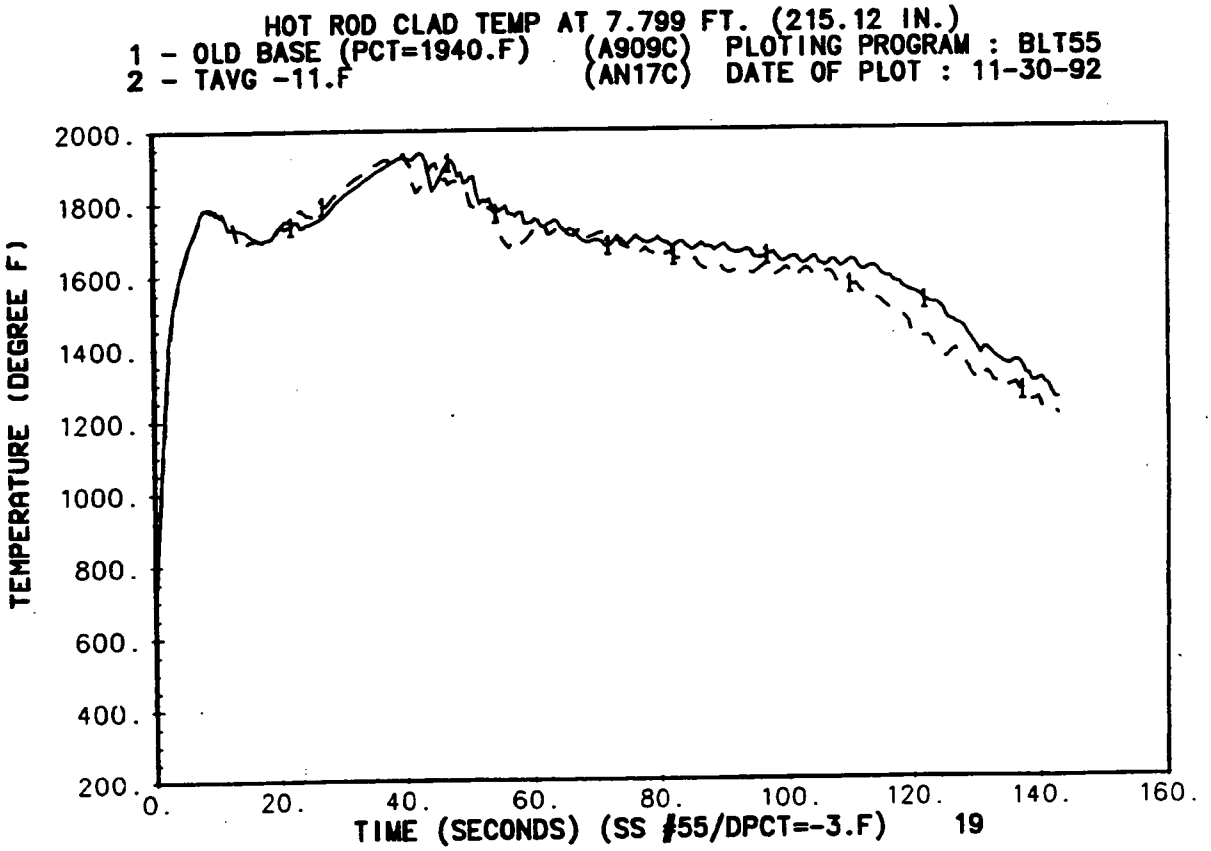

Figure 5-22. PCT Overlay (Case 2.2a)

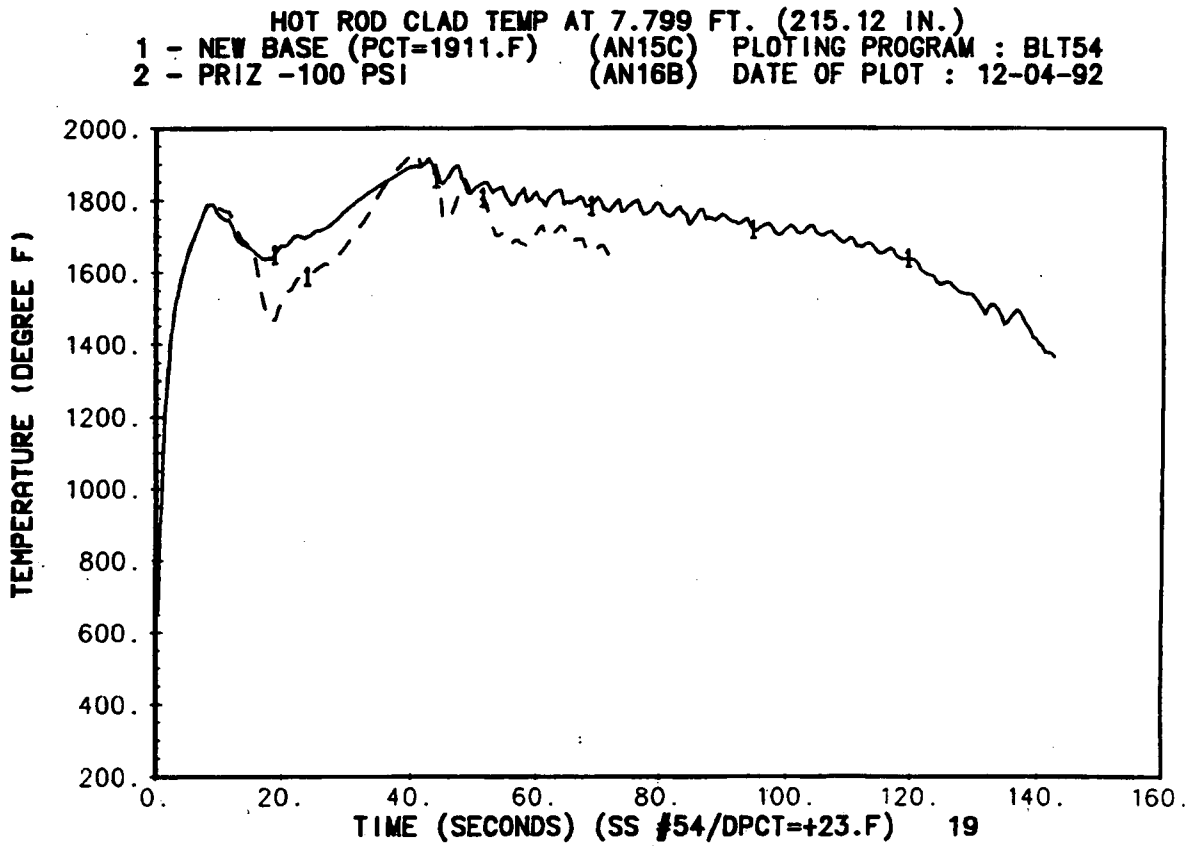

Figure 5-23. PCT Overlay (Case 2.2b)

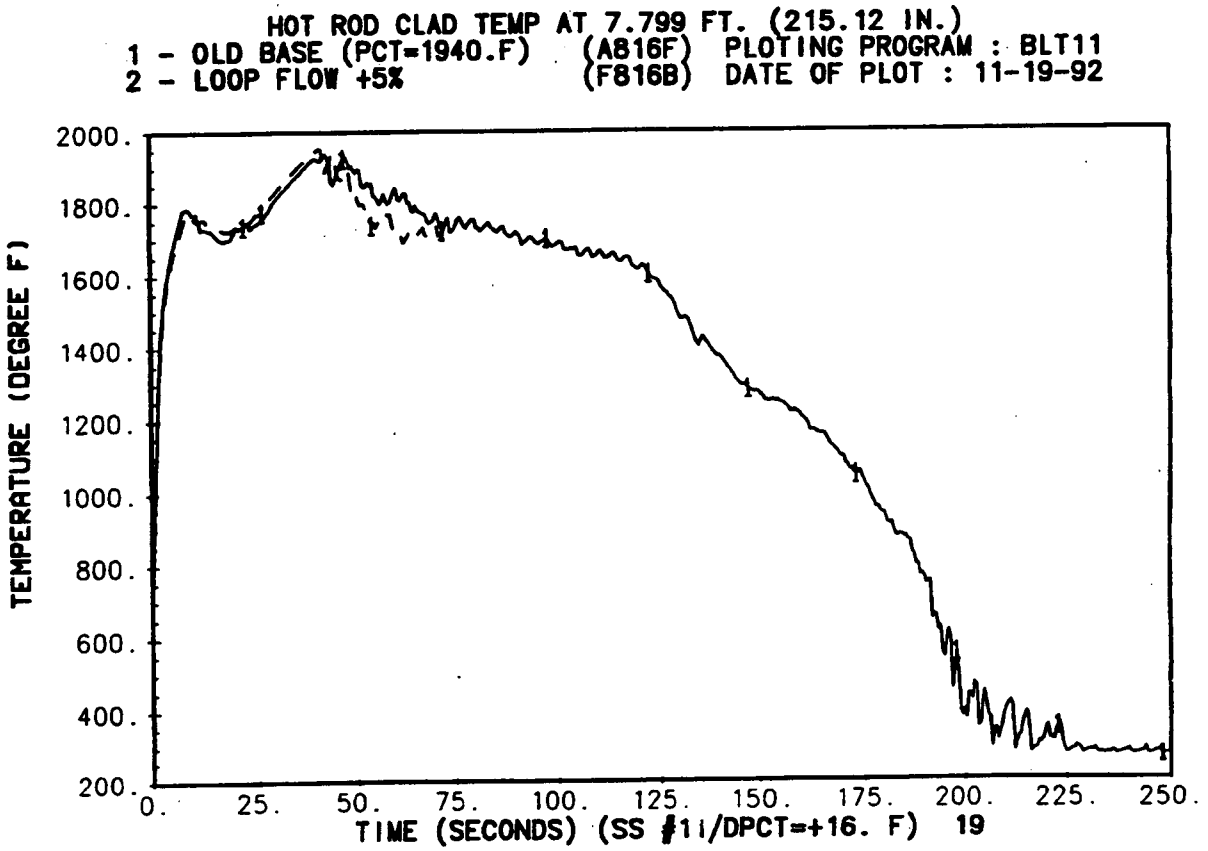

Figure 5-24. PCT Overlay (Case 2.2c)

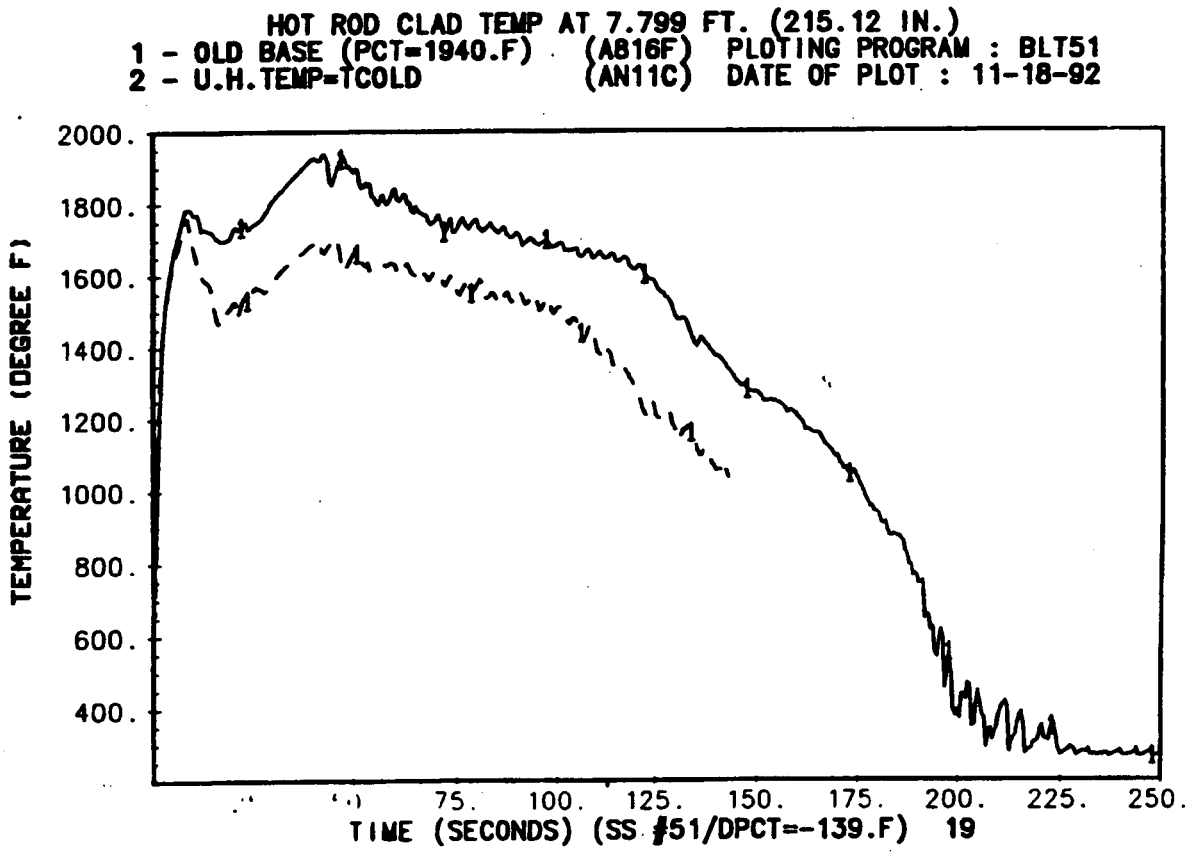

Figure 5-25. PCT Overlay (Case 2.2d)

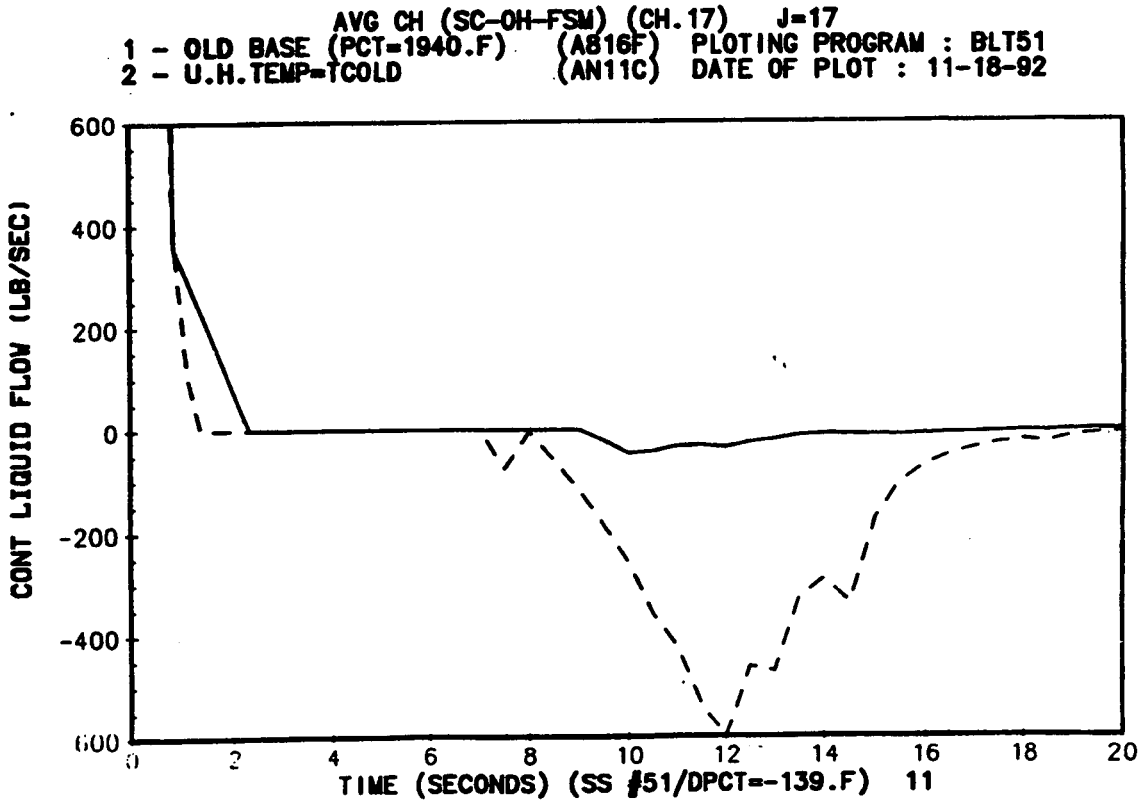

Figure 5-26. Liquid Flow at Top of Core Average Channel (Case 2.2d)

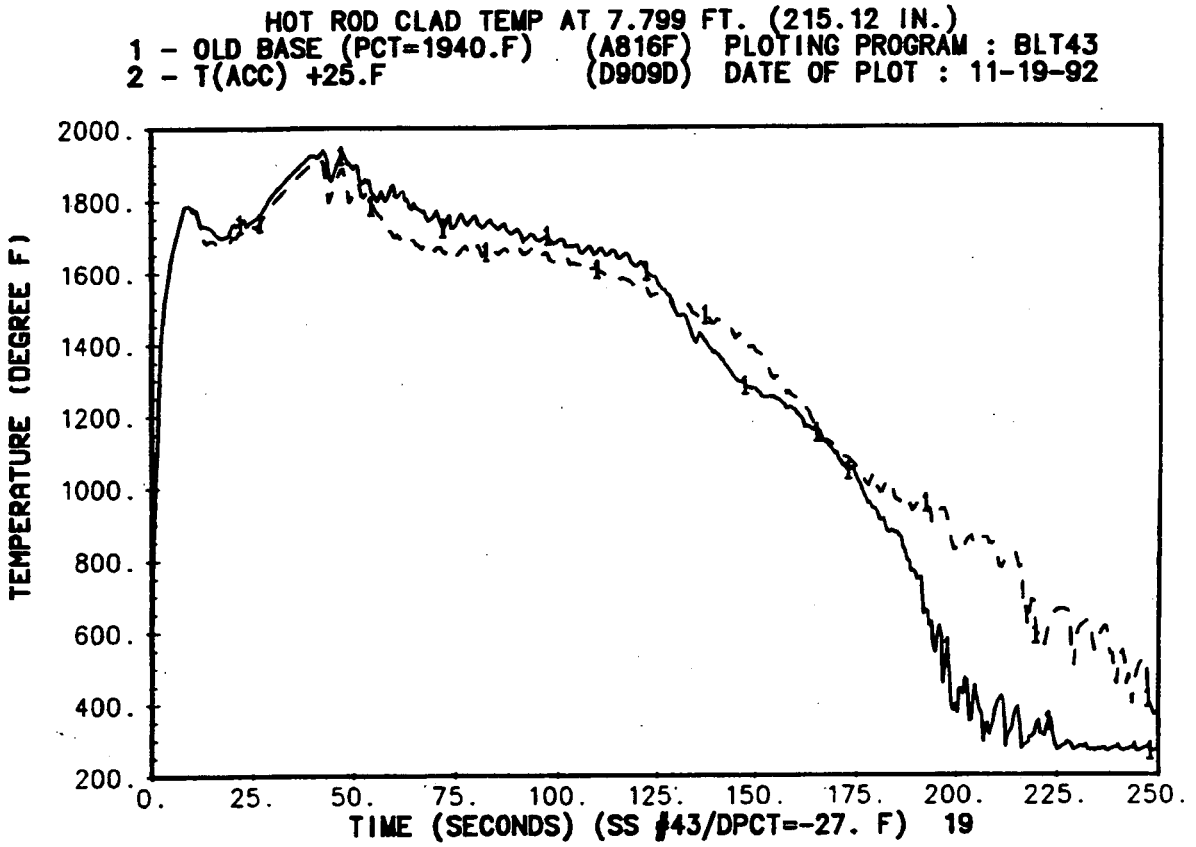

Figure 5-27. PCT Overlay (Case 2.2f)

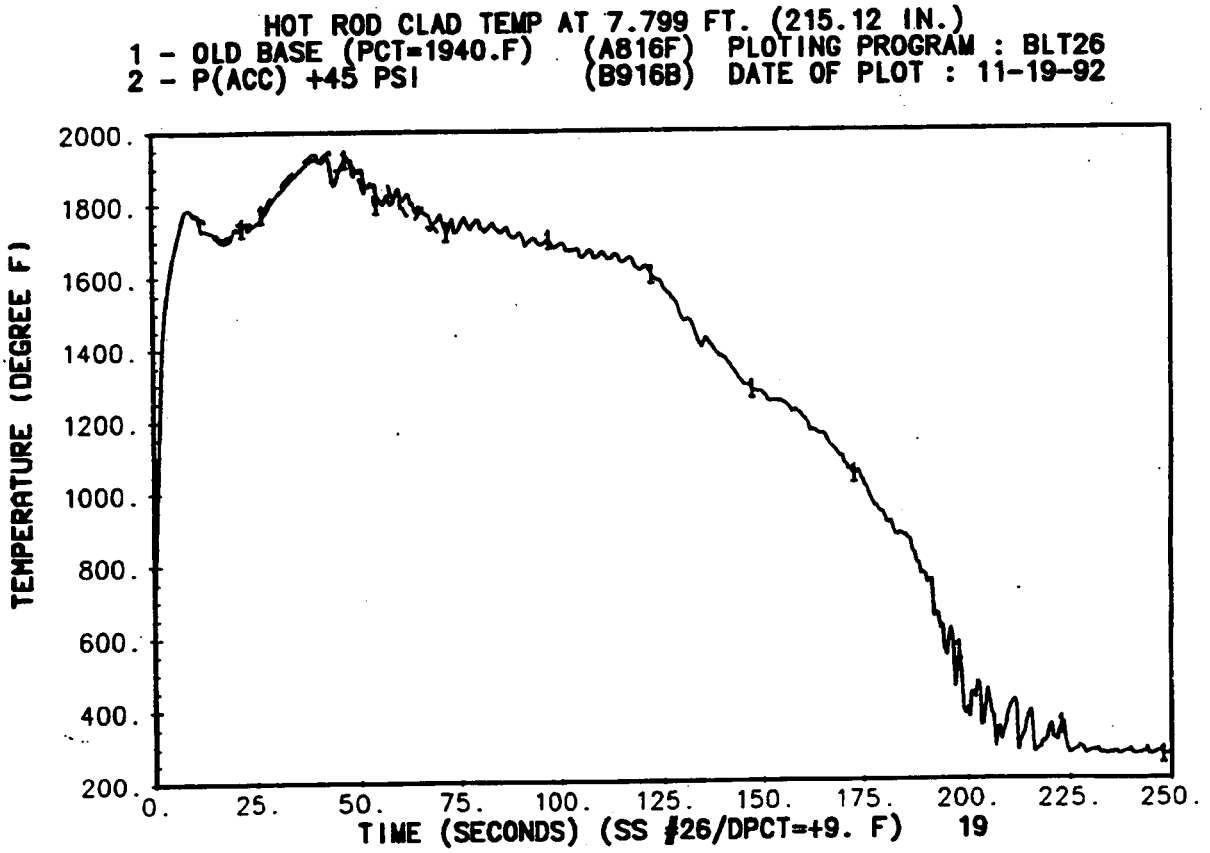

Figure 5-28. PCT Overlay (Case 2.2g)

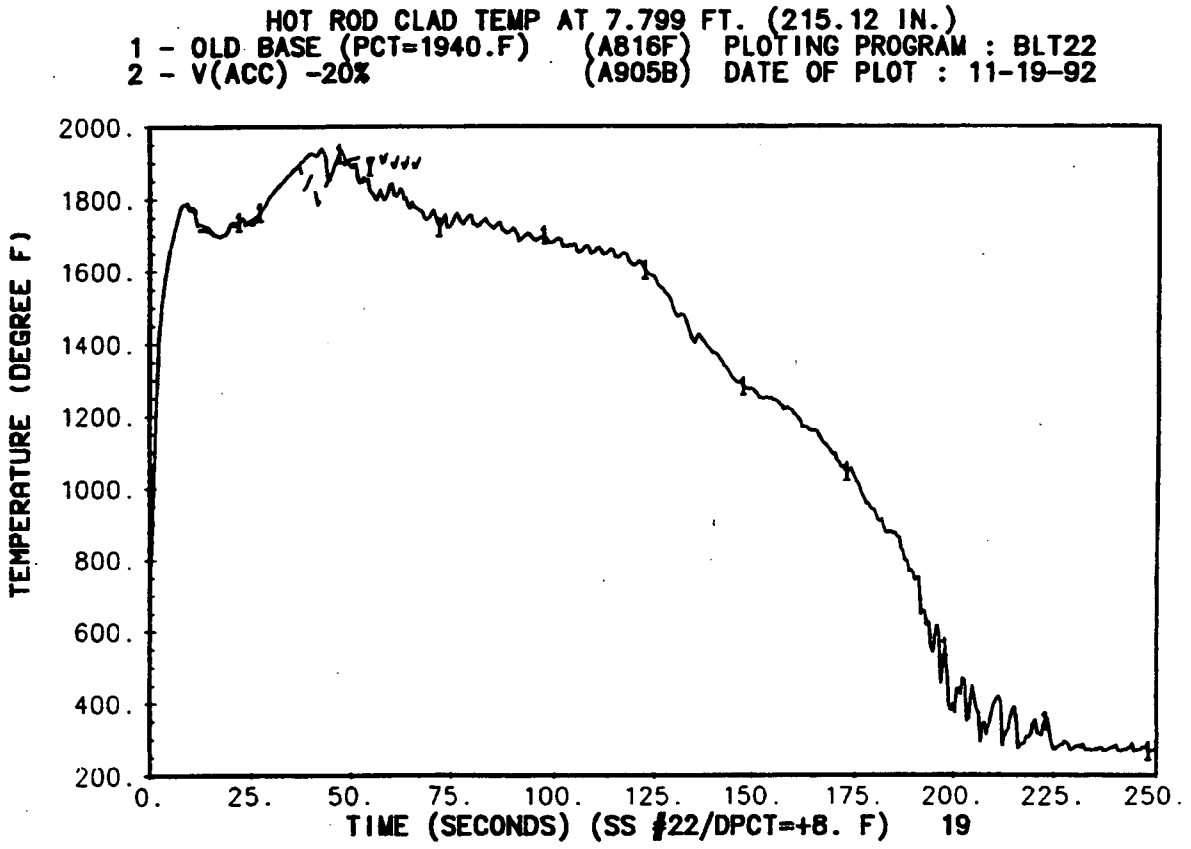

Figure 5-29. PCT Overlay (Case 2.2h)

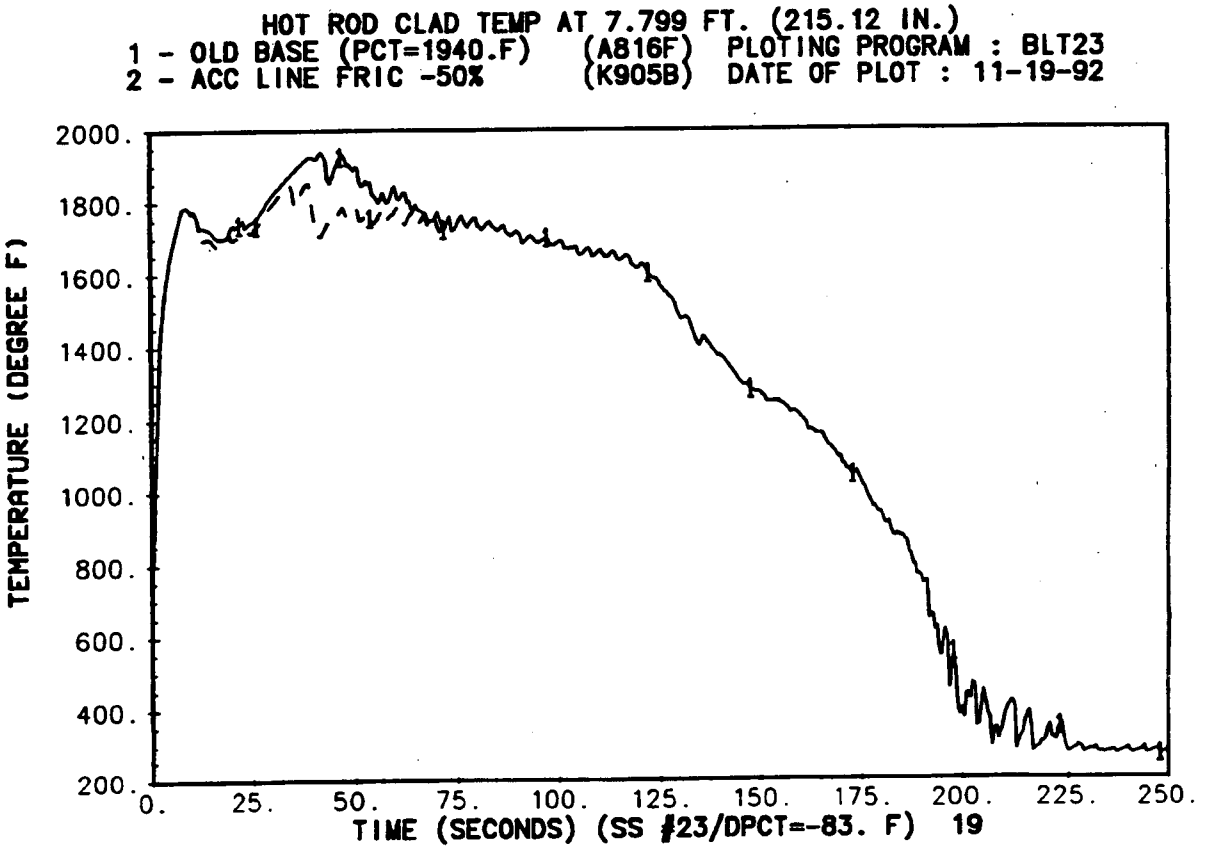

Figure 5-30. PCT Overlay (Case 2.2i)

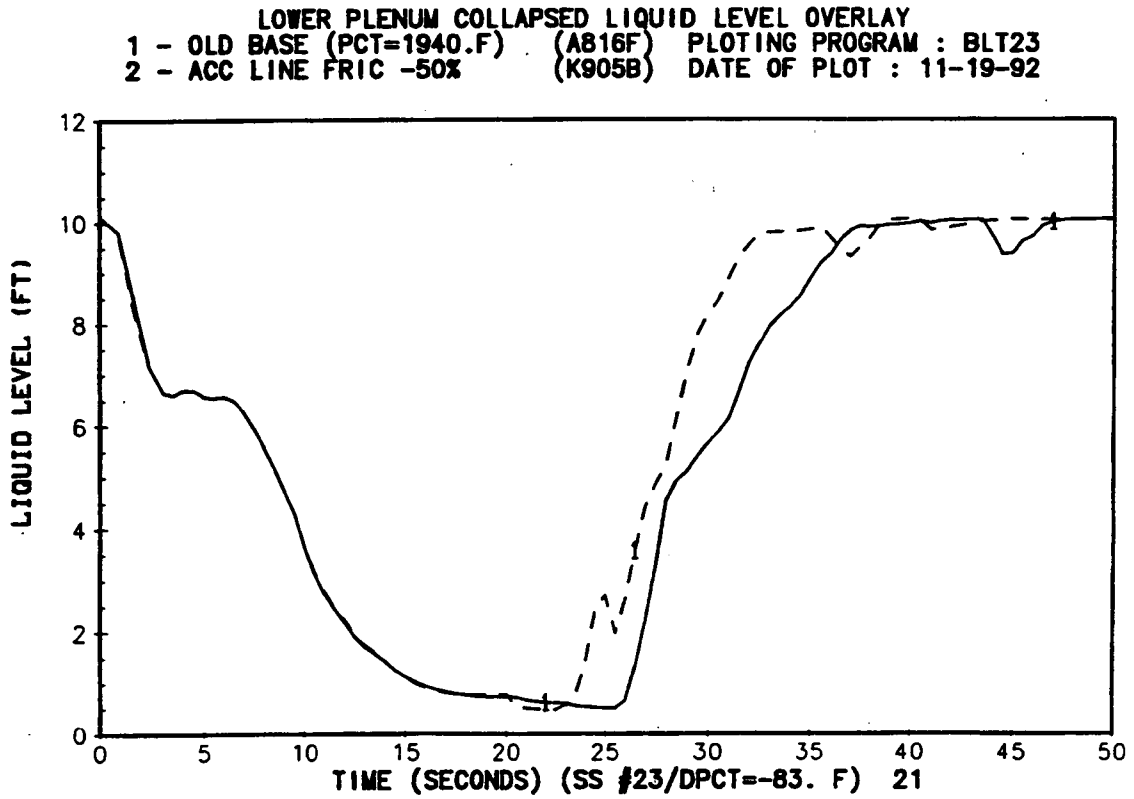

Figure 5-31. Lower Plenum Liquid Level (Case 2.2i)

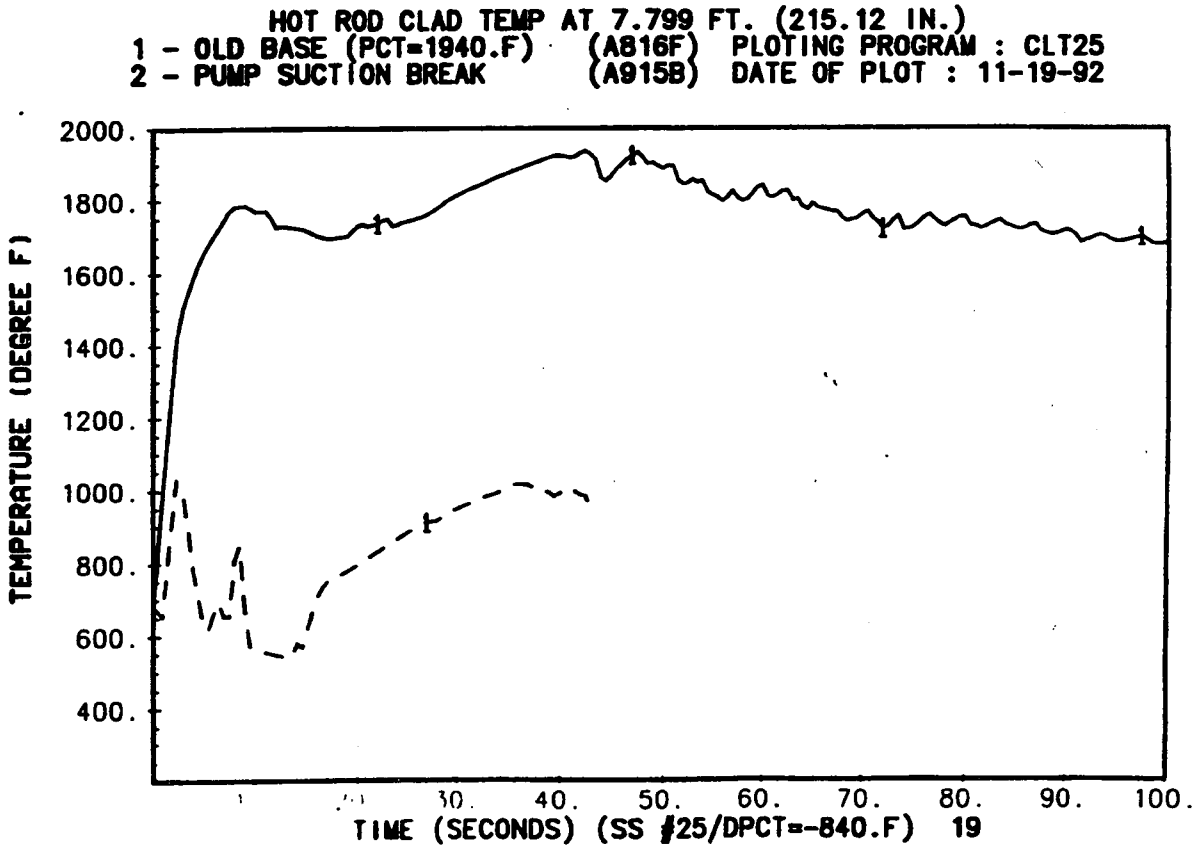

Figure 5-32. PCT Overlay (Case 3.0a)

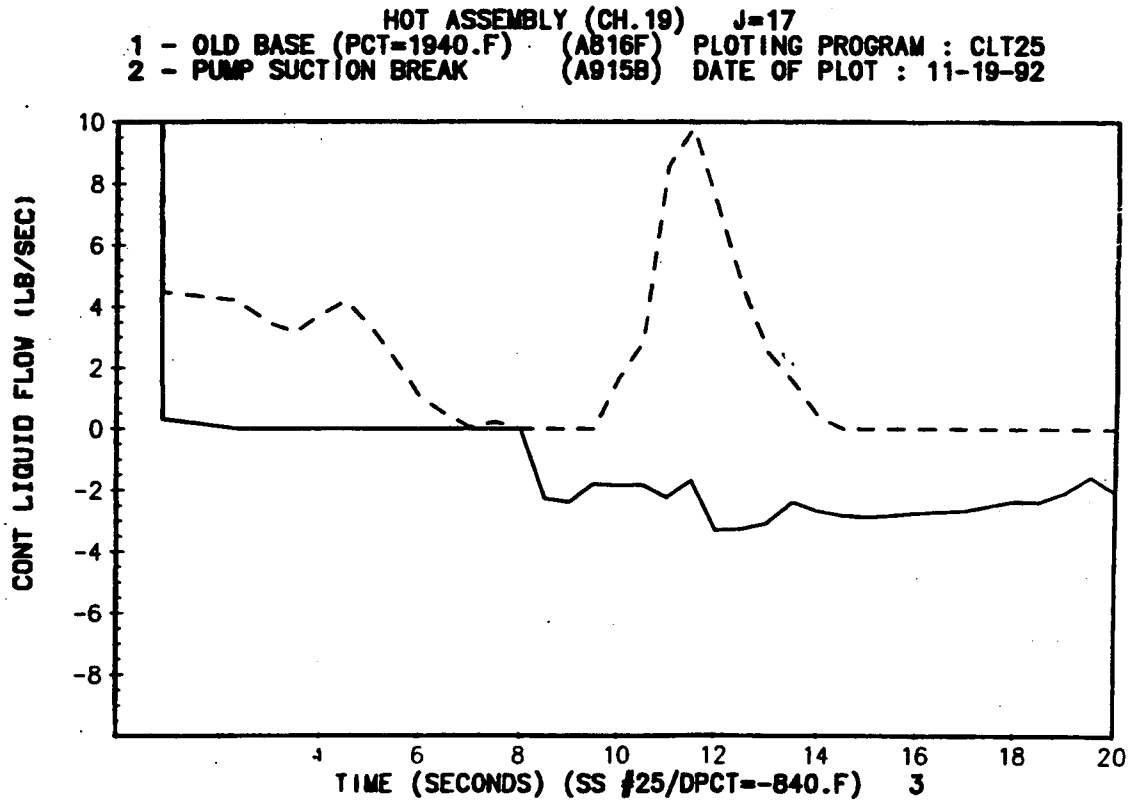

Figure 5-33. Liquid at Top of Hot Assembly (Case 3.0a)

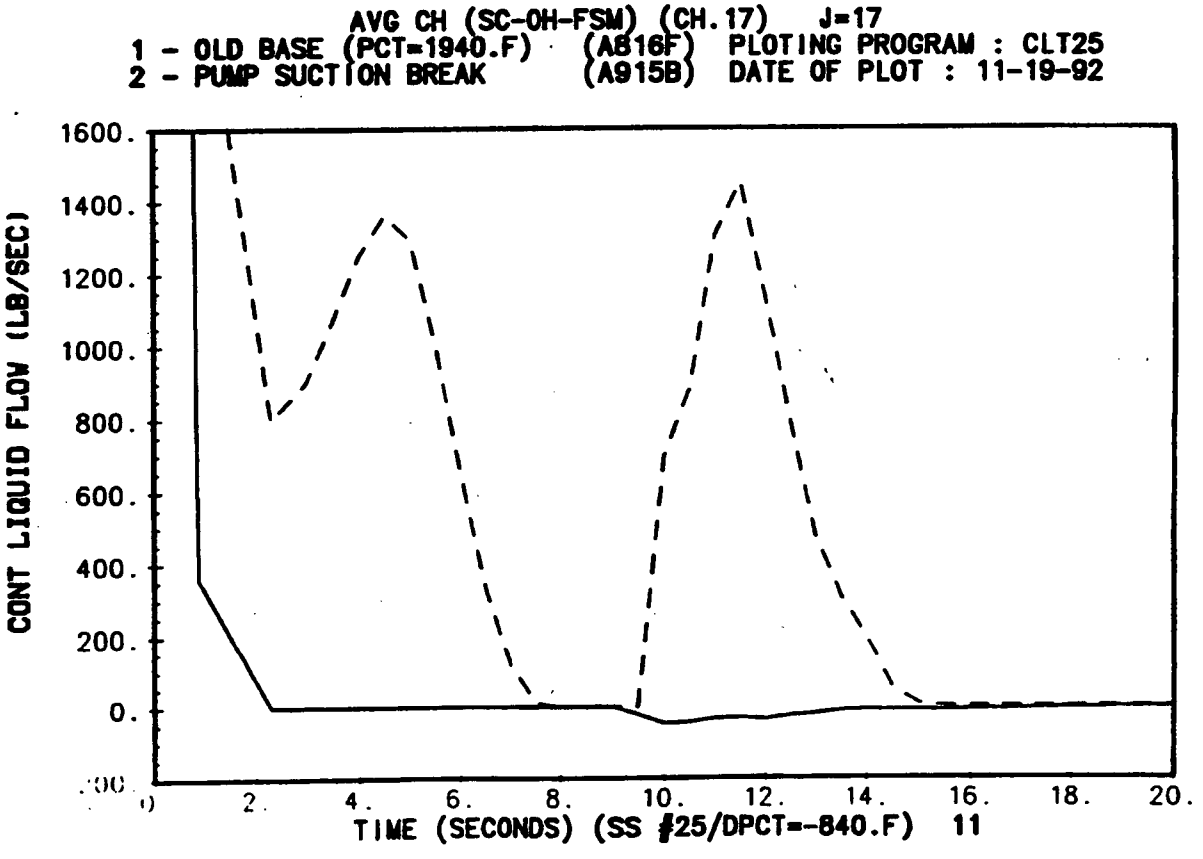

Figure 5-34. Liquid Flow at Top of Core Average Channel (Case 3.0a)

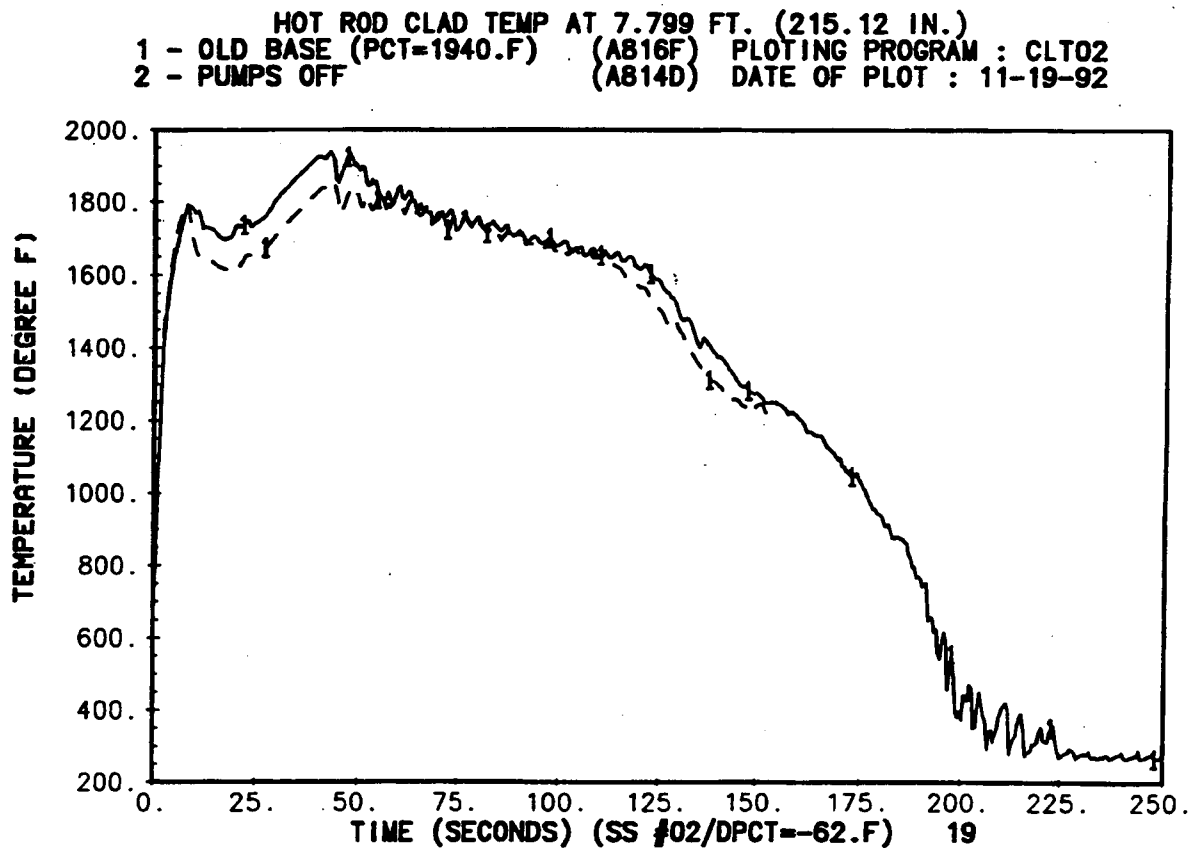

Figure 5-35. PCT Overlay (Case 3.0d)

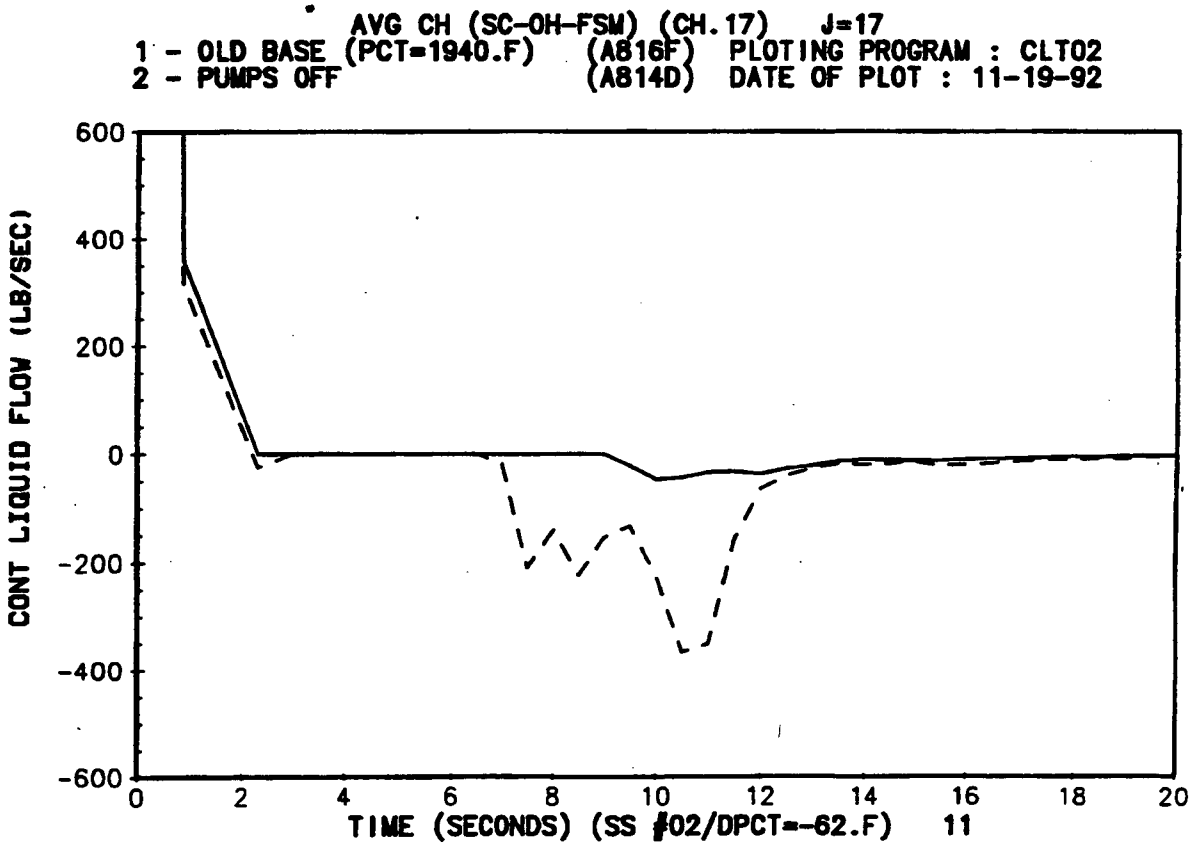

Figure 5-36. Liquid Flow at Top of Core Average Channel (Case 3.0d)

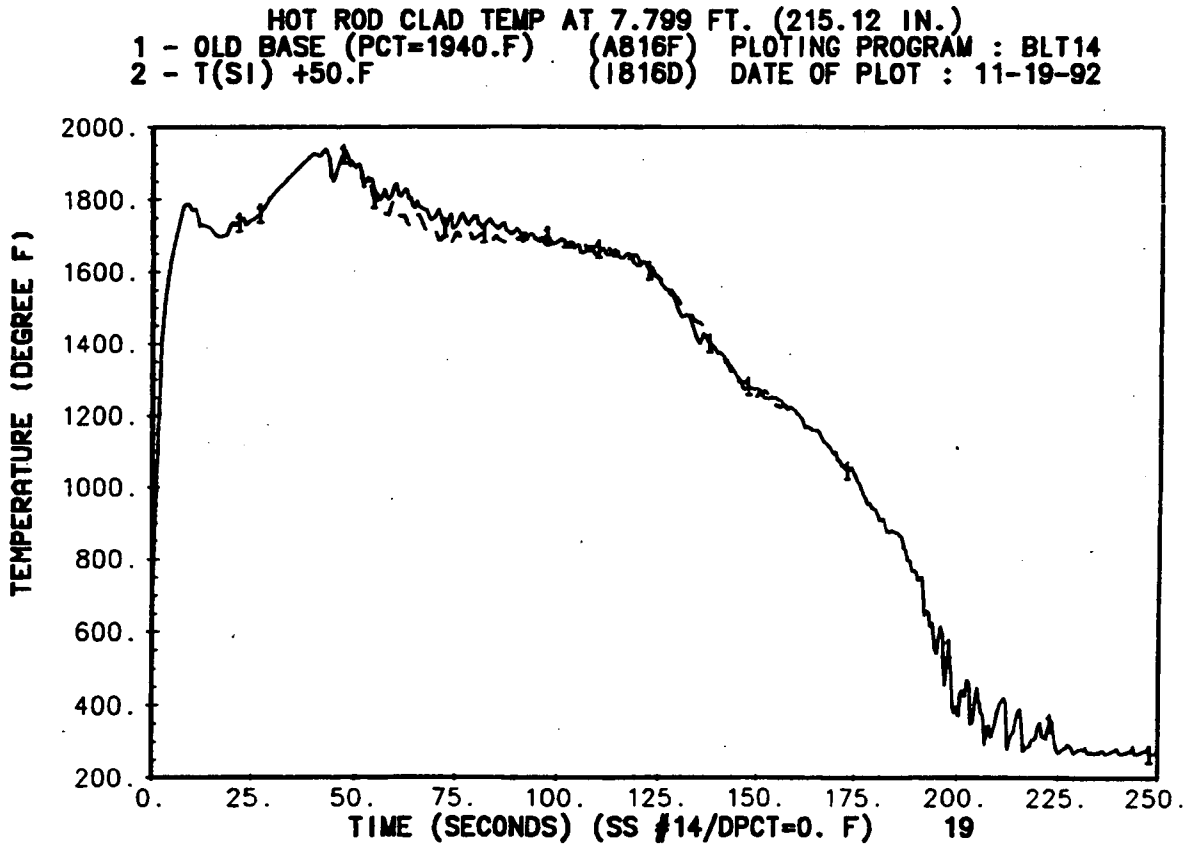

Figure 5-37. PCT Overlay (Case 3.0f)

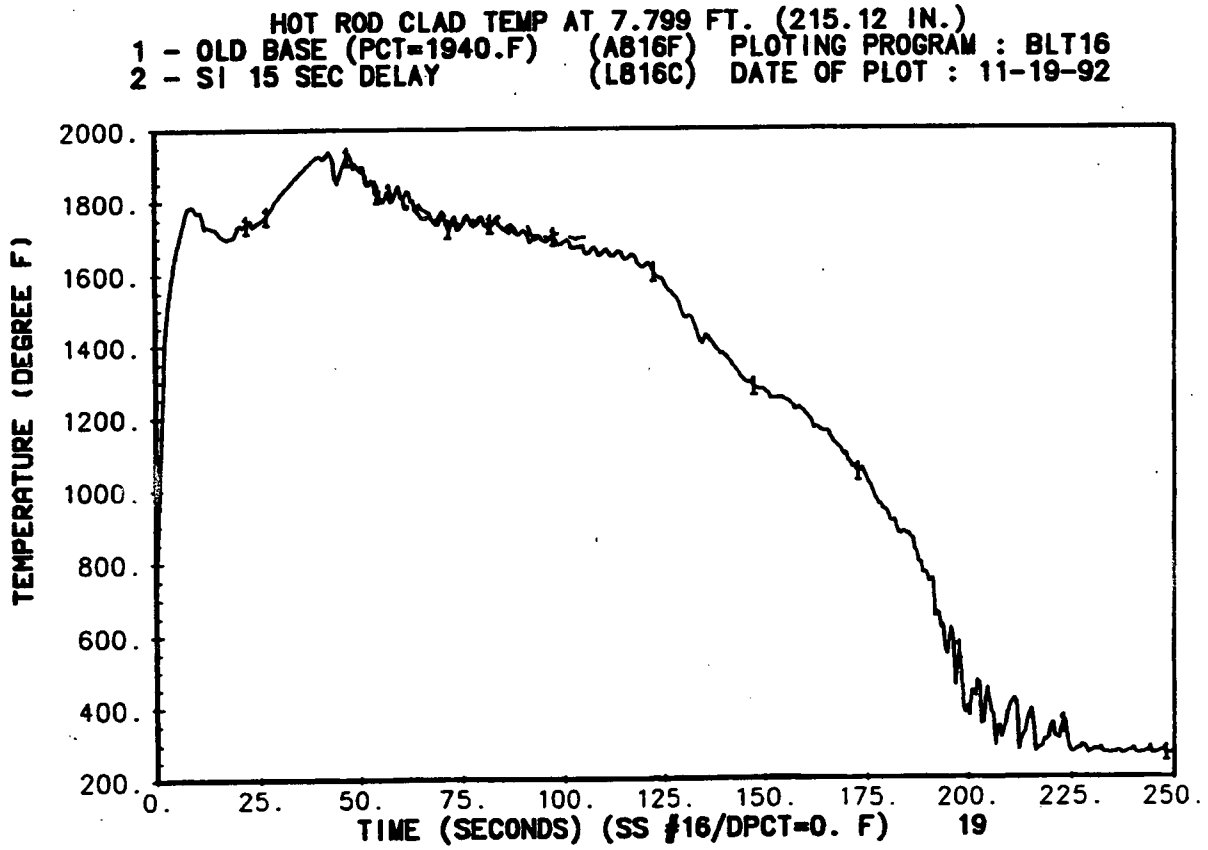

Figure 5-38. PCT Overlay (Case 3.0g)

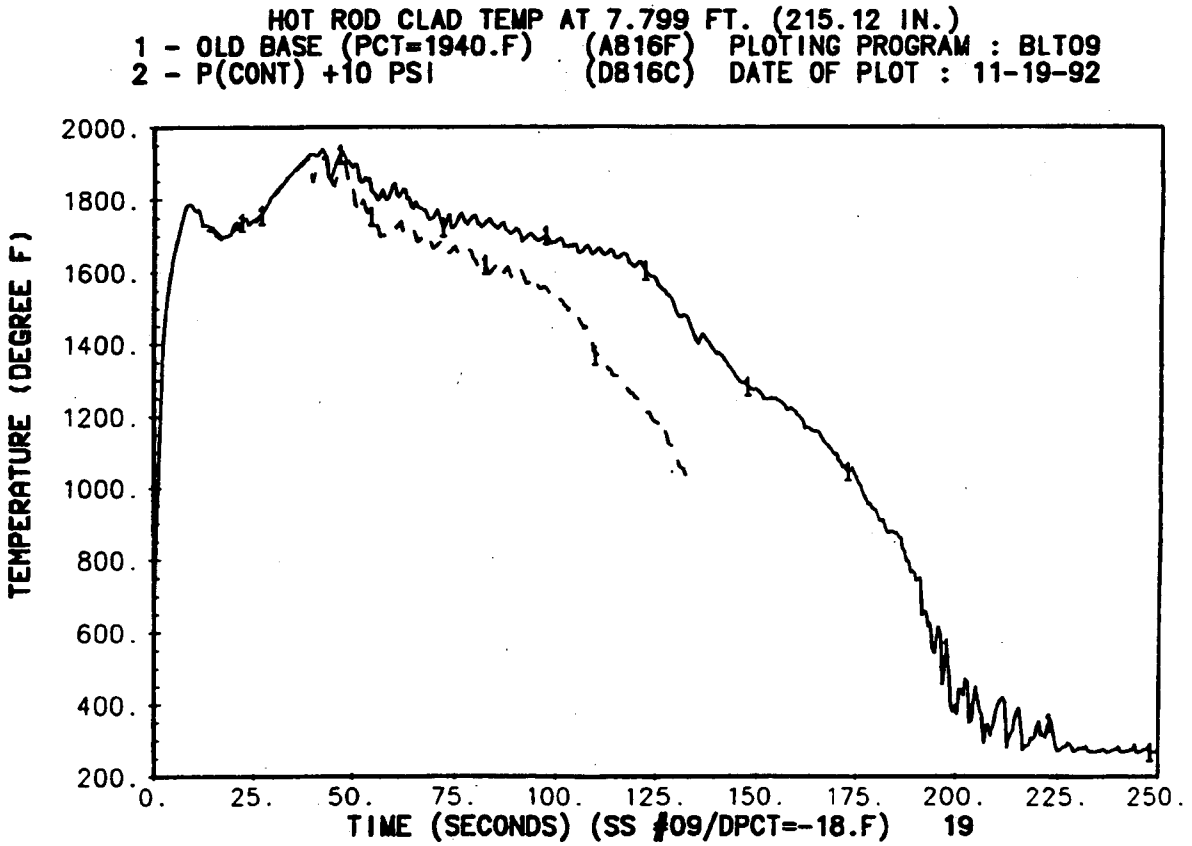

Figure 5-39. PCT Overlay (Case 3.0h)

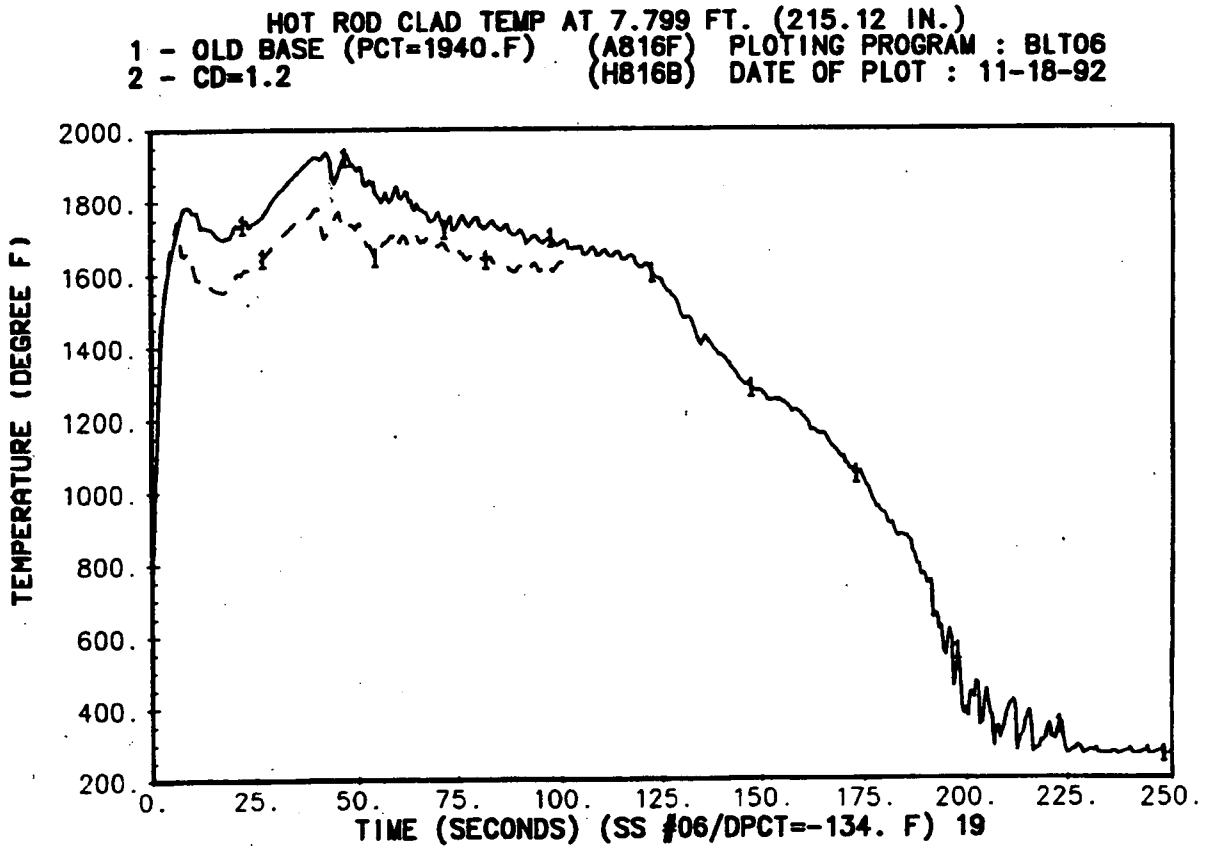

Figure 5-40. PCT Overlay (Case 4.0a)

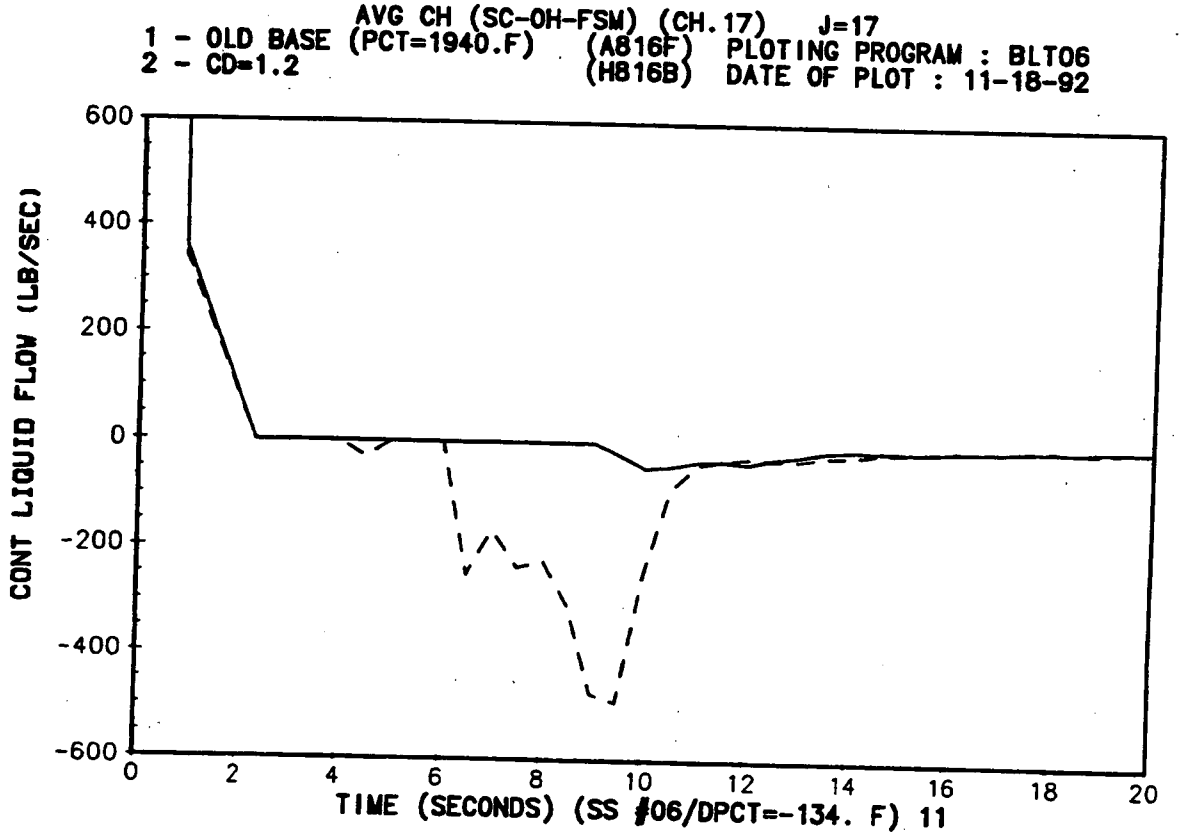

Figure 5-41. Liquid Flow at Top of Core Average Channel (Case 4.0a)

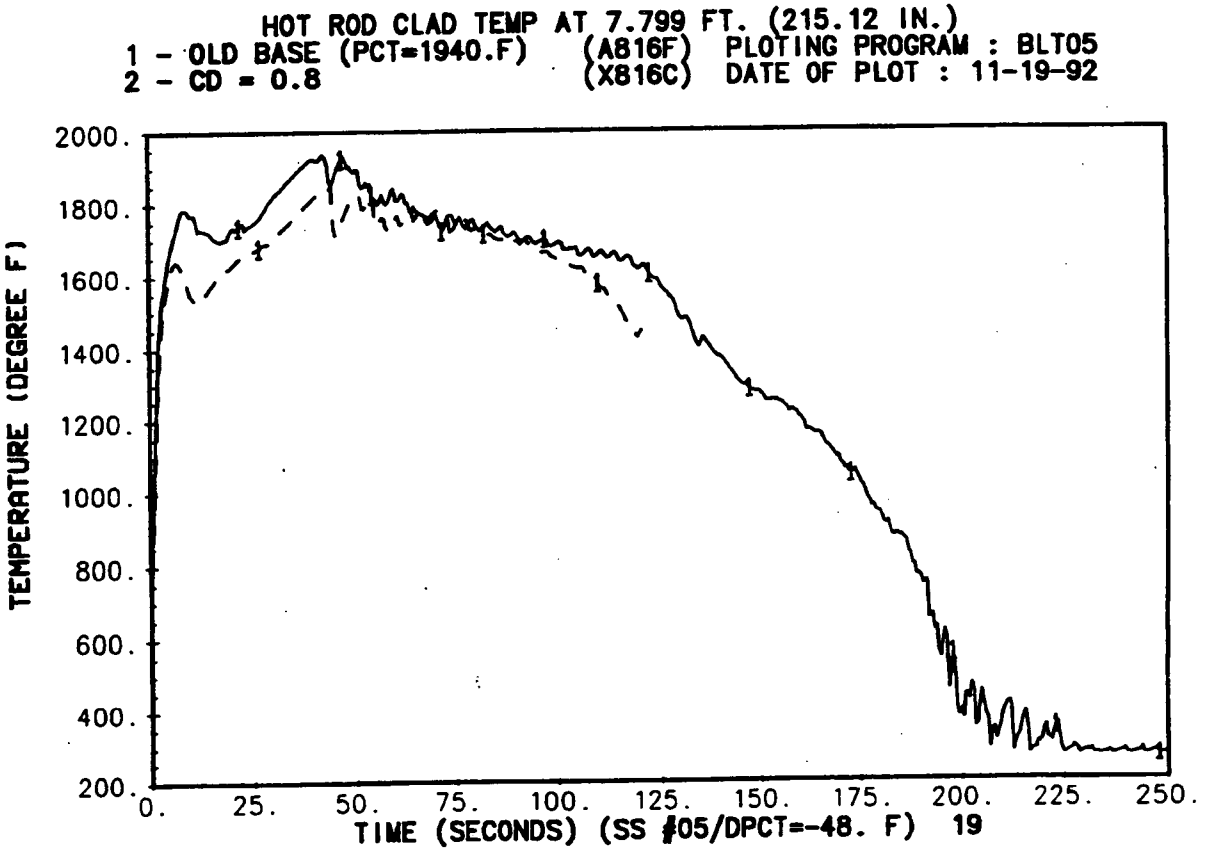

Figure 5-42. PCT Overlay (Case 4.0a)

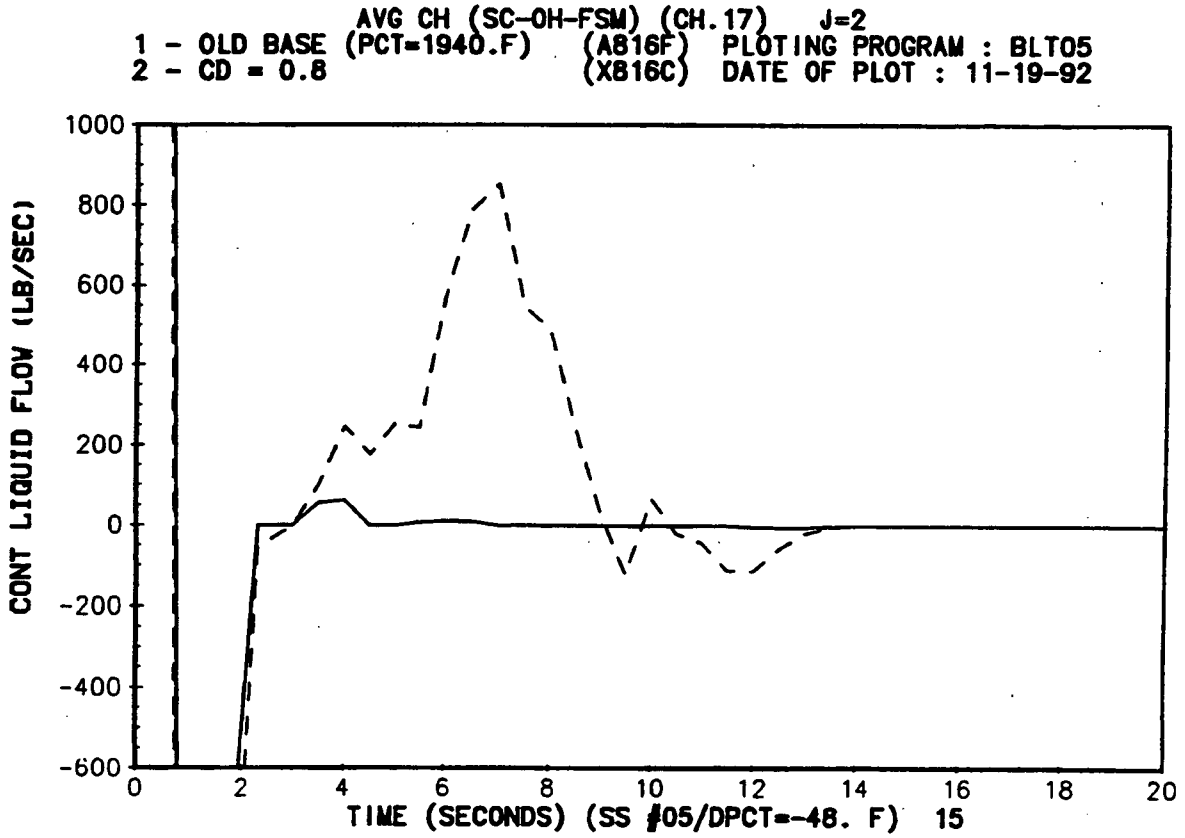

Figure 5-43. Liquid at Top of Core Average Channel (Case 4.0a)

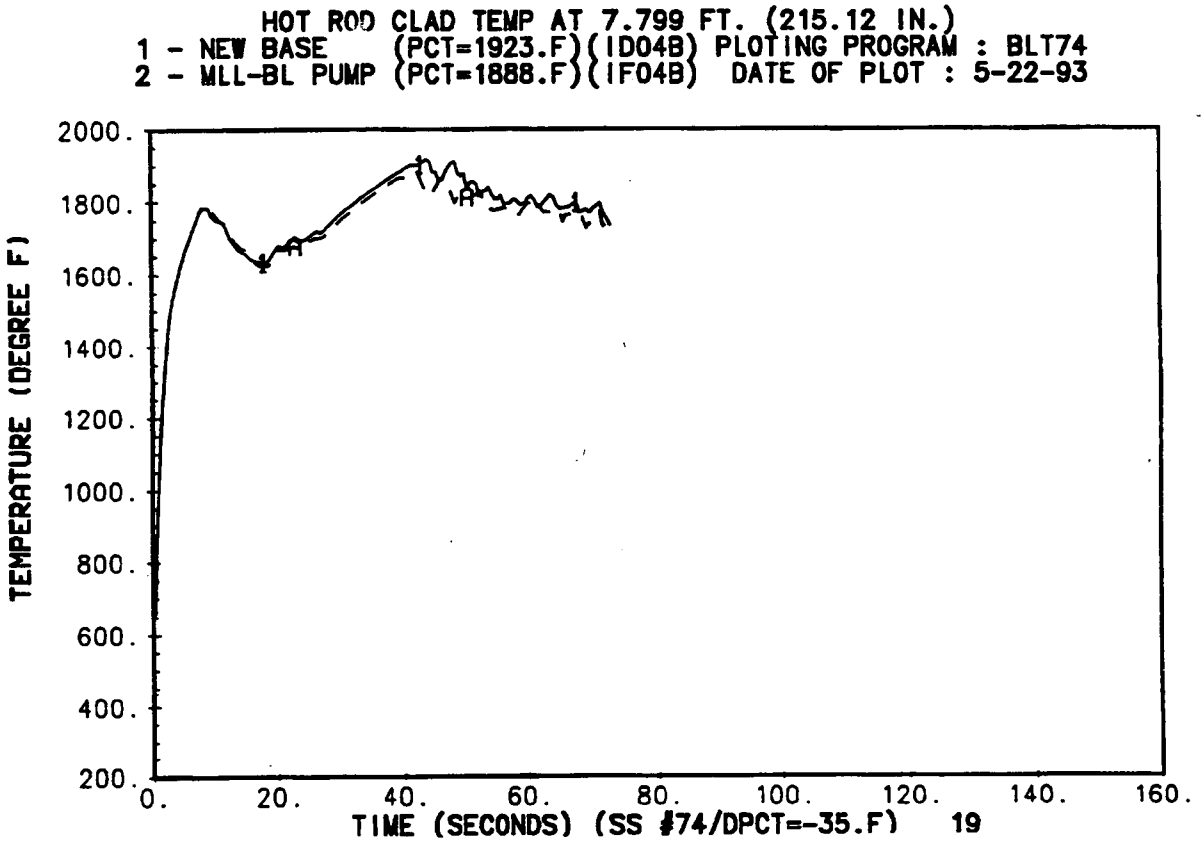

Figure 5-44. PCT Overlay (Case 4.0b)

5-5 Power Distribution Response Surface Results

The first step in the generation of the power distribution response surface is to define the minimum number of parameters which are required to distinguish different power shapes. As discussed in Section 21 of the CQD, describing the power shape in terms of the maximum linear heat rate and the one-third integrals of power has been used successfully in prior analyses. In this case, we will use the maximum linear heat rate as described by F_Q, the total hot rod power as described by $F_{\Delta H}$, and the two partial integrals ***PBOT*** and ***PMID***.

A cubic spline was used to generate axial power distributions which fit specific values of these four parameters. This was done in order to have a means of specifying exactly the power shape attributes while generating axial power distributions which reflect actual power distributions. While these shapes are purely mathematical constructions, they reasonably reflect actual shapes generated by the core design.

The second step is to define the range of variation of the shape parameters, and generate the corresponding shapes. The ranges are established from actual core design information which was presented in Section 21 of the CQD. It was shown that the range of partial integrals was affected by the peaking factor and other limits imposed on the design; the higher the peaking factor, the wider the possible distribution of partial integrals, reflecting more asymmetric shapes. For each range of peaking factors, a corresponding range of partial integrals can be established. The range of F_Q lies between the calculated baseload value and the maximum calculated value, $F_{Q,BE}$.

The third step is to generate a run matrix and corresponding power distributions for generation of PCT data. The design used for this analysis is described in Section 26 of the CQD. The power shape calculated results for IP2 are presented in Table 5-3.

The base case which is taken as a reference for this element is the result from shape 10. This shape was chosen as the reference because it is at the mid-point of the peaking factor range, and has moderate power shape skewing.

The results indicate that, as expected, power distributions with the highest linear heat rate result in high PCT. It should be noted, however, that the conditions for these cases will exist only rarely in the uncertainty evaluation. A second observation which was made during these calculations was that a second reflood peak sometimes appeared, particularly for top skewed shapes. In the case of IP2, this occurred for shape 13. It was decided to fit a response surface to the maximum reflood PCT, rather than fit two surfaces for two time periods. In Table 5-4, the maximum reflood PCT appears in the second column.

The response surfaces were obtained by least squares regression. The output from the response surface is the difference in °F from the reference shape PCT. The response surface is a polynomial with a constant coefficient and 5 or 6 additional terms.

Table 5-3
Power Shape PCT Data (IP2)

Shape No.	Attributes	$PCT_{2,RCTJ}(PCT-PCT*)$		
		j=1	j=2	j=3
1	High F_Q, $F_{\Delta H}$, bottom skewed	1920(55)	2232(253)	1860(-20)
2	High F_Q, $F_{\Delta H}$, top skewed	1960(95)	2172(193)	1973(73)
3	High F_Q, $F_{\Delta H}$, top skewed	1945(80)	2165(186)	2110(230)
4	High F_Q, $F_{\Delta H}$, top skewed	1935(70)	2123(144)	2000(120)
5	High F_Q, $F_{\Delta H}$, bottom skewed	1755(-110)	1905(-74)	1545(-335)
6	High F_Q, $F_{\Delta H}$, bottom skewed	1855(-10)	2053(74)	1750(-130)
7	Baseload F_Q, High $F_{\Delta H}$, uniform	1750(-115)	1784(-195)	1770(-110)
8	Nominal F_Q, High $F_{\Delta H}$, bottom skewed	1742(-123)	1905(-74)	1618(-262)
9	High F_Q, High $F_{\Delta H}$, bottom skewed	1880(15)	2111(132)	1800(-80)
10	Nominal F_Q, High $F_{\Delta H}$, top skewed	1865(0)	1979(0)	1880(0)
11	High F_Q, High $F_{\Delta H}$, top skewed	1875(10)	1982(3)	1884(4)
12	Nominal F_Q, High $F_{\Delta H}$, uniform	1818(-47)	1940(-39)	1778(-102)
13	Nominal F_Q, High $F_{\Delta H}$, uniform	1810(-55)	1901(-78)	1901(21)
14	Nominal F_Q, Low $F_{\Delta H}$, top skewed	1835(-30)	1889(-90)	1845(-35)
15	High F_Q, Low $F_{\Delta H}$, top skewed	1910(45)	2090(111)	1990(110)

5-6 Break Flow Response Surface Results

As discussed in Section 26 of the CQD, several variables affecting break flow were combined into two parameters.

A response surface equation is sought which describes the effect of break discharge coefficient (C_D) and broken loop nozzle loss coefficient (K_N) on PCT.

This response surface captures two effects found to be important: The effect of variations in break discharge coefficient, which is applied equally to both sides of the break, and the effect of variations in cold leg nozzle resistance, which changes the relative resistance between the flow path from the core to the break via the loop, and from the core to the break via the vessel lower plenum and downcomer.

The run matrix shown in Table 5-4 was performed for IP2 with the results also indicated in Table 5-4. The base case is taken as Run 1, which is one of the scoping base cases from Section 3. For the base case, the actual PCT is shown. For the other cases, the PCT change is shown.

Table 5-4
Break Parameter Results (IP2)

Run No.	Attributes	$\Delta PCT_j = PCT_j - PCT_{BASEj}$	
		j=1	j=2
1*	Nominal C_D, K_N	1838	1935
2	Nominal C_D, High K_N	-32	-5
3	Nominal C_D, Low K_N	-32	-106
4	Low C_D, Nominal K_N	-118	-43
5	Low C_D, High K_N	-217	-100
6	Low C_D, Low K_N	21	55
7	High C_D, Nominal K_N	-37	-129
8	High C_D, High K_N	-22	-56
9	High C_D, Low K_N	-141	-181

In all these cases there was no second reflood peak. The resulting response surfaces were obtained by least square fits after several trials with different combinations of parameters using methods similar to those employed for the power distributions.

5-7 Initial Condition Bias and Uncertainty

The purpose of this uncertainty element is to capture all the remaining uncertainties, which have a relatively minor effect on PCT. It is estimated from the scoping study results using the method outlined in CQD Section 26.

The PCT ranges and uncertainties are shown in Table 5-5 for IP2. The sensitivity values are estimated from the scoping study results, and are expressed in terms of the change in PCT for a 1 percent change in parameter value. P_{BASE} is the value of the parameters in the base PCT calculation. P_{NOM} is the expected parameter value in the plant. $P_{RNG\%}$ or P_{LIM} is the parameter range during normal operation, or an upper limit value based on scoping study results and/or technical specifications. The generic values were estimated by averaging the sensitivities among the three plants described in the CQD. These results are judged to provide a conservative estimate of the uncertainty from these parameters, owing to the conservative nature of the scoping analysis, provided that the range of the parameter is not increased beyond the range shown in the table.

Table 5-5
Initial Condition Bias and Uncertainty (IP2)

PARAM	P_{BASE}	P_{NOM}	$P_{RNG\%}$ or P_{LIM}	$\partial PCT/\partial P\%$		ΔPCT_{4j}		σ_{4j}	
				1	2	1	2	1	2
RIP	864	864	±10%		1*				10
PLOW	0.4	0.4	±200%		0.3*				26
T_{avg}	583	583	<587		3				1
P_{RCS}	2250	2250	<2310		7				11
T_{ACC}	105	105	<130		-1				--
P_{ACC}	655	655	±7%		2				8
V_{ACC}	795	795	±10%		-1				6
K_{ACC}	NOM	NOM	±20%		2*				23
T_{SI}	90	90	<90						
Initial Condition Bias, Uncertainty						0	0	0	39

* - generic value

SECTION 6
OVERALL PCT UNCERTAINTY EVALUATION

6-1 Combining the Uncertainties

The PCT equation was presented in Section 2. Each element of uncertainty is considered to be independent of the other. In words, the PCT equation can be described this way:

The code predicts a value of the hot rod PCT which is conservatively biased with respect to hot rod uncertainties, but is the expected value with respect to break flow, power distribution, and model uncertainties. The PCT is then adjusted by ΔPCT_1 to predict the expected PCT with respect to code model uncertainties, by ΔPCT_2 to predict the expected PCT when all possible power distribution variations are accounted for, by ΔPCT_3 to predict the expected PCT when all possible break flow parameter variations are accounted for, and by ΔPCT_4 to predict the expected PCT when remaining initial conditions are accounted for. Each bias element includes an inherent uncertainty.

Each bias component is considered a random variable, whose uncertainty and distribution is obtained directly, or is obtained from the uncertainty of the parameters of which the bias is a function. Since PCT_j is the sum of these biases, it also becomes a random variable. A PCT frequency distribution is constructed using the methods described in Sections 26 and 27 of the CQD. The resulting cumulative distribution is shown in Figure 6-1.

The estimate of the PCT at 95 percent probability is determined by finding that PCT below which 95 percent of the calculated PCT's reside. This estimate is the licensing basis PCT, under the revised ECCS rule.

The results for IP2, are given in Table 6-1. These results include an additional bias to account for the effect of ZIRLO© cladding. As expected, the difference between the 95 percent value and the average value increases with increasing time, as more parameter uncertainties come into play. It should also be noted that the average value of PCT is well below the base case values used for both the scoping and response surface studies. This indicates that the variations predicted by the response surfaces are conservative (see below).

Table 6-1
Overall Results (IP2)

Component	j=1	j=2
$PCT^{average}$	<1735	<1684
$PCT^{95\%}$	<1996	<2040
Max Oxidation	0	<10%
Tot Oxidation	0	<0.25%

6-2 Plant Operating Range

The expected PCT and its uncertainty developed above is valid for a range of plant operating conditions. In contrast to current Appendix K calculations, many parameters in the base case calculation are at nominal values. The range of variation of the operating parameters has been accounted for in the uncertainty evaluation. Table 6-2 summarizes the operating ranges for IP2. If operation is maintained within these ranges, the LOCA analyses developed in this report using WCOBRA/TRAC are considered to be valid.

Table 6-2
Plant Operating Range Allowed by the LOCA Analysis (IP2)

Parameter			Operating Range
1.0	**Plant Physical Description**		
	a)	Dimensions	No grid deformation during LOCA + SSE
	b)	Flow resistance	N/A
	c)	Pressurizer location	N/A
	d)	Hot assembly location	Anywhere in core
	e)	Hot assembly type	Fresh 15X15 OFA or V+ or burned, no restrictions Zirc-4 or ZIRLO cladding
	f)	SG tube plugging level	≤ 25%
2.0	**Plant Initial Operating Conditions**		
	2.1	Reactor Power	
		a) Core avg linear heat rate (AFLUX)	Core power ≤ 102% of 3216 MWt
		b) Peak linear heat rate (PLHR)	$F_Q \leq 2.5$
		c) Hot rod avg lr ht rt (HRFLUX)	$F_{\Delta H} \leq 1.7$
		d) Hot assembly avg ht rate (HAFLUX)	N/A
		e) Hot assembly pk ht rate (HAPHR)	N/A

Table 6-2 (Cont'd)
Plant Operating Range Allowed by the LOCA Analysis (IP2)

Parameter		Operating Range
	f) Axial power dist (PBOT, PMID)	Table 26-3
	g) Low power region rel pwr (PLOW)	.2 ≤PLOW ≤ .8
	h) Hot assembly burnup	≤ 75000 MWD/MTU, lead rod
	i) Prior operating history	All normal operating histories
	j) MTC	≤ 0 at HFP
	k) HFP boron	Normal letdown
	2.2 Fluid Conditions	
	a) T_{avg}	≤ 587°F
	b) Pressurizer pressure	≤ 2310 psia
	c) Loop flow	≥ 80600 gpm/loop
	d) T_{UH}	Current upper internals
	e) Pressurizer level	Normal level, automatic control
	f) Accumulator temperature	≤ 130°F
	g) Accumulator pressure	$612 \leq P_{acc} \leq 700$ psia
	h) Accumulator volume	$723\ V_{acc} \leq 875$ ft^3

Table 6-2 (Cont'd)
Plant Operating Range Allowed by the LOCA Analysis (IP2)

Parameter		Operating Range
	i) Accumulator fL/D	Current line configuration
	j) Minimum ECC boron	≥ 2000 ppm
3.0	**Accident Boundary Conditions**	
	a) Break location	N/A
	b) Break type	N/A
	c) Break size	N/A
	d) Offsite power	On
	e) Safety injection flow	≥ values used in base case
	f) Safety injection temperature	≤ 90°F
	g) Safety injection delay	≤ 38 seconds (with offsite power) ≤ 45 seconds (without offsite power)
	h) Containment pressure	Current Tech Specs
	i) Single failure	All trains operable
	j) Control rod drop time	N/A

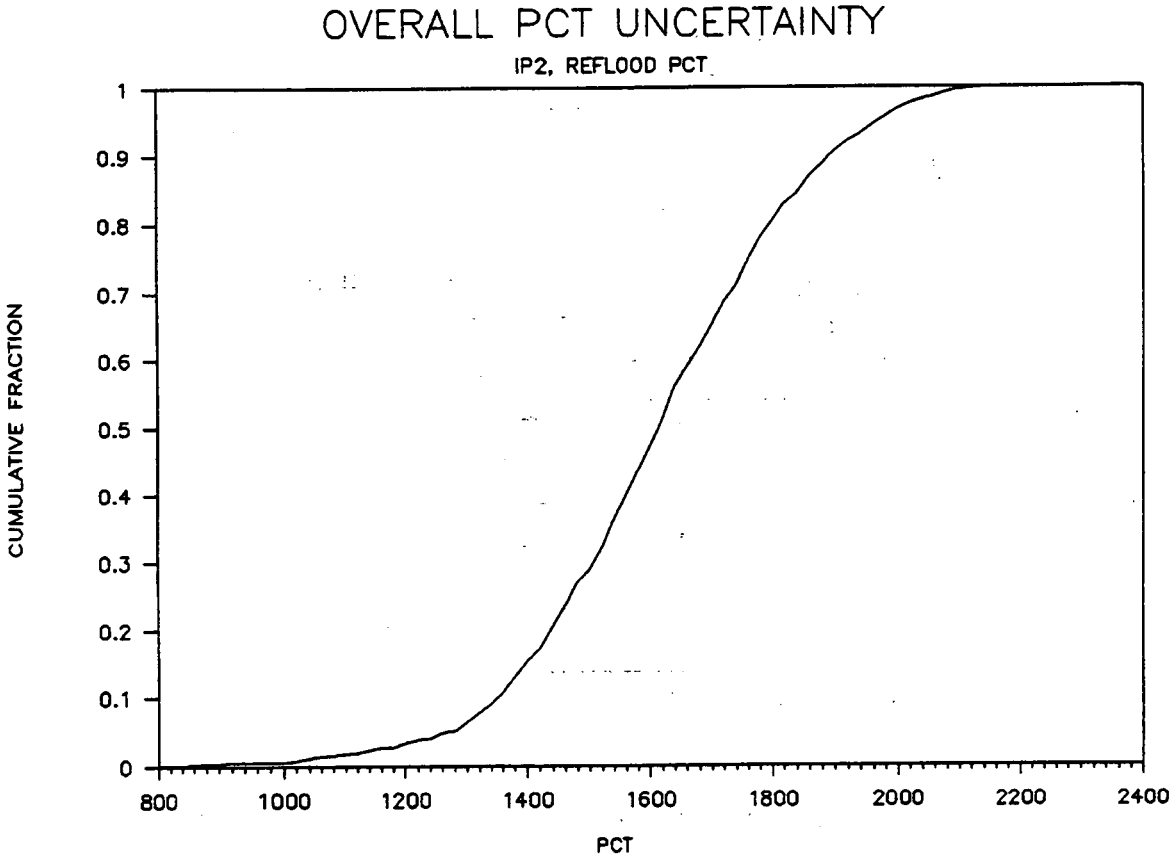

Figure 6-1. Cumulative PCT Distribution for IP2, Reflood PCT

SECTION 7
CONCLUSIONS

It must be demonstrated that there is a high probability that the limits set forth by 10 CFR 50.46 will not be exceed. The limits are:

1) Peak cladding temperature (PCT) less than 2200°F. The results in Table 6-1 indicate that this limit has been met.

2) Maximum cladding oxidation must be less than 0.17 times the cladding thickness before oxidation. Typically, the maximum oxidation occurs at the location where the cladding has burst, since this location includes oxidation on the inside. WCOBRA/TRAC calculates the maximum cladding oxidation as a percent of the cladding thickness. Examination of the calculated transient with the highest PCT (for these plants, the maximum PCT was obtained from power shape 1 or 3) shows the maximum oxidation values given in Table 6-1. Even these maximum possible values are well below the limit.

3) Maximum hydrogen generation must be less than 0.01 times the maximum theoretical amount. An accurate estimate of this quantity involves the calculation of the total oxidation on fuel rods of varying powers, then summing the oxidation over all the fuel rods in the core. Examination of the total oxidation on the hot assembly rod for the limiting transient discussed above indicates that for the hot assembly itself the total amount oxidized is less than 0.01 times the maximum theoretical amount (Table 6-1). Even assuming the entire core reacts as the hot assembly, this limit is met.

4) Coolable geometry must be maintained. This requirement is met both by demonstrating that PCT remains below 2200°F, and by demonstrating that seismic and LOCA forces are not sufficient to distort the fuel assemblies to the point that the core is uncoolable. For the plant described in this report, structural analyses described in the plants FSAR's demonstrate that no distortion occurs.

5) Long term cooling must be demonstrated. While WCOBRA/TRAC is typically not run past full core quench, all base calculations are run well past PCT turnaround and past the point where increasing vessel inventories are calculated. The conditions at the end of the WCOBRA/TRAC calculation indicate that the transition to long term cooling is under way even before the entire core is quenched.

This safety analysis therefore demonstrates that Indian Point Unit 2, with its revised operating range, continues to meet the requirements of 10CFR50.46.

SECTION 8
REFERENCES

10 CFR Part 50, "Acceptance Criteria for Emergency Cooling Systems for Light Water Cooled Nuclear Power Plants," Federal Register 39, (3), Jan. 4, 1988.

"Emergency Core Cooling Systems: Revisions to Acceptance Criteria," Federal Register V53, N180, pp. 35996-36005, Sept. 16, 1988.

Bordelon, F. M., 1974, "Containment Pressure Analysis Code," WCAP-8327-P-A.

Liles, D.R., et al., 1981, "TRAC-PD2, An Advanced Best Estimate Computer Program for Pressurized Water Reactor Loss-of-Coolant Accident Analysis," NUREG/CR-2054.

Paik, C.Y., and Hochreiter, L.E., 1986, "Analysis of FLECHT-SEASET 163-Rod Blocked Bundle Data Using COBRA-TF," WCAP-10735.

SECY-83-472, Information Report from W.J. Dircks to the Commissioners, "Emergency Core Cooling System Analysis Methods," Nov. 17, 1983.

Thurgood, M.J., et al., 1980, "COBRA-TF Development," 8th Water Reactor Safety Information Meeting.

Thurgood, M.J., et. al., 1983, "COBRA/TRAC - A Thermal-Hydraulics Code for Transient Analysis of Nuclear Reactor Vessels and Primary Coolant Systems," NUREG/CR-3046.

Westinghouse, 1992 and 1993, "Code Qualification Document For Best Estimate LOCA Analysis," WCAP-12945-P, Volumes I - V.

Wilson, G., et al., 1989, "Quantifying Reactor Safety Margins," NUREG/CR-5249.